UNIVERSITÀ DEGLI STUDI DI PADOVA

DIPARTIMENTO DI INGEGNERIA CIVILE, EDILE ED AMBIENTALE

Corso di Dottorato di Ricerca in
SCIENZE DELL'INGEGNERIA CIVILE ED AMBIENTALE
Ciclo XXIX

Multi-objective optimization of run-of-river hydropower: hydrologic disturbance, stream connectivity and economic profitability

Coordinatore: Ch.mo Prof. Stefano LANZONI

Supervisore: Ch.mo Prof. Gianluca BOTTER

Dottorando: Gianluca LAZZARO

ANNO ACCADEMICO 2016/17

Acknowledgements

At the end of this PhD, there are some people that deserve to be thanked.
I am really grateful to my supervisor, Gianluca Botter, whose ideas are behind every chapter of this thesis, but even more because his constant guidance and support have been fundamental for my personal growth.
Special thanks go to Stefano Basso, who first started working on these topics. Support received by Paolo, Giulia and Enrica, and the work done by some master students need also to be acknowledged.
I am grateful to all people of the ICEA Department at University of Padova for academic and technical support, in particular to the Head of the PhD School of Civil and Environmental Engineering, Stefano Lanzoni.
Comments and suggestions on an earlier version of this thesis by Maurizio Righetti and Ross Woods were really helpful.
These years have certainly been easier thanks to all my colleagues in Padova. In particular, Manuel, Valentina and Irma, who entirely shared this adventure with me.
I would like to thank Chris Soulsby and Doerthe Tetzlaff, who kindly hosted me within their research group in Aberdeen and provided data as well as valuable suggestions for this research. I want also to thank all the guys met during my period abroad, especially Luca and Bas, colleagues and friends.
Lastly, I want to express my gratitude to my girlfriend Valentina, my parents Silvio and Mara, my brother Lorenzo, and all my dearest friends.

Abstract

Although run-of-river hydropower represents a key source of renewable energy, it cannot prevent stresses on river ecosystems. This is especially true in mountain regions, where the outflow of a plant is placed several kilometres downstream of the intake, inducing the depletion of river reaches of considerable length. In this thesis, multi-objective optimization is used in the design of the capacity of run-of-river plants to identify optimal trade-offs between contrasting objectives: the maximization of the profitability and the minimization of the impact induced by the plant. The latter is quantified either as the upstream/downstream changes of a set of ecologically-relevant flow metrics, or as the loss of hydrological connectivity in the impacted river reaches. Optimal plant sizes are devised for several case studies belonging to catchments in Italy and UK. Results show that the duration of economic optimal design capacity is strongly affected by the nature of the flow regime at the plant intake. In particular, the analysis emphasizes the important distinction between persistent (reduced variability) and erratic (enhanced variability) streamflow regimes. Multi-criteria optimization indicates that in persistent regimes a trade-off between profitability and hydrologic impact is achieved reducing the plant capacity below the economic optimum, whereas distinct trade-offs are available depending on the relative importance of the different flow statistics. This work also confirms that water abstractions for human exploitation induce ecologically-meaningful and quantifiable impacts on the hydrologic connectivity of altered river reaches, which may limit significantly migratory movements of fish. The application of a probabilistic eco-hydrological model to reproduce the observed immigration rates of Atlantic salmon in a Scottish river shows that limitations of connectivity are more pronounced in years where exceedance probability of relatively high flow is low. The analyses conducted in this thesis show that residual flows represents a key decision variable to preserve the connectivity of impacted river reaches, and thus should be carefully considered in

planning environmental policy actions. The analytical tools developed in this thesis could provide a clue for evaluating the environmental footprint of run-of-river plants and improve sustainability of energetic exploitation of surface water.

Contents

Chapter 1

Introduction

Motivation

Global policies on energy production hint at the reduction of carbon dioxide dispersed in the atmosphere. Many government programs and research studies highlight the negative role of CO_2 in the climatic changes occurred during last decades [Anderegg et al., 2010; IPCC, 2014]. In this context, renewable energies represent an important source for energy production. Recently, different techniques have been developed and/or more intensively exploited. Hydropower is probably the most ancient form of renewable energy and provided 16.3 % of the world's electricity (3874 TWh) in 2013, more than the sum of all other renewable sources (5.7 %) and nuclear power (10.6 %), but much less than fossil fuel plants (67.4 %) [IEA, 2015]. Notwithstanding the development of hydroelectricity in the 20^{th} century, most of the world hydroelectric residual potential remains unexploited [Karki, 2008]. Top four hydropower producers are China, Canada, Brazil and United States, that collectively supply more than 50 % of the world hydroelectricity. Hydropower is a key energy source also in developing countries, whose hydro-potential is seen as the backbone for future social and economic development [Bartle, 2002]. Brazil, Venezuela, India and Nepal are actually promoting hydropower investments to support their domestic electricity demand and thus foster and/or sustain their economies.
The intense exploitation of hydro-electricity has been typically associated with the construction of conventional plants that rely on large dams. Dams induce dramatic changes in the landscape (large areas are permanently inundated) and significant alterations of the downstream flow regime. Conventional hydropower plants are close to their sat-

uration in most western countries, and they are often unpopular because of the huge environmental disturbance they induce on rivers and landscapes.

During last decades a new type of hydropower plants has become increasingly important: run-of-river hydropower plants. River flows in these plants are continuously diverted, processed and released back to the same river without any regulation. Their main advantage is thus that they do not need large dams to accumulate and regulate water in an artificial reservoir, thereby avoiding dramatic changes in the landscape and significant alterations of the flow regime in the entire river network downstream of the dam.

In 2013, global run-of-river hydropower installed capacity was 75 GW, about the 0.07 % of the overall hydropower, but worldwide the residual gross potential is 173 GW [Liu et al., 2013]. Asia holds the largest fraction (about 65 %) of this unexploited potential (about 110 GW).

In Italy, more than 3000 run-of-river hydropower plants (< 10 MW) were in operation in 2014, with an overall installed capacity of 3173 MW. Italy is the top European country for installed capacity and electricity generation, considering hydropower plants with less than 10 MW. The energy produced in 2014 was 12.3 TWh. Large hydropower plants ($\geq$ 10 MW) still represent the most important source of hydroelectricity of the country with about 45 TWh in 2014 (76 % of the total hydroelectric generation) whereas run-of-river plants contributed the remaining 24 % (14 TWh). The gross hydropower potential in Italy is estimated to be about 200 TWh/year, of which 38 TWh/year associated with run-of-river plants. The evaluation of net potential also requires an assessment of the technical and economic feasibility of hydropower production. Technical and economical constraints are likely to reduce the hydropower potential production to about 50 TWh/year. Estimates of the technical run-of-river hydropower potential range between 12.5 TWh and 20 TWh. The potential installed capacity available is around 4 GW.

The energy produced by a hydropower plant mainly depends on the net hydraulic head and processed flows. Conventional hydropower plants maximize both these variables since dams are usually high and turbines can process significant quantities of water thanks to regulation. This is not possible with run-of-river power plants that maximize either hydraulic head or processed flow depending on their functioning scheme and are thus usually characterized by lower energy productions than conventional plants, because of the lower head or mean flow.

The functioning scheme of run-of-river plants is different whether the plant is located in

Figure 1.1: Aerial view of the Isola Serafini run-of-river power plant (Piacenza, Italy).

plane or mountain areas.

In plane regions, run-of-river plants can process significant flows ($\sim 10^3$ m^3/s) with an associated hydraulic head which is usually limited (< 15 m). A weir containing turbines is usually placed in the river, and water is processed and then returned immediately downstream of the weir. To increase the hydraulic head these plants are usually placed in correspondence of localized drops along the river, e.g. cutting a meander of the pristine river path. In Figure 1.1, it is shown the Isola Serafini plant (Piacenza, Italy) actually managed by ENEL, the Italian national Authority for electricity, that is characterized by a capacity of 1000 m^3/s and a hydraulic head of 11 m, determining a maximum power of 79 MW and an annual energy production of about 500 GWh. The plant is built in correspondence of a meander along the plane course of the Po River, the largest Italian river ($\sim$ 70000 km^2 of contributing area).

This work however is focused on run-of-river plants in mountain regions. Therein, as shown in Figure 1.2, water is diverted from headwater channels, where contributing areas and, consequently, available streamflows are relatively small. In this case, the plant outflow, where diverted water is processed and then returned to the original stream,

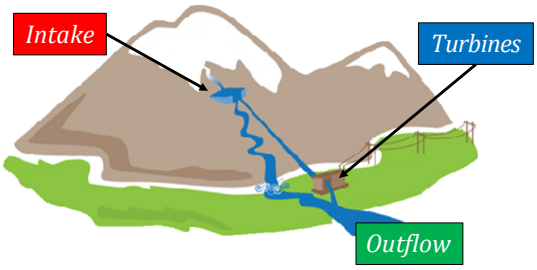

Figure 1.2: Functioning scheme of a run-of-river plant located in mountain area.

needs to be located several kilometres downstream of the intake to allow for a suitable increase of the head. Energy production from mountain run-of-river plants is usually limited compared to run-of-river plants in plane regions and even more if compared with conventional hydropower plants. For this reason, this kind of plants is usually referred as small hydropower (official Italian law requirement is maximum power < 10 MW).
Even though small hydro inflicts a smaller impact on aquatic ecosystems and local communities compared to large dams, it cannot prevent stresses on plant, animal, and human well-being [Kern et al., 2012]. Indeed, the entire river reach between the intake and the outflow is depleted of a significant quantity of water. This is evident from Figure 1.3 which shows two photos simultaneously taken during a visit to a plant located in the Alps, Italy (June 2014). Both pictures were taken from the plant intake, but Figure 1.3a shows the upstream reach (natural flow conditions), whereas Figure 1.3b emphasizes the significant depletion of water experienced by the stream downstream of the intake. Natural flow regime is then restored downstream of the outflow, where processed water returns to the original stream.
During recent years, this technology has been heavily subsidized through state incentives aimed at increasing national shares of green energy production through the growth of small hydropower plants [Liu et al., 2013]. Accordingly, an intensive exploitation of river flows, with a series of plants built in cascade along the same river has been promoted. Consequently, the disturbance on the flow regime, rather than being restricted to a single individual reach, is usually replicated across many different reaches along the same river

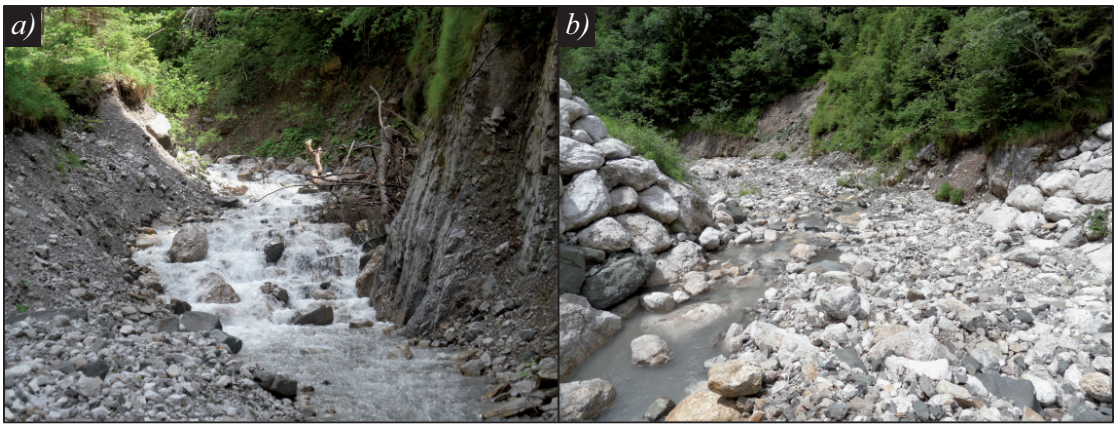

Figure 1.3: These photos were simultaneously taken during a visit to a plant in the Alps, Italy (June 2014) and show the different amount of water flowing upstream (a) and right downstream of the plant intake (b). In this case, the outflow is located 2 km downstream of the intake.

leading to significant large-scale impacts.

Worldwide, the cumulated longitudinal impact of run-of-river plants is raising concerns for the health of riverine ecosystems and creates social aversion toward this type of infrastructure. In the Piave river basin (Italy), for instance, several small hydropower plants have been recently added to the existing network of reservoirs and pipelines, and many others may be completed in the upcoming years. After the completion of the proposed projects, in the upper part of the Piave River, the overall length of reaches impacted by run-of-river plants would raise to 150 km (Figure 1.4). As a result, about one-third of the streams of two major tributaries like the Cordevole and the Boite rivers would be heavily depleted. The negative cumulative effect of run-of-river systems operating along the same river threatens the ability of stream networks to supply ecological corridors for plants, invertebrates, or fishes, and support biodiversity [Muneepeerakul et al., 2008; Rodriguez-Iturbe et al., 2009; Ziv et al., 2012] and has originated harsh social conflicts involving regional authorities, green organizations, energy companies, and local population. Nowadays, the prediction of the long-term impacts associated with the expansion of run-of-river projects remains highly uncertain. As the decommissioning of run-of-river hydropower plants is not considered an economically feasible option, the only reliable solution to the emerging conflicts among water users seems to be a wiser management of the available resources.

Objectives and outline of this thesis

The need of reconciling contrasting social interests (economic interests of energy producers and environmental issues) puts the focus on the need of developing methods enabling an objective assessment of the economic and environmental outcomes of different design solutions. With these premises, the objectives of this thesis can be identified as follows:

- define tools for the preliminary design of the plant capacity of run-of-river power plants devoted to maximize the energy produced or the economic profitability;
- identify and quantifying the main disturbances induced on the natural flow regime and the loss of hydrological connectivity between the intake and the outflow of a plant, and their negative reach-scale drawbacks on riverine ecosystems;
- utilize multi-objective tools to identify sustainable plant capacities simultaneously maximizing contrasting goals such as the maximization of the economic profitability and the minimization of hydrologic disturbances.

Developed tools have been applied to run-of-river plants located in the north-eastern part of the Alps (Italy) where the massive development of small hydropower is actually posing some concerns on the sustainability of this new technology. Moreover, the multi-objective design of a run-of-river plant has been carried out in a pristine catchment located in the Highlands of Scotland (UK). Here, the impact induced by water abstraction on fluvial ecosystems can be properly quantified through the simulated impact of altered flow regimes on migratory movements of fish communities.

The remainder of this work is organized as follows:

- Chapter 2 describes how the energy production, the economic profitability and the hydrologic disturbance of run-of-river plants at the reach-scale can be quantified; a mathematical framework to simultaneously combine contrasting objectives such as economic maximization and environmental protection is also formally introduced;
- Chapter 3 shows the application of methods for a preliminary design of run-of-river plants maximizing the energy production or the economic profitability to three case studies located in the Alps, Italy;
- Chapter 4 focuses on the hydrologic disturbance induced by plants on the river reach between the intake and the outflow, and it presents results of a multi-objective design approach trading between economic and environmental needs;
- Chapter 5 analyses the disturbance induced by water diversions on the mobility of fish communities along the river network, thereby investigating potential losses of

hydrological connectivity inside the catchment to define the plant capacity simultaneously allowing energy production and fish migrations.

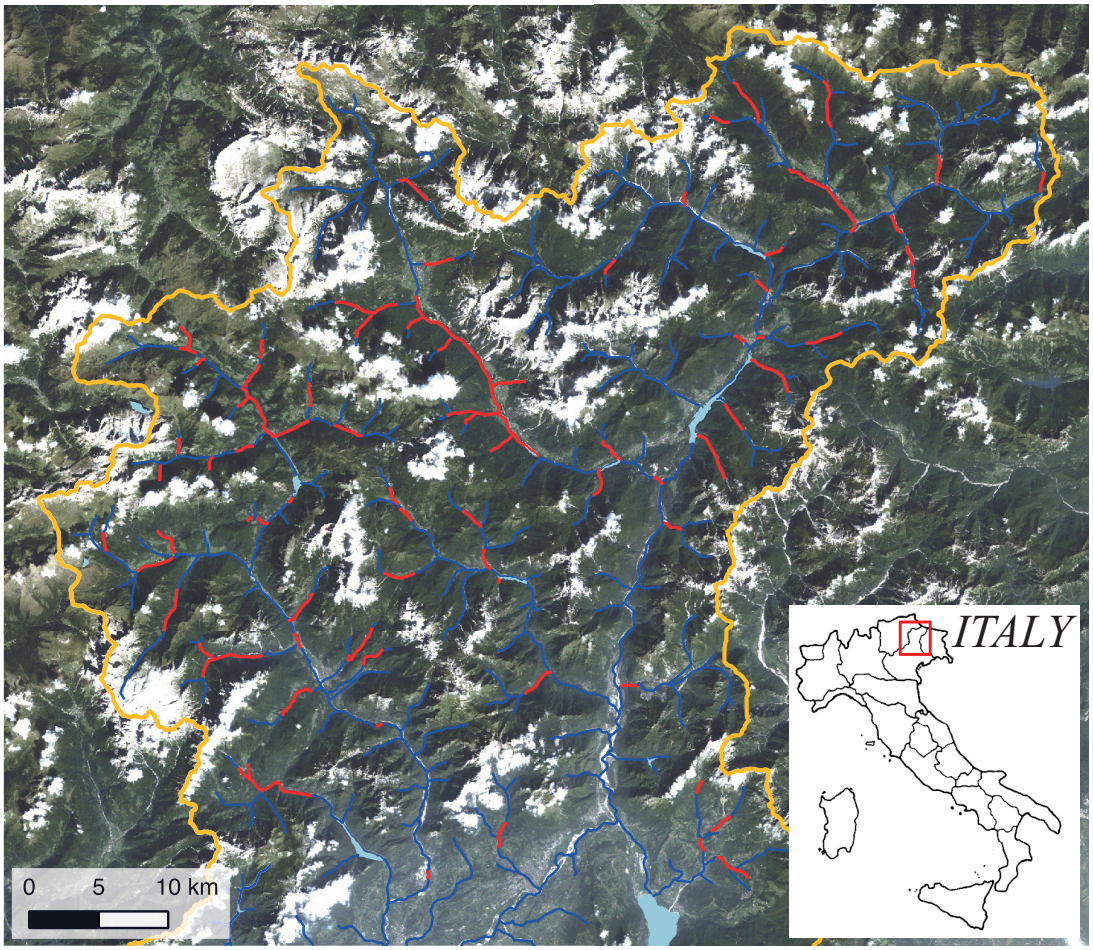

Figure 1.4: River network of the Piave basin (blue lines) showing the extent of the river reaches impacted by the run-of-river power plants recently proposed (red lines). The map has been drawn exploiting data available on-line on the website of the Veneto region (http://bur.regione.veneto.it/).

Chapter 2

Methods

The amount of energy produced by hydropower plants mainly depends on the sequence of streamflows workable by the plant during its lifetime. The choice of the maximum flow that a plant can process (i.e. the plant capacity Q) is known to be strongly influenced by the hydrologic regime of the river. Flow availability observed at a river cross section strongly fluctuates in time at multiple time-scales, mirroring fluctuations of climatic drivers such as rainfall and evapotranspiration (e.g. [Zanardo et al., 2012; Botter et al., 2013; Botter, 2014]). Surface water resources are indeed the by-product of complex processes with strong stochastic components. As a consequence, streamflows show a strong intra-seasonal variability mainly related to rainfall stochasticity, inter-seasonal variations due to seasonal features of climate, and inter-annual fluctuations driven by long-term variations of climate and landscape.

Streamflow availability and variability are usually portrayed by hydrologists and engineers by means of the probability density function ($p(q)$) of streamflows or, alternatively, by the flow duration curve ($D(q)$). The shape of $p(q)$ (or $D(q)$) places a substantial constraint on the optimal capacity (i.e., the maximum flow a plant can process) and other design attributes of a run-of-river plant.

Estimating natural flow regime at the plant intake thus represents the first (and probably the most important) task engineers are forced to face in the design process, since it directly influences most of the associated hydraulic and mechanical design problems. The best way of assessing $p(q)$ (or $D(q)$) would be the use of long-term flow measurements in the river section where the plant intake will be built. Unfortunately, in remote small mountain basins where plant intakes are commonly placed, there is a lack of flow

measurements that is usually overtaken by means of alternative techniques. Empirical approaches are usually applied which try to get information on the streamflow availability from rainfall-runoff models based on precipitation data series which need only sporadic flow measurements for calibration. Flow estimates can also be made based on previous studies on the same area which analysed the specific contribution of the catchment where the plant is being built or based on similarity with other nearby gauged basins.

In this work, a mechanistic-stochastic and parsimonious model for streamflow dynamics (based on a water balance forced by Poisson rainfall) is used to assess the probability distribution of streamflows and the related flow duration curve at the plant intake. The model has been introduced by Botter et al. [2007] and following extensive applications in different regions of the world have proved its ability to reproduce the probability distributions of the observed streamflows in watersheds characterized by different climatic and geological settings [Botter et al., 2010; Ceola et al., 2010; Botter et al., 2013; Basso et al., 2015].

The mathematical formulation of the model is briefly reported at the beginning of this chapter (Section 2.1), since the relationship between analytical expressions of the streamflow pdf ($p(q)$) provided by the model and different technical problems that are typically associated with the realization of run-of-river hydropower plants represents the core of this thesis.

2.1 Availability of water resources at the plant intake

Water resources available at the intake of run-of-river power plants can be estimated according to a mechanistic analytical model in which streamflow dynamics are driven by a catchment-scale soil-water balance forced by stochastic daily rainfall. When infiltration of rainfall brings enough water in the root zone to fill the soil-water deficit resulting from evapotranspiration, soil moisture exceeds the field capacity and such excess of water is eliminated through the catchment hydrologic response. Model details are provided below based on the work introduced by Botter et al. [2007] and then developed by Botter et al. [2013] and Basso et al. [2015].

Daily rainfall can be described as a Poisson process with frequency λ_p $[T^{-1}]$ and exponentially distributed intensities with average α $[L]$. As a consequence, the sequence of events producing streamflow can also be approximated by a Poisson process similar to

the main rainfall, although characterized by a reduced frequency, $\lambda < \lambda_p$ $[T^{-1}]$.
The ratio between λ and λ_p is a number which is always lower than one and represents the rainfall-runoff coefficient ($\phi = \lambda/\lambda_p$). Different values of ϕ are usually observed among different catchments, mainly due to different underlying climates and soil types and covers. For example, humid catchments can be characterized by rainfall-runoff coefficients close to 1 in seasons where the effect of evapotranspiration is negligible (e.g. winter), implying that flow-producing rainfall events have a frequency which is similar to that of rainfall due to the relatively high saturation of the catchment, and consequently the reduced filtering effects of soil moisture dynamic. Conversely, in dry seasons ϕ approaches zero and flow-producing rainfall events are uncommon due to high evapotranspiration-driven water losses from the catchment. Soil moisture is thus very low and runoff production can only be seen in correspondence of intense rainfall events capable of saturating the root zone or exceeding the rate of infiltration of soil. The rainfall-runoff coefficient at a river cross section exhibits inter-seasonal fluctuations driven by seasonal patterns of climatic variable (rainfall and evapotranspiration). In fact, dry seasons (e.g. summer) are characterized (on average) by values of ϕ lower than those observed during humid seasons (e.g. winter).
Once that flow-producing events occur, the release of water is usually modelled assuming a linear storage-discharge relation:

$$\frac{dq(t)}{dt} = -k\, q(t) + \xi_t \,, \tag{2.1}$$

where q is the specific streamflow (per unit catchment area). In eq. (2.1), the first term on the right-hand side expresses the exponential decay of the flow between the events, which is a function of the mean residence time of water inside the catchment ($\tau = 1/k$). The second term (ξ_t $[L/T^2]$) formally embeds the series of stochastic jumps induced on q by the sequence of flow pulses. Each pulse ξ_t determines a sudden increase of streamflow followed by an exponential-like recession. Provided that the system is linear, the overall streamflow is the sum of the contribution of different effective pulses taking place. Flow-producing events have instantaneous durations and produce a sequence of positive jumps in the dynamics of q. Interarrival times between these jumps are exponentially distributed with mean $1/\lambda$. Given the exponential distribution of rainfall depths, the extents of the jumps experienced by q are random and exponentially distributed with mean αk (k times pulse depth).
Under these assumptions, the master equation associated with the probability density

function (pdf) of flow q at time t, $p(q,t)$, reads:

$$\begin{aligned}\frac{\partial p(q,t)}{\partial t} &= \frac{\partial\left[k\,q\,p(q,t)\right]}{\partial q} - \lambda\,p(q,t) \\ &+ \frac{\lambda}{\alpha k}\int_0^q p\,(q-z,t)\;exp[-z/(\alpha k)]\,dz. \end{aligned} \tag{2.2}$$

The steady-state pdf of specific river discharge is thus given by the solution of the master equation for $t \to \infty$, which leads to eq. (2.3).

$$p(q) = \frac{\Gamma(\lambda/k)^{-1}}{\alpha k}\,\left(\frac{q}{\alpha k}\right)^{\frac{\lambda}{k}-1}\,exp\left(-\frac{q}{\alpha k}\right), \tag{2.3}$$

where $\Gamma(x)$ is the complete Gamma-function of argument x.

The application of eq. (2.3) is based on the assumption that the flow regime reaches steady state at the seasonal time scale. This assumption proved to be valid in a wide range of case studies where the model was applied [Botter et al., 2010, 2013; Botter, 2014], even at time windows smaller than a season [Park et al., 2014]. Model performances may deteriorate in catchments characterized by strongly different seasonal climates, rapidly shifting from dry to humid conditions, where steady conditions could be difficultly achieved within a season.

Water resources availability in practical applications is usually represented through flow duration curves, which are the cumulative probability distributions of such flows. The analytical expression of flow duration curve is shown by eq. (2.4).

$$D(q) = \int_q^\infty p(q)\,dq = \frac{\Gamma(\lambda/k)^{-1}}{\alpha k}\,\int_q^\infty \left(\frac{q}{\alpha k}\right)^{\frac{\lambda}{k}-1}\,exp\left(-\frac{q}{\alpha k}\right)\,dq. \tag{2.4}$$

Parameters required to define the natural flow regime are: mean daily rainfall depth, α; mean frequency of flow-producing rainfall events, λ; and inverse of the mean residence time of water inside the catchment, k.

The analytical mechanistic model allows the river flow pdf to be expressed as a gamma-distribution with shape parameter $\frac{\lambda}{k}$ and rate parameter αk (eq. (2.3)). The mean and variance of the streamflow distribution are $\lambda\alpha$ and $\lambda\,k\,\alpha^2$ (respectively), implying that the coefficient of variation of daily flows (CV_q) is $\sqrt{k/\lambda}$. This represents the basis for a quantitative classification of flow regimes, as discussed below.

When flow-producing rainfall events are relatively frequent, such that their mean inter-arrival is smaller than the duration of the flow pulses delivered from the contributing catchment ($\lambda > k$), the range of streamflows observed at a station between two subsequent events is reduced, and a persistent supply is guaranteed to the stream from

catchment soils. Therefore, river flows are weakly variable around the mean (Figure 2.1, lower) and quite predictable. This type of regime (hereafter termed persistent) is typically expected during humid, cold seasons in slow-responding catchments (high λ, low k). When the mean interarrival between flow-producing rainfall events is larger than the typical duration of the resulting flow pulses ($\lambda < k$), a wider range of streamflows is observed between events because the reach is allowed to dry significantly before the arrival of a new pulse. The temporal patterns of streamflows are thus more unpredictable (Figure 2.1, upper), leading to erratic regimes with significant streamflow fluctuations. Under these circumstances, the preferential state of the system is typically lower than the mean. Erratic regimes are likely expected in fast-responding catchments during seasons with sporadic rainfall events (low λ, high k). However, this type of regime can frequently be observed during hot, humid seasons (where relatively high rainfall rates are compensated by enhanced evapotranspiration). The characterization of river flow

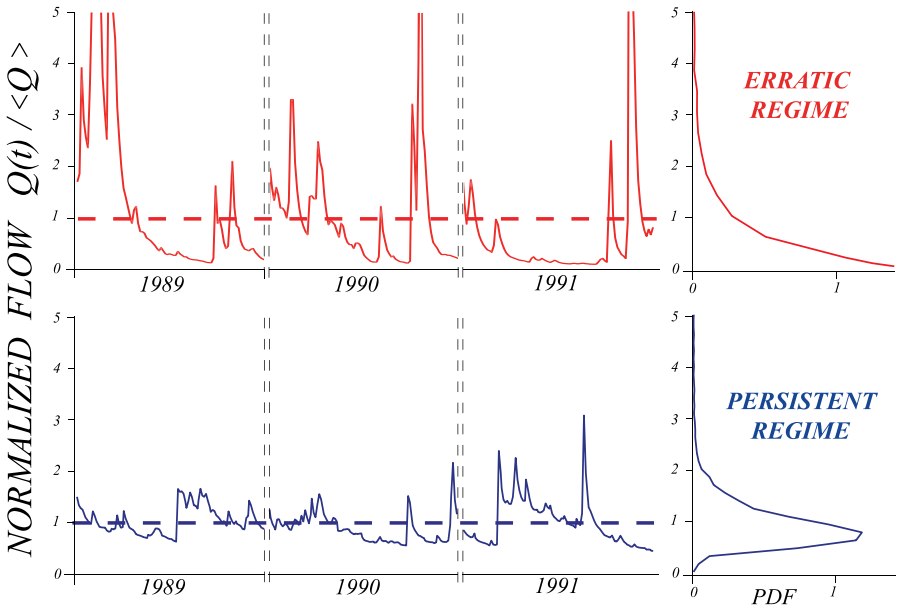

Figure 2.1: Typical behaviour of river flow dynamics in erratic and persistent regimes.

regimes relies on the specification of three (α, λ and k) model parameters, which can be estimated by combining rainfall and discharge data.

The mean rainfall depth, α, is estimated by using daily rainfall data recorded in several stations located within or nearby the considered basin. When synchronous data from

different stations are available for the same catchment, rainfall records are first interpolated to obtain spatially averaged rainfall series. The value of α is the average daily rainfall depth during wet days.

The average frequency of streamflow-producing events, λ, can be estimated by equalling the observed mean specific discharge, $< q >$, and the analytical mean of q (which is the equal to the product $\alpha\,\lambda$) according to the stochastic model (i.e., $\lambda =< q > /\alpha$). This can be done only when discharge data measured in the same river or in similar, nearby catchments are available. However, alternative estimation methods exist to overcome the lack of flow measurements. These alternative procedures are based solely on soil and climatic features of basins (see Botter et al. [2013]; Doulatyari et al. [2015]).

The recession rate, k, is derived from observed streamflows through a regression analysis. In particular, k is the slope of the linear regression between the estimated temporal derivatives of q (dq/dt) and the corresponding observed discharges [Brutsaert and Nieber, 1977]. Details about the computation of k can be found in Basso et al. [2015]. Alternative procedures for the calculation of k exist, that consist in estimating the mean residence time of water in the catchment.

Despite the fact that some of the related hydrological processes are somewhat simplified (e.g., rainfall dynamics, hydrological response of the catchment) and other processes are completely disregarded (e.g., geomorphological and hydrodynamic dispersion in the river network), the above approach provides a robust linkage between the river flow regime and a few (directly measurable) rainfall and landscape attributes of the contributing catchment. Hence, it represents a simple, parsimonious and useful tool for the preliminary estimate of water resources at the plant intake.

2.2 Flows worked by the plant

Once that the distribution of flows at the plant intake is known ($p(q)$ or $D(q)$, see eqs. 2.3 and 2.4), the operation rules of a run-of-river power plant have to be taken into account to define the pdf of flows worked by the plant $p_w(q_w)$ [Basso and Botter, 2012]. Figure 2.2 shows the functioning scheme of a run-of-river plant equipped with a single turbine ($n_T = 1$) coping with Minimum Flow Discharge (MFD) withdrawal. Due to flow requirements downstream of the intake, the flow which can be diverted from a river to the plant is the difference between the incoming streamflow q and the MFD (when such difference is positive). Moreover, the actual range of streamflows processed by the

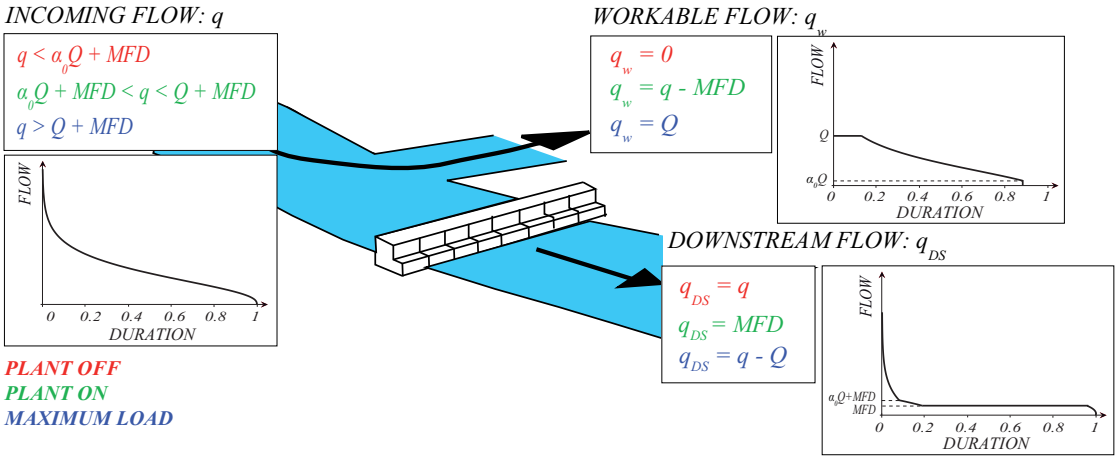

Figure 2.2: Scheme of functioning of a run-of-river hydropower plant with the derivation to the plant which respect the prescription of Minimum Flow Discharge in the river.

plant depends on the technical constraints of the turbine, namely its capacity Q, and the minimum workable flow (i.e. cut-off flow), which is usually expressed as a fraction of Q (i.e., $\alpha_0 Q$, where α_0 usually ranges between 0.1 and 0.2 mainly depending on the type of turbines installed). In particular, when the flow which could be diverted ($q - MFD$) is lower than the cut-off flow, water cannot be processed and $q_w = 0$. This happens with probability $1 - D(\alpha_0 Q + MFD)$, as shown by the following equations:

$$\begin{aligned} \int_0^{\alpha_0 Q} p_w(q_w)\, dq_w &= 1 - \int_{\alpha_0 Q}^{\infty} p(q_w + MFD)\, dq_w = \\ &= 1 - \int_{\alpha_0 Q + MFD}^{\infty} p(q)\, dq = \\ &= 1 - D(\alpha_0 Q + MFD) \end{aligned} \tag{2.5}$$

On the other hand, when the diverted flows are in between the cut-off flow and the capacity of the plant, they are entirely processed by the plant, and $q_w = q - MFD$. Finally, when the flow which could be diverted exceeds the capacity of the plant, only the flow Q is actually taken from the river and processed. This happens with a probability equal to $D(Q + MFD)$, as the following expression demonstrates:

$$\begin{aligned} \int_Q^{\infty} p_w(q_w)\, dq_w &= \int_Q^{\infty} p(q_w + MFD)\, dq_w = \int_{Q + MFD}^{\infty} p(q)\, dq = \\ &= D(Q + MFD) \end{aligned} \tag{2.6}$$

In practical applications, sediment concentrations associated with very high flow conditions may stop plant operation because of potential abrasion damages to turbines. However, the relatively low frequency of those high flows suggests that a reasonable estimate of flows worked by a run-of-river plant can be achieved even if this situation is not taken into account by the model. The pdf of the flows which are processed by the plant hence corresponds to the incoming streamflow pdf, $p(q)$, (dashed line in Figure 2.3) simply translated leftward by a value equal to the MFD, with the two tails of the original distribution becoming two atoms of probability associated to $q_w = 0$ and $q_w = Q$. The

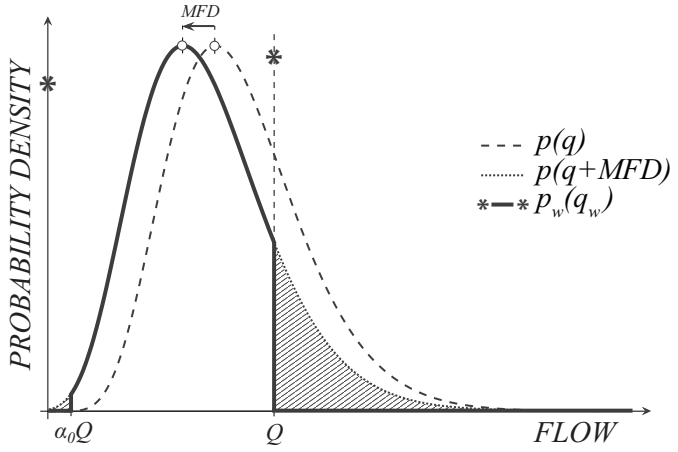

Figure 2.3: Probability distributions of streamflows ($p(q)$, dashed line), of river flows which can be diverted (dotted line) and pdf of flows workable by an hydropower plant ($p_w(q_w)$, solid line and stars) equipped with a single turbine and coping with Minimum Flow Discharge requirements.

probability distribution of the workable flows $p_w(q_w)$ of a plant equipped with a single turbine and coping with Minimum Flow Discharge requirements can thus be expressed as:

$$p_w(q_w) = p(q_w + MFD) \;\text{ if }\; \alpha_0 Q < q_w < Q \tag{2.7}$$

while probabilities of having $q_w = 0$ or $q_w = Q$ are respectively equal to $[1 - D(\alpha_0 Q + MFD)]$ (eq. 2.5) and $[D(Q + MFD)]$ (eq. 2.6).
Considerations on the flow processed by a plant equipped with a single turbine can be easily extended to the case of a plant with n_T identical turbines, each having a capacity Q/n_T. The MFD withdrawal rule in this case can be mathematically described through

eq. (2.8).

$$q_w = \begin{cases} 0 & \text{if } q < \frac{\alpha_0}{n_T} Q + MFD \\ q - MFD & \text{if } \frac{\alpha_0}{n_T} Q + MFD \leq q < Q + MFD \\ Q & \text{if } q \geq Q + MFD \end{cases} \tag{2.8}$$

In this case, Q is the total capacity of the plant and $\frac{\alpha_0}{n_T} Q$ defines the cut-off flow of a single turbine. In eq. (2.8), the first condition represents the switching off of the plant because the water supply is insufficient to maintain the MFD downstream of the intake and activate one turbine. The last condition in eq. (2.8) expresses the fact that, for large incoming flows ($q \geq Q + MFD$), the plant capacity is completely exploited and $q_w = Q$.

The number of simultaneously operating turbines (n_o) is a function of the amount of flow being processed. If streamflow available in the river is lower than the threshold $\frac{\alpha_0}{n_T} Q + MFD$, $n_o = 0$. When the available flows exceed the threshold ($\frac{\alpha_0}{n_T} Q + MFD$), one turbine is activated. Streamflows diverted to the plant may also increase above $\frac{Q}{n_T}$, in this case a second turbine needs to be activated. If the second turbine processes a flow larger than $\frac{\alpha_M Q}{n_T}$ and the flow processed by the first turbine, $q_w - \frac{\alpha_M Q}{n_T}$, is larger than $\frac{\alpha_M Q}{n_T}$, the efficiency of both the turbines will be maximum ($\eta = \eta_M$). Note that the conditions $q_w \geq \frac{Q}{n_T}$ and $q_w - \frac{\alpha_M Q}{n_T} \leq \frac{\alpha_M Q}{n_T}$ can be simultaneously fulfilled if $\alpha_M \leq 0.5$, a condition which is verified for all the turbine types commonly employed in run-of-river plants. This operation is then re-iterated every time the activation of an additional turbine is required by the increase of diverted flows. Hence, n_o depends on the magnitude of the processed flow q_w, scaled to the plant capacity Q, according to the following equation:

$$n_o = \begin{cases} 1 & \text{if } \frac{q_w}{Q} < \frac{1}{n_T} \\ 2 & \text{if } \frac{1}{n_T} \leq \frac{q_w}{Q} < \frac{2}{n_T} \\ \ldots & \\ n_T - 1 & \text{if } \frac{n_T - 2}{n_T} \leq \frac{q_w}{Q} < \frac{n_T - 1}{n_T} \\ n_T & \text{if } \frac{q_w}{Q} \geq \frac{n_T - 1}{n_T} \end{cases} \tag{2.9}$$

The probability distribution of the workable flows $p_w(q_w)$ of a plant equipped with n_T turbines and coping with Minimum Flow Discharge requirements can thus be expressed as:

$$p_w(q_w) = p(q_w + MFD) \text{ if } \frac{\alpha_0}{n_T} Q < q_w < Q \tag{2.10}$$

while probabilities of having $q_w = 0$ or $q_w = Q$ are respectively equal to $[1 - D(\frac{\alpha_0}{n_T}Q + MFD)]$ and $[D(Q + MFD)]$.
The comparison between eq. (2.7) and eq. (2.10) suggests that when n_T turbines are installed, the cut-off flow decreases from $\alpha_0 Q$ to $\frac{\alpha_0}{n_T}Q$ (being n_T a positive integer) with an higher range of discharges that can be efficiently processed by the plant.

2.3 Energy production

The energy produced by a run-of-river hydropower plant mainly depends on three variables.

- the net hydraulic head, calculated as the difference between the gross hydraulic head and the energy losses within the plant;
- the workable flow (q_w);
- the turbine efficiency, which mainly depends on the turbine type and on the ratio between flow worked by the plant q_w and the maximum workable flow Q (i.e. the plant capacity).

In the following mathematical derivations, the plant capacity will be considered as the only decision variable, thereby assuming the remaining design attributes of the plant to be known or derivable on the basis of the capacity.
The energy produced by a hydropower plant during a time period ΔT is the time integral of the time dependent power generated during ΔT:

$$E(Q) = \rho g \, \eta_P \int_0^{\Delta T} H(t) \, \eta \left(\frac{q_w(t)}{Q} \right) q_w(t) \, dt \tag{2.11}$$

where Q is the plant capacity (i.e., design flow), ρ is the water density, g is the standard gravity, η_P is the efficiency of the plant, η is the turbine efficiency and H is the net hydraulic head.
Following Najmaii and Movaghar [1992], Voros et al. [2000], Montanari [2003], Anagnostopoulos and Papantonis [2007] and Santolin et al. [2011], in the forthcoming calculations the head H will be considered constant. Hence both the head losses and possible reductions of the gross head for incoming flows larger than Q will be neglected.
For time periods ΔT much longer than the correlation scale of streamflows [Botter et al., 2010] (e.g. few years, a decade, the lifetime of the plant), incoming streamflows can be assumed to be ergodic, and the frequencies characterizing the different values of q_w in

equation (2.11) are described by the probability density function of workable flows, p_w, previously defined in Section 2.2. Therefore, the time integral of equation (2.11) can be replaced by a weighted integral over q_w, the weighting factor being p_w:

$$E(Q) = \Delta T\, H\, \rho g\, \eta_P \int_0^{\infty} \eta\left(\frac{q_w}{Q}\right) p_w(q_w)\, q_w\, dq_w \tag{2.12}$$

When the expression of the workable flow pdf given by equation (2.10) is used, equation (2.12) becomes:

$$\begin{aligned} E(Q) \;=\; & \Delta T\, H\, \rho g\, \eta_P \left[\int_{\frac{\alpha_0}{n_T}Q}^{Q} \eta\left(\frac{q_w}{Q}\right) p(q_w + MFD)\, q_w\, dq_w + \right. \\ & \left. + \eta(1)\, Q\, D(Q + MFD)\right] \end{aligned} \tag{2.13}$$

The second term within the square brackets on the right hand side of equation (2.13) is originated from the atom of probability in correspondence of $q_w = Q$, while the first term derives from the continuous part of the workable flow pdf.

The assessment of the produced energy $E(Q)$ requires to specify the efficiency function $\eta(x)$, where $x = \frac{q_w}{Q}$. The efficiency pertaining to each turbine type can be represented by means of specific curves characterized by distinctive shapes and working ranges. Examples of efficiency curves for different types of turbines [ESHA, 1998] are displayed with thick grey lines in Figure 2.4. The actual turbine efficiency curve will be approximated by a piecewise linear function: for x lower than α_0, the efficiency of the turbine is null; between α_0 and α_M, efficiency grows linearly from η_0 to η_M; for x larger than α_M, the efficiency is maximum η_M. The approximation can be formulated in analytical terms through the following expression:

$$\eta(x) = \begin{cases} 0 & \text{if } x < \alpha_0 \\ \frac{x-\alpha_0}{\alpha_M-\alpha_0}(\eta_M - \eta_0) + \eta_0 & \text{if } \alpha_0 \le x < \alpha_M \\ \eta_M & \text{if } x \ge \alpha_M. \end{cases} \tag{2.14}$$

In general, when n_T turbines are installed, the efficiency of the plant, $\eta(\frac{q_w}{Q})$ can be expressed as:

$$\eta(x) = \begin{cases} 0 & \text{if } x < \frac{\alpha_0}{n_T} \\ \frac{\eta_M-\eta_0}{\frac{\alpha_M}{n_T}-\frac{\alpha_0}{n_T}}(x - \frac{\alpha_0}{n_T}) + \eta_0 & \text{if } \frac{\alpha_0}{n_T} \le x < \frac{\alpha_M}{n_T} \\ \eta_M & \text{if } x \ge \frac{\alpha_M}{n_T} \end{cases} \tag{2.15}$$

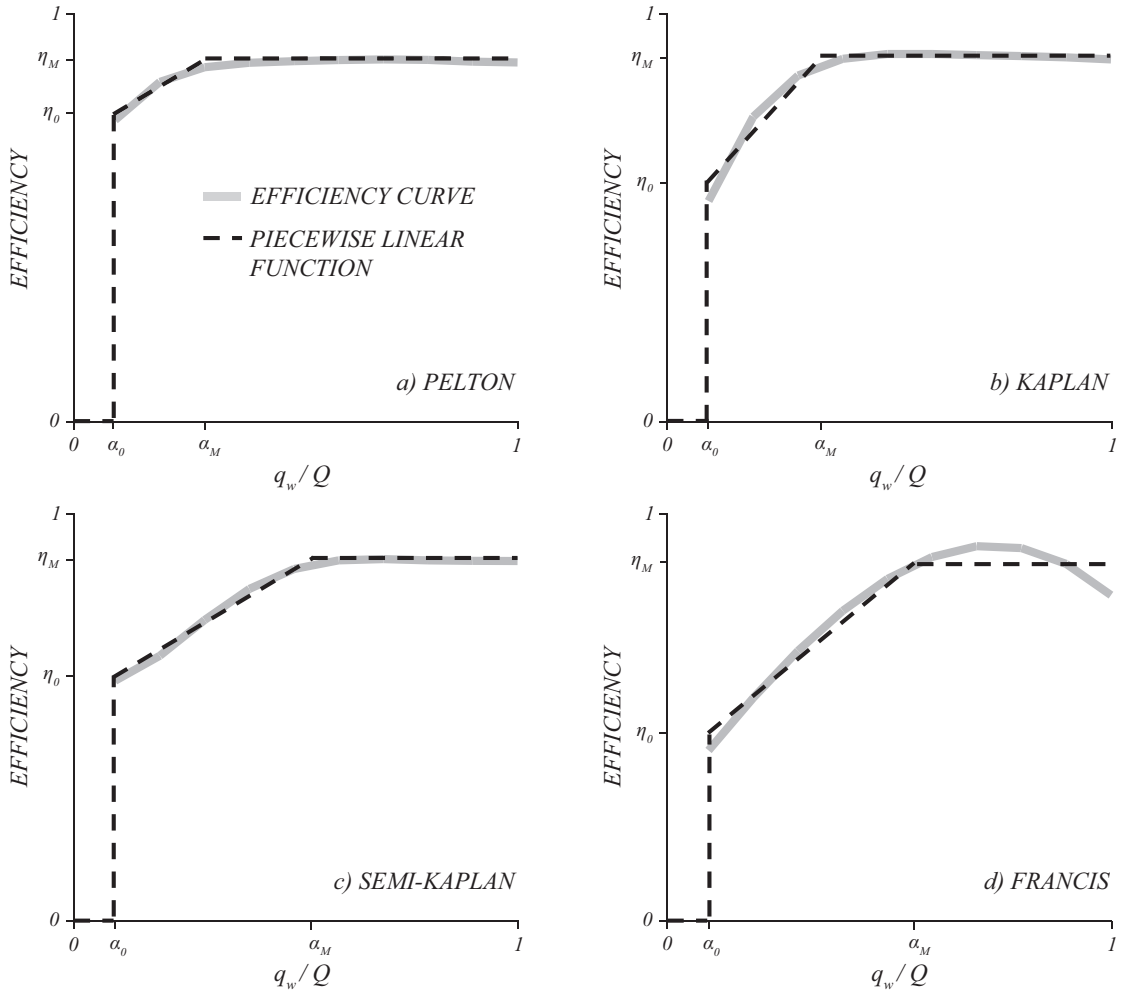

Figure 2.4: Efficiency curves for different turbine types (solid grey lines), taken from literature [ESHA, 1998]. The approximation given by the piecewise linear (dashed lines, equation (2.14)) functions is displayed for the different cases, with the validity boundaries of the different parts of these functions (α_0 and α_M) and the corresponding efficiency values (η_0 and η_M).

Note that eq. (2.15) is exactly equal to eq. (2.14) when n_T is set to 1.
The energy produced by a run-of-river power plant can thus be computed by combining equations (2.13) and (2.15).

2.4 Economic profitability

In real-world practical application, run-of-river power plants are designed based on economic issues. Indeed, investors are mainly interested in the profits they can get from hydropower plants and not in the energy produced by the plant. Due to the non-linear increase of costs with the size of the plant, profits (calculated as revenues minus costs) are not proportional to the energy produced. The revenues generated by a run-of-river hydropower plant can be calculated by multiplying the produced energy by the selling price of energy from renewable sources e_p, which is assumed here to be constant. Indeed, in most EU countries a feed-in tariff fixed by national laws exists to promote the production of energy from renewable sources [Liu et al., 2013; Lucchetti et al., 2013; Scarlat et al., 2013]. Feed-in tariffs depend on the maximum power of the plant which in turn affects also the duration of state incentives. The aim of these laws is to promote run-of-river energy generation providing incentives to support economic feasibility of these zero-emissions power plants.
To make a proper economic assessment of hydropower projects, the ergodicity hypothesis underlying equation (2.13) will be applied within each year of ΔT, so that the annual revenue $R_1(Q)$ is the same every year. Hence, annual proceeds $R_1(Q)$ can be calculated as:

$$R_1(Q) = e_p \, E_1(Q) \tag{2.16}$$

where $E_1(Q)$ is $E(Q)$ expressed by equation (2.21) with $\Delta T = 1$ year.
The overall present value $R_n(Q)$ of every cash inflow occurring during n years (e.g. the duration of state incentives or the lifetime of the plant) can be computed by means of the following expression:

$$R_n(Q) = \sum_{k=1}^{n} \frac{1}{(1+r)^k} \, R_1(Q) = \frac{1}{r} \left(1 - \frac{1}{(1+r)^n} \right) R_1(Q) = \hat{r} R_1(Q) \tag{2.17}$$

where r is the (constant) annual discount rate and $\hat{r} = \frac{1}{r} \left(1 - \frac{1}{(1+r)^n} \right)$ is an auxiliary variable expressing the multiplier used to compute the present value of the overall cash

inflows.

Typically hydropower plants are characterized by initial investment costs much higher than the corresponding operation expenses (e.g. Aggidis et al. [2010]). Therefore, costs incurring during the functioning of the plant could be neglected (e.g. Fahlbuch [1983]) to focus only on the construction expenses.

Several past studies have investigated the relationship between construction costs and some key features of a hydropower plant, chiefly the nominal power and the hydraulic head [Gordon and Penman, 1979; Gordon, 1981, 1983; Gordon and Noel, 1986; Ogayar and Vidal, 2009; Aggidis et al., 2010]. Following those papers, the construction costs are expressed as a function of the design flow (all the other terms being constants) as:

$$C(Q) = a\,Q^b \tag{2.18}$$

where a and b are empirical coefficients. Typical values for a and b can be derived from previous studies or via empirical estimates of the relationship between construction costs and plant features (e.g. Ogayar and Vidal [2009]; Aggidis et al. [2010]). While a can be highly variable from site to site, the parameter b has been found to be weakly variable around 0.6 in most cases [Aggidis et al., 2010].

Following Anagnostopoulos and Papantonis [2007]; Basso and Botter [2012]; Lazzaro et al. [2013]; Lazzaro and Botter [2015], the economic value of the plant can be expressed through the Net Present Value (NPV), which is an economic index used to quantify the reliability of an investment. The NPV of a sequence of cash inflows/outflows is defined as the sum of every cash flow discounted back to its present value. In this case all future cash flows are incoming flows (the proceeds obtained from the selling of the produced energy). Conversely, the only outflow is assumed to occur at time zero, and it is represented by the construction cost of the plant, evaluated here by assuming that the plant could be completed during the first year and neglecting possible financings and the related interests. Hence, the NPV can be computed as:

$$NPV(Q) = R_n(Q) - C(Q) = \hat{r}\,R_1(Q) - \,a\,Q^b = \hat{r}\,e_p\,E_1(Q) - a\,Q^b \tag{2.19}$$

When designers can deal with observed streamflow data, the ergodicity of incoming streamflow can be relaxed and the above expression becomes:

$$NPV(Q) = R_{_n}(Q) - C(Q) = \sum_{k=1}^{n} \frac{1}{(1+r)^k}\,e_p\,E_k(Q) \;-\; a\,Q^b \tag{2.20}$$

In eq. (2.20), $E_k(Q)$ represents the amount of energy produced during the k-th year ($k = 1, ..., n$) and n represents the number of years for which the feed-in tariff e_p is guaranteed.

2.5 Plant capacity optimization

This section focuses on the derivation of mathematical expressions aimed at supporting designers in the choice of the plant capacity of run-of-river power plants. Based on the expressions derived in previous sections of this chapter, plant capacities can be identified that maximizes the energy production (energetic optimal plant capacity, Q_{EN}) or the profitability of the investment (economic optimal plant capacity, Q_{NPV}).
An energetic optimal plant capacity exists because of the presence of a minimum workable flow (i.e. the cut-off flow, $\alpha_0 Q$), which is introduced in practical applications to avoid processing low discharges inefficiently. Therefore, Q_{EN} is the capacity in correspondence of which the marginal increment of energy production due to increased capacity is balanced by the marginal loss of energy generated by the lowest flows, induced by the corresponding increase of the cut-off flow.
For the sake of simplicity, mathematical expressions of Q_{EN} and Q_{NPV} will be presented in the following only for the case of a plant equipped with a single turbine. Similar considerations however could be generalized to the case of n_T turbines, with an unavoidable increased complexity of mathematical expressions.
Main assumptions made up to this point are summarized below:

- the plant capacity Q (i.e. the maximum flow that the plant can process) is the only decision variable, thereby assuming the remaining design attributes of the plant to be known or derivable on the basis of the capacity;
- the distribution of flows at the plant intake provided by eqs. 2.3 and 2.4 is assumed to be ergodic (i.e. to be time invariant);
- a Minimum Flow Discharge withdrawal strategy governs water abstraction for hydropower purposes, therefore the method implicitly considers the release of a base flow (i.e. the MFD) downstream of the intake;
- feed-in tariffs for energy selling are considered to be constant during the lifetime of run-of-river hydropower plants.

The energy produced by a plant equipped with a single turbine is the combination of equations (2.13) and (2.14).

$$\begin{aligned} E(Q) &= \Delta T\, H\, \rho g\, \eta_P \left\{ \int_{\alpha_M Q}^{Q} \eta_M\, p(q_w + MFD)\, q_w\, dq_w + \right. \\ &+ \eta_M\, Q\, D(Q + MFD) + \\ &\left. + \int_{\alpha_0 Q}^{\alpha_M Q} \left[\frac{q_w - \alpha_0 Q}{\alpha_M Q - \alpha_0 Q} (\eta_M - \eta_0) + \eta_0 \right] p(q_w + MFD) q_w dq_w \right\} \end{aligned} \tag{2.21}$$

The value of Q which gives the best result in terms of produced energy can be obtained computing the derivative dE/dQ and setting it equal to zero. The value of Q satisfying the equation $dE/dQ = 0$ provides the optimal energetic plant capacity Q_{EN}.

$$\begin{aligned} \frac{dE}{dQ} &= \Delta T H \rho g \eta_P \left\{ \frac{d}{dQ} \left[\int_{\alpha_M Q}^{Q} \eta_M p(q_w + MFD) q_w dq_w \right] + \right. \\ &+ \frac{d}{dQ} \left[\eta_M Q D(Q + MFD) \right] + \\ &\left. + \frac{d}{dQ} \left[\int_{\alpha_0 Q}^{\alpha_M Q} \left(\frac{q_w - \alpha_0 Q}{\alpha_M Q - \alpha_0 Q} (\eta_M - \eta_0) + \eta_0 \right) p(q_w + MFD) q_w dq_w \right] \right\} \end{aligned} \tag{2.22}$$

Using the Leibniz integral rule to calculate the first and the last derivatives at the r.h.s. of equation (2.22), the following equation is obtained:

$$\begin{aligned} \frac{dE}{dQ} &= \Delta T H \rho g \eta_P \left\{ \eta_M Q p(Q + MFD) - \eta_M \alpha_M^2 Q p(\alpha_M Q + MFD) + \right. \\ &+ \eta_M D(Q + MFD) - \eta_M Q p(Q + MFD) + \\ &+ \frac{\eta_M - \eta_0}{\alpha_M - \alpha_0} \left[\alpha_M^3 Q p(\alpha_M Q + MFD) - \alpha_0^3 Q p(\alpha_0 Q + MFD) + \right. \\ &\left. - \int_{\alpha_0 Q}^{\alpha_M Q} \frac{1}{Q^2} q^2 p(q + MFD) dq \right] + \\ &- \frac{\eta_M - \eta_0}{\alpha_M - \alpha_0} \alpha_0 \left[\alpha_M^2 Q p(\alpha_M Q + MFD) - \alpha_0^2 Q p(\alpha_0 Q + MFD) \right] + \\ &\left. + \eta_0 \left[\alpha_M^2 Q p(\alpha_M Q + MFD) - \alpha_0^2 Q p(\alpha_0 Q + MFD) \right] \right\} \end{aligned} \tag{2.23}$$

Reducing the first and fourth terms inside the braces at the r.h.s. of the above equation, after grouping and reordering the other terms, equation (2.23) gives:

$$\begin{aligned} \frac{dE}{dQ} &= \Delta T H \rho g \eta_P \left\{ \eta_M D(Q + MFD) - \frac{\eta_M - \eta_0}{\alpha_M - \alpha_0} \int_{\alpha_0 Q}^{\alpha_M Q} \frac{q^2}{Q^2} p(q + MFD) dq + \right. \\ &+ p(\alpha_M Q + MFD) \alpha_M^2 Q \left(-\eta_M + \alpha_M \frac{\eta_M - \eta_0}{\alpha_M - \alpha_0} - \alpha_0 \frac{\eta_M - \eta_0}{\alpha_M - \alpha_0} + \eta_0 \right) + \\ &\left. + p(\alpha_0 Q + MFD) \alpha_0^2 Q \left(-\alpha_0 \frac{\eta_M - \eta_0}{\alpha_M - \alpha_0} + \alpha_0 \frac{\eta_M - \eta_0}{\alpha_M - \alpha_0} - \eta_0 Q \right) \right\} \end{aligned} \tag{2.24}$$

Finally, reducing the terms within the round brackets of the above equation and changing the integration variable of the integral, equation (2.24) becomes:

$$\begin{aligned}\frac{dE}{dQ} &= \Delta T\, H\, \rho g\, \eta_P \left[\eta_M\, D(Q+MFD) + \eta_0\, \alpha_0\, Q\, D'(\alpha_0 Q + MFD) + \right. \\ &\left. + \int_{\alpha_0}^{\alpha_M} \left(\frac{\eta_M - \eta_0}{\alpha_M - \alpha_0}\, x \right) Qx\, D'(Qx + MFD)\, dx \right] \end{aligned} \tag{2.25}$$

The condition providing the capacity which maximizes the produced energy, Q_{EN}, can be obtained by setting $dE/dQ = 0$ in equation (2.25). Therefore, Q_{EN} satisfies:

$$\begin{aligned} D(Q+MFD) &= -\frac{\eta_0}{\eta_M}\alpha_0 Q D'(\alpha_0 Q + MFD) + \\ &+ \int_{\alpha_0}^{\alpha_M} \left(\frac{1 - \eta_0/\eta_M}{\alpha_M - \alpha_0} \right) Qx^2 D'(Qx + MFD) dx \end{aligned} \tag{2.26}$$

The condition providing the capacity which maximizes the NPV, Q_{NPV}, can be obtained by calculating $dNPV(Q)/dQ$ through equations (2.16), (2.18) and (2.19), and setting it equal to zero. Q_{NPV} hence should satisfy:

$$\begin{aligned} &\left[\eta_M\, D(Q+MFD) + \eta_0\, \alpha_0 Q\, D'(\alpha_0 Q + MFD) \; + \right. \\ &\left. + \int_{\alpha_0}^{\alpha_M} \left(\frac{\eta_M - \eta_0}{\alpha_M - \alpha_0} \right) Qx^2\, D'(Qx + MFD)\, dx \right] \hat{r}\, e_p\, H\, \rho g\, \eta_P \;=\; a\, b\, Q^{b-1} \end{aligned} \tag{2.27}$$

The comparison of equations (2.26) and (2.27) shows that, as expected, $Q_{NPV} < Q_{EN}$ except when the costs of the plant are negligible.

2.6 Hydrologic disturbance between the intake and the outflow

Among the objectives of this thesis is the definition of tools aimed at informing and supporting a sustainable design of run-of-river power plants, accounting not only for the produced energy or the economic profitability, but also the minimization of the hydrologic disturbance.

In catchments belonging to mountain areas, the compliance of the MFD may not suffice to mitigate the hydrologic alteration produced by water diversion in the reach between the intake and the outflow of the plant. The hydrologic disturbance on the flow regime induced by a hydropower plant can be quantified by comparing the probability density

functions of the river flows upstream and downstream of the plant intake (Figure 2.5). The latter strongly depends on the rule by which the withdrawal is conducted and the plant operation.

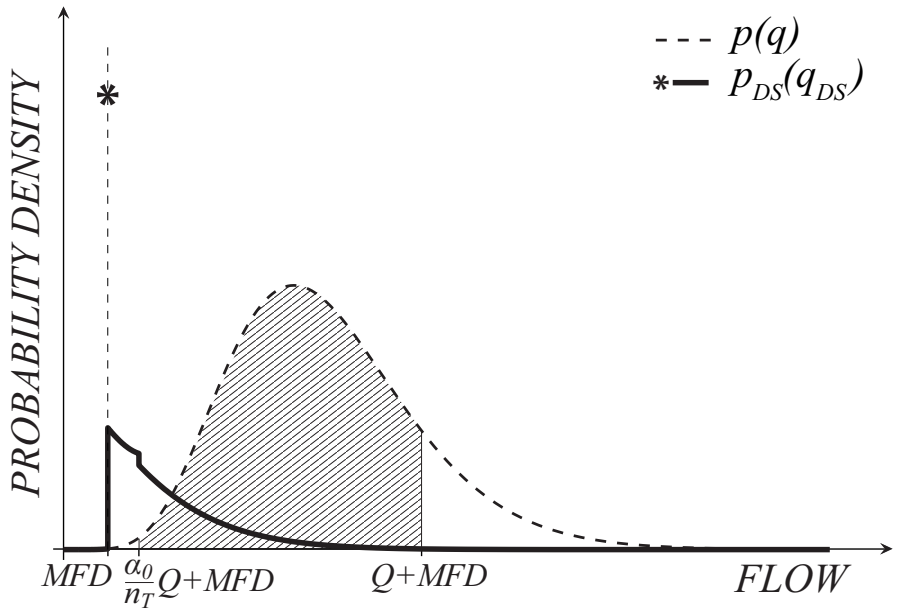

Figure 2.5: Probability distributions of streamflows ($p(q)$, dashed line), and pdf of flows between the intake and the outflow of the plant ($p_{ds}(q_{ds})$, solid line and stars) equipped with a multiple turbines and coping with Minimum Flow Discharge requirements.

If a plant equipped with n_T turbines is managed coping with a *MFD* withdrawal rule, the downstream flow pdf ($p_{DS}(q_{DS})$) is made up of four different parts. When the incoming flows are smaller than $\frac{\alpha_0}{n_T}Q + MFD$, the plant is not working and the incoming flows are entirely left to the river ($q_{DS} = q$, see eq. 2.10). In this range, the downstream flow pdf thus resembles the incoming flow pdf. When the incoming flows are larger than Q+*MFD*, only a flow equal to the maximum capacity Q can be processed and the exceedance is released to the river ($q_{DS} = q - Q$). The range of flows $MFD < q_{DS} < \frac{\alpha_0}{n_T}Q + MFD$ originates from both these different operational conditions, and hence the downstream flow pdf is the sum of the two corresponding contributes. Finally, when the incoming flows are comprised between $\frac{\alpha_0}{n_T}Q + MFD$ and $Q + MFD$, the plant is processing flows smaller than the plant capacity, thereby originating an atom of probability in $q_{DS} = MFD$.

In conclusion, when a *MFD* withdrawal strategy is used, the downstream flow pdf is:

$$p_{DS}(q_{DS}) = \begin{cases} p(q_{DS}) & \text{if } q_{DS} < MFD \\ p(q_{DS}) + p(q_{DS}+Q) & \text{if } MFD < q_{DS} \leq \frac{\alpha_0}{n_T}Q + MFD \\ p(q_{DS}+Q) & \text{if } q_{DS} > \frac{\alpha_0}{n_T}Q + MFD \end{cases} \tag{2.28}$$

plus a finite probability for $q_{DS} = MFD$, which is equal to $[D(\frac{\alpha_0}{n_T}Q + MFD) - D(Q + MFD)]$.

The strong hydrologic disturbance is evident when comparing the probability density functions upstream (natural) and downstream (altered) of the plant intake. Flows maintained in the river downstream of the plant intake are clearly lower on average, due to the removal of a significant fraction of incoming streamflows for energy production, but also show an increased variability. In fact, the flow pdf observed in the altered river reach is characterized by a finite probability concentrated in $q_{DS} = MFD$ and by the translated tail of the original streamflow distribution, representing incoming flows large enough to saturate the plant capacity. However, focusing only on the upstream/downstream modification of the streamflow pdf might not be sufficient to obtain a complete description of the alteration of the flow regime. More specific information on ecologically-relevant features of the flow regime like the temporal auto-correlation of river flows and their inter-annual variability should be included in the analysis.

A standard choice to quantify the regime alteration that occurs between the intake and the outflow of a run-of-river plant could be through the assessment of the upstream/-downstream changes of the following seasonal flow statistics [Richter et al., 1996; Tealdi et al., 2011; Destouni et al., 2013; Lazzaro et al., 2013]: i) the mean flow (μ); ii) the coefficient of variation of daily flows (CV); iii) the correlation scale of streamflows (I); and iv) the Regime Instability (RI) as defined by Botter et al. [2013].

The selected flow statistics are meaningful indicators of the hydrologic alteration induced by the plant, and summarize a variety of diverse physical and hydrologic features of the river flow regime, as discussed below.

The mean flow mainly depends on long-term climate conditions like seasonal rainfall amounts and potential evapotranspiration [Budyko, 1974].

The coefficient of variation of daily flows expresses the interaction between the stochasticity of rainfall (suitably filtered by vegetation) and the timescale of the hydrologic response [Botter et al., 2007].

The correlation of streamflows is the integral of the temporal autocorrelation function of

river flows ($I = \int_0^\infty \rho(\tau) d\tau$, with τ expressing the time lag), and mainly depends on recession attributes [Botter et al., 2010; Muneepeerakul et al., 2010], which in turn express key morphologic and hydrogeologic properties of the contributing catchment [Biswal and Marani, 2010; Harman et al., 2009].

The Regime Instability is half the mean of the integral of the difference (in modulus) between the seasonal streamflow probability density functions (pdfs) pertaining to consecutive years [Botter et al., 2013]:

$$RI = \frac{0.5}{n-1} \sum_{i=1}^{n-1} \int_0^\infty |p_i(Q) - p_{i+1}(Q)| \, dQ \ , \tag{2.29}$$

where $p_i(Q)$ is the seasonal streamflow pdf during the year i and n represents the number of years for which incentives are available. If $RI = 0$, the seasonal streamflow pdfs during different years are completely overlapping (high long-term predictability). Conversely, RI approaches unity when the streamflow pdfs in different years are completely disjointed (enhanced long-term variability). The Regime Instability encapsulates the inter-annual changes of rainfall and hydrologic features, which is mainly a byproduct of the hydroclimatic fluctuations involved in the water cycle [Botter et al., 2013; Reynolds et al., 2015].

Furthermore, each of these flow attributes controls different types of ecosystem services. The mean flow quantifies the average water availability (magnitude) in the river, a feature that is typically related to the stream ecosystem size [Sabo et al., 2009; Postel and Richter, 2003] and determines the touristic and anthropogenic exploitability of the reaches downstream of the intake. The coefficient of variation of daily flows quantifies the intra-seasonal flow variability and provides information about the frequency and duration of high and low flows (i.e., floods and droughts). A wide range of ecological and biological processes is known to be influenced by the flow variability, like macroinvertebrate grazing rates [Ceola et al., 2013], food chain length [Sabo et al., 2010], riparian vegetation dynamics [Doulatyari et al., 2014] and exchanges between the river and the floodplain [Tockner et al., 2010]. The correlation of streamflows is a measure of the short-term rate of change of streamflows, and hence is crucial for fish movement and for triggering behavioral responses of stream biomes. High values of I determine an increased probability to observe similar water stages for prolonged periods, and thus facilitate the completion of critical life-cycle stages like reproduction [Poff and Ward, 1989; Lytle and Poff, 2004]. The Regime Instability quantifies the inter-annual flow vari-

ability which is deemed to be a key determinant of river biodiversity, because critical life-stages in fishes (spawning, egg hatching, migrations) are often triggered by specific seasonal patterns of hydrologic conditions [Poff et al., 1997; Lytle and Poff, 2004]. The inter-annual variability of flow regimes may also contribute to define the frequency of flood events, that are able to revitalize or reset stream ecosystems [Ledger et al., 2013]. The seasonal values of the four hydrologic indexes described above are calculated upstream and downstream (DS) of the intake, averaged among the seasons and then combined to obtain the following dimensionless indexes of hydrologic alteration:

$$\begin{aligned}
\Delta\mu(Q) &= \frac{|\mu - \mu_{DS}(Q)|}{\mu} \\
\Delta CV(Q) &= \frac{|CV - CV_{DS}(Q)|}{CV} \\
\Delta I(Q) &= \frac{|I - I_{DS}(Q)|}{I} \\
\Delta RI(Q) &= \frac{|RI - RI_{DS}(Q)|}{RI}
\end{aligned} \tag{2.30}$$

The four indexes in eq. (2.30) quantify the relative change in the flow statistics produced by the plant in the reach between the intake and the outflow. These indexes are all downward bounded by zero (absence of disturbance) and they only depend on the plant capacity, which is the only variable of the optimization. The use of the modulus in eq. (2.30) is based on the assumption that the effect of a unit decrease of each index is equivalent to that produced by a unit increase of the same index. The tenet is that any anthropogenic change in the flow regime with respect to natural conditions brings detrimental effects on aquatic ecosystems, regardless of the nature of the change (increase/decrease) [Lytle and Poff, 2004].

Note that the four hydrologic indexes considered in this work respond in a quite heterogeneous manner to flow diversions of the type produced by run-of-river plants, which implies that the degree of disturbance of different indicators shows independent patterns with the plant capacity.

A single hydrologic disturbance index, $D_H(Q)$, was defined to represent the overall degree of alteration of flow regimes. D_H was defined as a function of the plant capacity Q combining the four alteration indexes in eq. (2.30). First, it was assumed that all the flow statistics in eq. (2.30) equally contribute to the overall hydrologic alteration, which can be thus calculated as the average of the disturbances induced by the plant

on the mean discharge, the coefficient of variation, the correlation scale and the regime instability:

$$D_H(Q) \quad = \quad [\Delta\mu(Q) + \Delta CV(Q) + \Delta I(Q) + \Delta RI(Q)] \ / \ 4 \tag{2.31}$$

Eq. (2.31) assumes a linear link between hydrologic drivers and environmental drawbacks, which is a standard procedure in analysis of hydrologic alteration, where different classes of attributes are separately evaluated and then averaged [Richter et al., 1996]. However, one may wonder if the flow statistics considered in eq. (2.30) are actually equally influential in terms of ecosystem services, and which is the most appropriate combination of weights that properly accounts for the actual ecological and environmental significance of the different flow metrics in a given case study. The issue could be tackled by listing the various ecosystem services supplied by the stream (including provisioning, supporting, regulating and cultural services), and then analysing the impact of each flow metric on the ecosystem services involved. However, predicting the response of a given ecosystem service to changes in hydraulic and hydrologic features of the stream is a challenging task, because of the multi-dimensionality of the problem and the number of information required to predict the hydro-chemical, morphological and ecologic response of rivers to altered flow conditions [Bombino et al., 2009; Comiti et al., 2011; Bombino et al., 2014]. The problem is further complicated by the inherent difficulty in commensurating different types of ecosystem services, and by the presence of compensating effects (e.g. an increase in the flow variability may enhance the exchange of nutrients with riparian and hyporeic regions, thereby compensating detrimental effects on water quality induced by reduced streamflows). Thus, one may wonder if the huge effort required to complete this type of analysis is worthwhile (or just feasible) for practical applications.

Here, the problem is tackled from a different perspective, by suitably randomizing the weights assigned to each statistic. The procedure is designed to circumvent a detailed evaluation of the effects of the flow statistics on the relevant ecosystem services, and enables a preliminary identification of cases where additional analysis are recommended - because the choice of the weights might have a critical impact on the results. Accordingly, the hydrologic disturbance index, $D_H(Q)$, can be modified by weighting the contributions of the different flow metrics through random weights $\gamma_i = w_i / \sum w_i$, where

w_i ($i \in [1,4]$) are independent random numbers uniformly distributed in the range [0,1]:

$$D_H(Q) = \gamma_1 \Delta\mu(Q) + \gamma_2 \Delta CV(Q) + \gamma_3 \Delta I(Q) + \gamma_4 \Delta RI(Q) \tag{2.32}$$

In the proposed framework, the hydrologic disturbance in the river reach between the intake and the outflow is thus assessed for any possible combination of weights.
Needless to say. other types of ecologically meaningful hydrologic metrics can be identified in contexts where the focus of the analysis is on a limited number of ecological processes that are directly influenced by specific features of the flow regime.

2.7 Multi-objective optimization

In previous sections of this chapter, a set of tools for energetic and economic evaluations of run-of-river power plants has been introduced together with a method enabling the assessment of the hydrologic disturbance induce by these plants in the river reach between the intake and the outflow. A further step can be made by coupling those methodologies aiming at creating a new tool for the preliminary design of economically and ecologically feasible run-of-river power plants.
Incommensurable goals such as the maximization of the economic profitability (or the energy produced) and the minimization of the hydrologic disturbance can be simultaneously addressed through a multi-objective optimization. Optimization techniques for multi-objective problems can exploit the concept of Paretian efficiency. The Paretian efficiency is a tool that is used to identify optimal allocation strategies in presence of multiple conflicting objectives [Loucks et al., 2005].
Given a set of ν conflicting goals and m alternative solutions of a problem, a ν-dimensional vector ($\boldsymbol{f}$) that represents the overall objective function is evaluated for each alternative. Each element of $\boldsymbol{f}$ represents the degree of fulfillment of any objective guaranteed by the considered solution. Frequently, a null value for the k-th component of the objective function ($f_k = 0$) implies that the k-th objective is fully achieved. The optimization is typically performed through the minimization of the euclidean norm of the vector $\boldsymbol{f}$ (Figure 2.6) [Lu et al., 2011; Rye et al., 2012; Pargett et al., 2014], even though alternative definitions of optimality (e.g. the maximization of the curvature) are available in the literature [Castelletti et al., 2010].

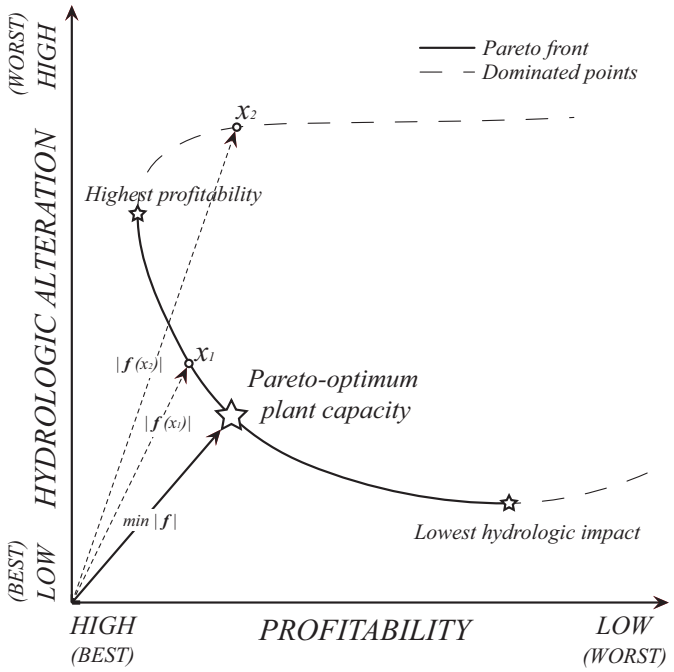

Figure 2.6: Example of Pareto front resulting from a multi-objective optimization problem. The considered conflicting objectives are the economic value of the run-of-river hydropower plant (x-axis) and the hydrologic alteration on the river reach between the intake and the outflow (y-axis). The Pareto-optimal capacity is that minimizing the distance from the origin (where the incommensurable objectives would be simultaneously fulfilled).

Paretian efficiency can be used not only to identify the best allocation of the available resources but also to produce a set of dominant solutions (Pareto front) to guide and constrain the choice of decision makers. An allocation is considered to be Pareto-dominant whenever it doesn't exist any other allocation that simultaneously improves all the conflicting goals, implying that the degree of satisfaction for a single objective can be improved only at the expense of other goals. The definition of the Pareto front in complex multi-objective optimization problems may require complex numeric techniques, such as metaheuristic algorithms that incorporate elements of structured randomness for search and follow empirical guidelines [Reed et al., 2013].

The unknown decision variable in this case is represented by the capacity Q of a run-of-river power plant whose definition is made dependent on the simultaneous fulfilment of the following contrasting objectives: i) the maximization of the economic profitability

of the investment; and ii) the minimization of the disturbance of the flow regime in the river reach between the intake and the outflow. These are contrasting goals because the maximization of the earnings requires significant water abstractions from the river that strongly impact the hydrologic regime.

The objective function that expresses the profitability of run-of-river plants and the associated degree of hydrologic alteration can be defined as a function of the plant capacity Q as follows.

Provided that the economic value of the plant is measured by its NPV (Section 2.4), the economic component of the objective function, $f_1(Q)$, is defined as:

$$f_1(Q) = \frac{NPV_{max} - NPV(Q)}{NPV_{max} - NPV_{min}} \tag{2.33}$$

where NPV_{max} and NPV_{min} are the maximum and minimum economic values of the run-of-river plant. Owing to the normalization introduced in eq. (2.33) [Marler and Arora, 2004; Wang et al., 2009; Stanimirovic et al., 2011], f_1 ranges between 0, which represents the maximum profitability ($NPV = NPV_{max}$), and 1 ($NPV = NPV_{min}$). This procedure corresponds to using the maximum potential NPV as a reference value to evaluate the marginal impact of suitable decrease (or increase) on the profitability of the project.

Regardless of the choice of the hydrologic disturbance index (eq. (2.31) or eq. (2.32)), the objective function expressing the hydrologic alteration (f_2) can be then defined as:

$$f_2(Q) = \frac{D_H(Q) - D_{H,min}}{D_{H,max} - D_{H,min}} \tag{2.34}$$

where $D_{H,min}$ and $D_{H,max}$ are the minimum and maximum values of $D_H(Q)$. In analogy with eq. (2.33), when the hydrologic alteration is minimum, $f_2 = 0$, while f_2 tends to unity when the hydrologic alteration approaches its maximum possible value.

In the analysis, the plant capacity Q has been varied from 0 up to a maximum plant capacity, Q_{max}, whose duration is 0.01. The values of NPV and D_H are calculated for each value of Q using eq. (2.20) and eq. (2.31) (or eq. (2.32)). Then, the minimum and maximum values of NPV and D_H are calculated for $Q \in [0, Q_{max}]$, and f_1, f_2 are computed via eqs. (2.33) and (2.34).

In the case at hand, the numerical analysis of $\boldsymbol{f}(Q)$ is particularly simple and does not require the use of sophisticated stochastic algorithms due to the limited number of objectives, which can be readily calculated as a function of the plant capacity (single

decision variable). In particular, f_1 and f_2 are found to be continuous and smoothed functions of Q, thereby allowing the capacity to be treated as a discrete variable with a suitable spacing.

Chapter 3

Energetic and economic optimization

The analytical tools for the energetic and economic optimization of the plant capacity introduced in Sections 2.3, 2.4 and 2.5 are here applied to three case studies located in the Piave river basin (north-east of Italy, see Figure 1.4). Selected case studies belong to a set of existing, proposed or under-construction plants that underwent Environmental Impact Assessment and for which design documents are available on-line (http://bur.regione.veneto.it/). The assessment of the hydrologic regime at the plant intake, and the consequent choice of the economic optimal plant capacity made by designers in these real case studies are thus available. The methodology outlined in Section 2.5 has been applied to the considered case studies to obtain optimal plant capacities maximizing the energy produced (Q_{EN}, eq. 2.26) and the Net Present Value (Q_{NPV}, eq. 2.27) aiming at comparing choices made by designers with the application of the methodology outlined in Sections 2.3, 2.4 and 2.5.

3.1 Study area and data

Three run-of-river power plants located in the Piave river basin (north-east of Italy) are considered in this application. Creeks from which processed water is withdrawn give the name to the plants: namely, the Valfredda plant, the Piova plant and the Ru delle Rosse plant.

The Valfredda plant is going to be built in the Valfredda Creek, a small tributary of the

Biois Creek, belonging to the Cordevole River catchment (one of the major tributary of the Piave River). Catchment area upstream of the plant is about $4\,km^2$ and the hydraulic head between the intake ($1753\,m\,a.s.l.$) and the turbine ($1549\,m\,a.s.l.$) is about $204\,m$.

The Piova plant withdraws water from the Piova Creek, a small tributary of the Piave River flowing in the heart of the Dolomites. Catchment area is equal to $30\,km^2$ and the hydraulic head is about $52\,m$, being the intake at $742\,m\,a.s.l.$ and the turbine at $690\,m\,a.s.l.$.

The Ru Delle Rosse plant exploits streamflows of a small tributary of the Cordevole Creek named Ru Delle Rosse. Catchment area at the plant intake is about $3\,km^2$ and the hydraulic head between the intake ($1450\,m\,a.s.l.$) and the turbine ($1160\,m\,a.s.l.$) is equal to $290\,m$.

The main technical and economic characteristics of these plants are reported in Table 3.1, jointly with the major features of the corresponding contributing catchments. The average length of the reaches impacted by plant in the selected case studies is about $1\,km$.

Flow regime at the intake of each plant is described through the flow duration curve ($D(q)$) provided by the plant designers and available in the correspondent technical report. Parameters λ/k and $\alpha\,k$ in eq. (2.4) have thus been defined to match the empirical duration curve used by designers for choosing project plant capacities ($Q_{PROJECT}$). Estimates of $D(q)$ by plant designers have been performed exploiting empirical methods, provided that streamflow measurements at the sites of interest are completely lacking, as frequently happens in small headwater catchments. A critical analysis of the procedure used by the designers to determine the hydrologic regime is avoided here, since the focus of this work is not on the estimate of $D(q)$ in ungauged sites.

Information about turbines and related efficiency curves needs to be provided to the model to assess energetic and economic optimal plant capacities. Same turbine number and type as in technical reports were considered. Every case study considerd in this application is equipped with a single turbine but, as expected, turbine type is different depending on the characteristics of each plant. Pelton turbines have been chosen in the two cases characterized by hydraulic head larger than $100\,m$ (Valfredda and Ru Delle Rosse power plants). In the Piova power plant, instead, a Francis turbine has been installed because of the smaller hydraulic head (about $50\,m$). Table 3.1 reports the pa-

rameters of the piecewise linear functions approximating the efficiency curves of Pelton and Francis turbines.

Run-of-river plants can benefit from government incentives on green energy production. The energy selling price e_p and the duration of incentives n which are the same for each case study. In particular, $e_p = 0.22$ €/kWh and $n = 15$ years, according with the Italian law on small hydropower.

Last information required to compute the economic optimal capacity relates to the plant costs. While the value of b in equation (2.18) has been assumed constant and equal to 0.6, the parameter a has been calculated for each case study based on the overall construction costs of the plant ($C_{PROJECT}$) and the related proposed capacity ($Q_{PROJECT}$) as shown in the technical report of each plant.

$$a = \frac{C(Q_{PROJECT})}{Q_{PROJECT}^{0.6}} = \frac{C_{PROJECT}}{Q_{PROJECT}^{0.6}} \tag{3.1}$$

Table 3.1 summarizes all input data for each case study considered in this application of the proposed methodology for the energetic and economic optimization of the plant capacity. All discharges are considered per unit area (specific discharges):

$$[cm/d] = [m^3/s] \cdot \frac{60 \cdot 60 \cdot 24}{A\,[km^2]} \tag{3.2}$$

Unit transformation introduced by eq. (3.2) makes easier the comparison between case studies characterized by different contributing catchments.

3.2 Results and Discussion

Natural flow regimes at the plant intake, as defined on the basis of flow duration curve estimated by plant designer, are persistent in the Valfredda and Piova creeks. Parameter λ/k is larger than 1 in those streams, thereby implying that daily streamflow variability is reduced ($CV < 1$, see Section 2.1). Conversely, $\lambda/k = 0.3$ characterizes the erratic streamflow regime at the intake of the Ru delle Rosse plant whose daily discharges are highly variable and continuously range between strong drought and flood conditions. Specific mean flow is lower in the erratic (0.16 cm/d) than in persistent (0.23-0.26 cm/d) case studies. The difference in terms of streamflow regime is evident in Figure 3.1: flow duration curves have a different shape and, in particular, discharges characterized by duration larger than 0.5 are very close to 0 in the erratic case study (Figure 3.1c, Ru

	Valfredda	Piova	Ru delle Rosse
Hydrological features			
Catchment area [km^2]	4	30	3
Minimum Flow Discharge [cm/d]	0.052	0.047	0.041
Mean discharge [cm/d]	0.23	0.26	0.16
$\alpha\, k$ [cm/d]	0.077	0.034	0.563
λ/k [-]	3.0	8.0	0.3
Hydropower plant			
Intake height [m a.s.l.]	1753	742	1450
Outflow height [m a.s.l.]	1549	690	1160
Hydraulic head [m]	204	52	290
Impacted length [km]	1.3	1.1	0.8
Turbine type	Pelton	Francis	Pelton
α_0	0.10	0.10	0.10
α_M	0.30	0.50	0.30
η_0	0.75	0.46	0.75
η_M	0.89	0.86	0.89
Cost function			
$Q_{PROJECT}$ $[cm/d]$	0.31	0.33	1.02
$C(Q_{PROJECT})$ [M€]	1.0	1.5	1.2
a [M€/$(\frac{cm}{d})^b$]	2.00	2.90	1.19

Table 3.1: Technical and economic characteristics of the considered run-of-river power plants and hydrological features of the contributing catchments. All discharges are considered per unit area (specific discharges).

delle Rosse). In persistent regimes instead durations close to 1 (base flow which is always exceeded) are usually associated with finite discharges, around 0.05/0.1 cm/d in Figure 3.1a and Figure 3.1b.

Different shapes of the flow duration curve in the selected case studies determined different optimizations of the plant capacity. Results are graphically presented in Figure 3.1 and detailed in Table 3.2. In particular, economic optimal capacities, Q_{NPV}, obtained through the analytical method under the actual MFD prescription are relatively close to the project design flows $Q_{PROJECT}$, except that for the Ru delle Rosse power plant (Figure 3.1c), where the capacity suggested by the designers is much higher than the analytical estimate. This choice is not motivated in the technical reports available, but probably it can be explained by the need of increasing the plant capacity to deal with the enhanced variability of flows. However, the size of the Ru delle Rosse plant was exaggerated and closer to the maximization of the energy produced.

The duration of economic optimal capacity is strongly dependent on the incoming streamflow regime. As shown in Figure 3.1, the duration of Q_{NPV} is 0.20 and 0.27 in the persistent case studies (respectively, in the Valfredda and Piova creeks), while a larger plant capacity is suggested by the model when incoming daily streamflows are highly variable, such as in the erratic case study analysed (Figure 3.1c). In the latter, Q_{NPV} has a duration of 0.07 resulting in a economic optimal plant capacity that, in terms of specific discharge, is almost double ($Q_{NPV} = 0.62$ cm/d) than in persistent case studies ($Q_{NPV} = 0.33$ cm/d). The choice of a relatively higher capacity in erratic than in persistent flow regimes, confirmed by technical reports of real-case applications, implies that in the former cases it is more convenient to activate the plant less frequently and thus process less probable but larger streamflows (those located in the tail of the flow distribution). Model simulation of economic plant optimization determined a Net Present Value for the investors which is, respectively, 1.67, 4.84 and 0.88 M€. The Piova power plant produces very high proceeds, mainly thanks to the higher catchment contributing at the plant intake.

The energetic optimization individuates plant capacities which are higher than the correspondent economic optima. Indeed, when energy production is maximized, plant construction costs are not included in the model and thus $E(Q)$ peaks in correspondence of discharges which are higher than those determining peaks of $NPV(Q)$. In Figure 3.1 and Table 3.2, there are no particular relationships between values suggested for Q_{EN},

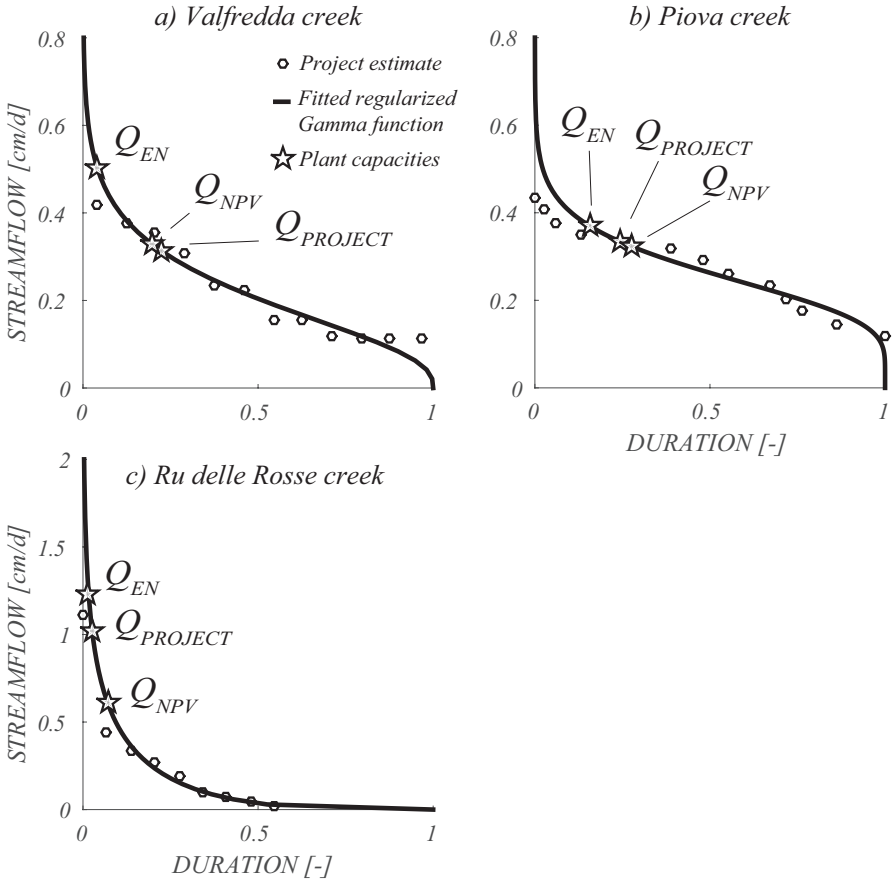

Figure 3.1: Flow duration curves of the Valfredda, Piova and Ru delle Rosse creeks assumed by designers (circles) and fitted (solid lines). Energetic (Q_{EN}) and economic (Q_{NPV}) optimal capacities compared against design flows ($Q_{PROJECT}$) (stars). All discharges are considered per unit area (specific discharges).

	Valfredda	Piova	Ru Delle Rosse
MFD [cm/d]	0.052	0.047	0.041
Q_{EN} [cm/d]	0.50	0.37	1.24
E [GWh]	17.9	40.5	12.5
Q_{NPV} [cm/d]	0.33	0.33	0.62
NPV [M€]	1.67	4.84	0.88
$Q_{PROJECT}$ [cm/d]	0.31	0.33	1.02

Table 3.2: Comparison between the plant capacities $Q_{PROJECT}$ chosen by the designers and those resulting from the maximization of the NPV (Q_{NPV}) or the energy produced Q_{EN}. All discharges are considered per unit area (specific discharges).

or for its relative duration, and incoming streamflow regimes. Mean annual energy production ranges between 0.8 GWh (Ru delle Rosse) and 2.7 GWh (Piova). As expected, the Piova power plant is again the one producing more energy.

The potential of the proposed method as a flexible and simple design tool for practical application emerges in this chapter. In particular, the duration of economic optimal capacity is found to be strongly dependent on the incoming streamflow regime, evidencing the role played by flow variability in the design of run-of-river power plants. Water resources availability at the plant intake needs to be carefully investigated when planning hydropower plants, especially in mountain remote areas where different flow regimes might occur depending on climatic and landscape information.
Proposed tools aim at supporting the preliminary design of capacities of run-of-river plants based solely on soft data (i.e. topographic and climatic data).

Chapter 4

Multi-objective optimization of the plant capacity: profitability and hydrologic disturbance

This chapter illustrates the application of a multi-objective optimization in the design of the capacity of run-of-river plants to identify optimal trade-offs between two contrasting objectives: the maximization of the profitability and the minimization of the hydrologic disturbance between the intake and the outflow. The latter is evaluated considering different flow metrics: mean discharge, temporal autocorrelation, and streamflow variability.

The Net Present Value and the dimensionless indexes of hydrologic alteration are calculated as a function of the plant capacity Q by means of eq. (2.20) and eq. (2.30), which are based on the availability of long-term flow measurements. In contrast with what has been done in the previous application, the assessment of water availability at plant intakes by means of the identification of streamflow distributions (or, alternatively, flow duration curves) has not been performed. Case studies for this application were indeed chosen based on the availability of flow measurements in the same stream, or in similar nearby catchments.

Results of the multi-criteria optimization of the plant capacity are presented for two case

studies located in the Alps and featured by contrasting flow regimes and show that the optimal design capacity is strongly affected by the flow regime at the plant intake. Implications in terms of policy actions are also discussed at the end of this chapter.

4.1 Study area and data

The application presented in this chapter has been performed selecting two case studies featured by contrasting flow regimes in correspondence of two run-of-river plants recently proposed along the major tributaries of the Piave river: the Boite and the Cordevole rivers. Given the key role of the Piave river and its ecosystem in supporting the tourism of the Veneto region, the selected case studies can be considered noteworthy examples of the need for reconciling hydropower exploitation and riverine ecosystem protection. The Boite river is the second major tributary of the Piave river with a total length of 45 km and a catchment area exceeding 400 km^2 (orange outlined area in Figure 4.1a). The Boite flows across an area which heavily relies on tourism and includes outstanding places like Cortina d'Ampezzo (the 'Pearl of Dolomites'). Although the critical role of landscape and environment for attracting tourists and enhancing local and regional economy, the Boite is impacted by the presence of 8 run-of-river plants along its main course (white points and dotted lines in Figure 4.1). Moreover, a reservoir with a capacity of about one million of cubic meters was built in the 60s a few kilometers upstream of the confluence with the Piave river (white diamond in Figure 4.1) . The case study considered in this analysis is an hydropower plant under construction along the course of the Boite river, whose intake is located two kilometers downstream of Cortina d'Ampezzo (drainage area = 220 km^2, blue region in Figure 4.1a). In this case, diverted flows will be returned back to the river 12 km downstream of the intake. The intake and the outflow are indicated as red dots in Figure 4.1a. Technical information available indicates a proposed plant capacity of 13.5 m^3/s and an hydraulic head of 240 m leading to 13 MW of mean annual electrical power produced by means of two Francis turbines. Although having a nominal power larger than 1 MW, this plant can still be considered a run-of-river plant since it processes water with a limited storage upstream of the weir. Regulation capacity is thus prevented even in this case. The minimum flow discharge in the Boite river is prescribed by the Water Authority as 0.6 m^3/s in winter and summer and 0.8 m^3/s in spring and fall. All these data are freely accessible through the website of the Water Resources division of the Regional Agency (http://www.regione.veneto.it).

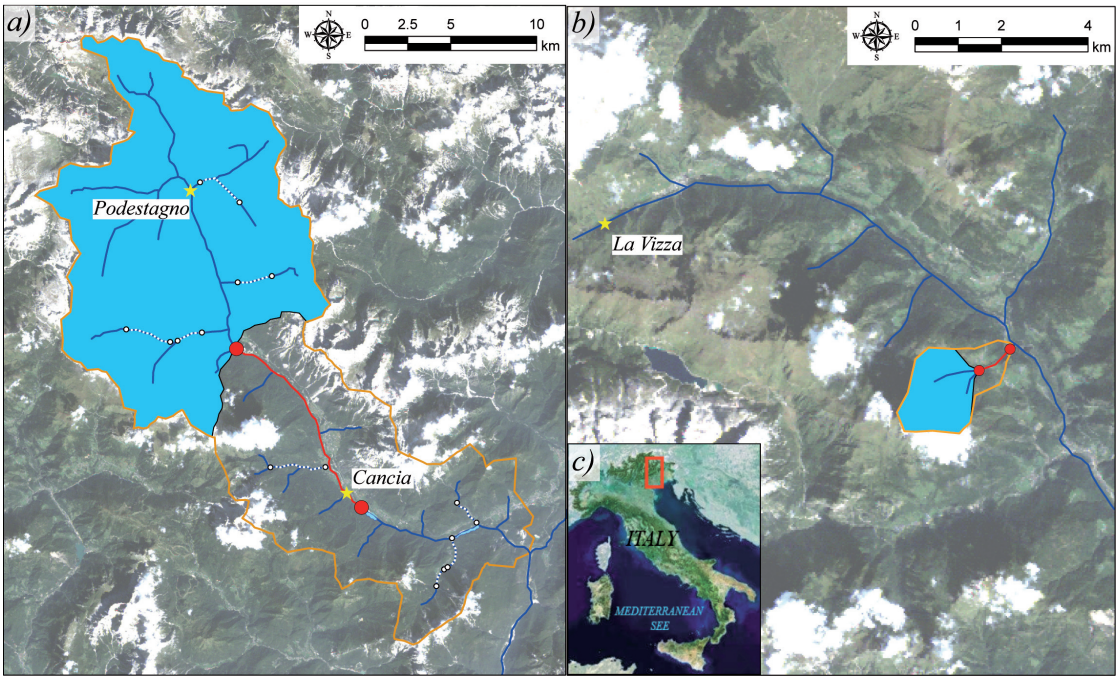

Figure 4.1: Location of the case studies considered in this chapter: (a) Boite river and (b) Ru delle Rosse creek. The map highlights the altered reaches (red lines) between the intakes and the outflows (red dots), and the contributing catchment of each plant (blue regions). White dots and dashed lines in (a) individuate other plants already built in the Boite river basin. The figures also show the location of the gauging stations (yellow stars) available nearby the plant intakes. Panel c shows the location of the Piave river in Italy.

Long-term daily streamflow data are required to quantify the Net Present Value and the alteration induced by the plant between the intake and the outflow. Streamflow measurements are available along the Boite river in two gauging stations: Podestagno (82 km^2, 1992-2008) and Cancia (313 km^2, 1986-2008) (Figure 4.1a). Both these data sets could be potentially used to estimate the flow regime at the plant intake, which is located in between these gauging stations. However, only the daily records available at Cancia were used because of the longer period of record and the reduced distance from the intake. Discharge data observed at Cancia were multiplied by a scaling factor represented by the ratio between the catchment area at the intake and the contributing area in correspondence of the gauging station (0.70). The flow regime of the Boite river is featured by a weak variability of daily flows around the mean and it can be classified as persistent.

A second case study has been identified in the Ru Delle Rosse creek, a small stream which belongs to the catchment of the Cordevole river. The plant, as introduced in Section 3.1, is featured by a contributing area at the intake of about 3 km^2, a capacity of 0.35 m^3/s and it should produce a mean annual power of about 120 kW exploiting an hydraulic head of 290 m.

The absence of streamflow measurements in the considered catchment requires to assess the Net Present Value of the plant and the hydrologic alteration by means of streamflow records gathered in a nearby cross-section, properly scaled with the contributing area. The streamflow series considered is the daily record available at La Vizza (1985-2007), a gauging station located along the Cordevole river, about 10 km upstream of the confluence with Ru Delle Rosse creek, in a nearby valley featured by similar climatic conditions and with analogous size (8 km^2). The use of flows measured in a nearby station is a reasonable assumption owing to the uniformity of climate, rainfall and soil use/type along single tributaries of the Piave river (see Botter et al. [2010]).

All the streamflow data used in this application were gathered and provided by the Regional Environmental Agency (ARPAV) using ultrasound hydrometers and by means of a stage-discharge relation, which is continuously updated. Missing data were less than 1 % (Boite river) and 3 % (Ru delle Rosse creek), and were not considered in the analysis because of the negligible impact on the results of the optimization.

The plants considered in this application will take advantage of the following incentives: $e_P = 0.12$ €/kWh for 30 years for the plant along the Boite river; and $e_P = 0.22$ €/kWh

for 15 years for the plant along the Ru delle Rosse creek. Feed-in energy tariff and duration of state incentives are different in the Boite river case study, because the plant has a nominal power larger than 1 MW, therefore it benefits a reduced energy selling price but guaranteed for a prolonged time periods, according with the actual legislation.
Provided that streamflow measurements at the gauging station of Cancia are available only for 23 years, the available measurements have been artificially extended by adding the first 7 years of streamflow data at the end of the measurement period. Alternative procedures (like replacing the first 7 years with the last 7 of the record) provide analogous results.
Information about the plant costs was gathered based on preliminary projects using the same procedure outlined in Section 3.1. The corresponding parameters of the cost function are summarized in Table 4.1, jointly with the major features of the plants.

4.2 Results and Discussion

Figure 4.2 shows the behaviour of all economic (NPV) and hydrologic (μ, CV, I, RI) indexes for both the case studies as a function of the plant capacity Q. To facilitate the comparison between the two plants, the horizontal axes have been normalized by the corresponding plant capacities that maximize the NPV (Q_{NPV}). The two plots on the top illustrate how the NPV changes with the plant capacity Q. For small values of Q, the NPV is very low (or even slightly negative) because the amount of flow processed by the plant yields earnings comparable with the construction costs. The maximum profitability is obtained for $Q = 7.5$ m^3/s (NPV = 67 M €) in the Boite river and $Q = 0.23$ m^3/s (NPV = 1.1 M€) in the Ru Delle Rosse creek. The duration of Q_{NPV} in the two cases is 0.25 and 0.07 respectively, reinforcing the critical role played by flow regimes in the definition of the optimal duration of plant capacity as found in Section 3.2. In agreement with analyses performed in the previous chapter, the duration of the economically optimal capacity is smaller when the flow variability is enhanced. Simulated economic performances of the Ru delle Rosse plant is slightly higher compared to the economic optimization performed in Section 3.2 because of the different approach followed to determine water resources availability at the plant intake (fit of the designer flow duration curve vs scaled discharges from a similar nearby catchment).
Figure 4.2c-l shows how the flow statistics mentioned in Section 2.6 change in between the intake and the outflow as a function of the plant capacity. The assessment of hy-

	Boite	Ru delle Rosse
Hydrological features		
Catchment area [km^2]	220	3
Minimum Flow Discharge [m^3/s]		
- winter and summer	0.6	0.014
- spring and fall	0.8	0.014
Mean discharge [m^3/s]	6	0.1
Hydropower plant		
Intake height [m a.s.l.]	1107	1450
Outflow height [m a.s.l.]	867	1160
Hydraulic head [m]	240	290
Impacted length [km]	12.1	0.8
Plant capacity [m^3/s]	13.5	0.35
Number of turbines	2	1
Type of turbines	Francis	Pelton
α_0	0.10	0.10
α_M	0.50	0.30
η_0	0.46	0.75
η_M	0.86	0.89
η_P	0.95	0.95
Mean annual power [kW]	13000	122
Maximum power [kW]	30000	995
Annual energy production [GWh]	113.8	1.1
Cost function		
$Q_{PROJECT}$ [m^3/s]	13.5	0.35
$C_{PROJECT}(Q_{PROJECT})$ [M€]	122	1.2
a [M€/$(\frac{m^3}{s})^b$]	25.7	2.3
b [-]	0.6	0.6

Table 4.1: Technical and economic characteristics of the considered run-of-river power plants and hydrological features of the contributing catchment.

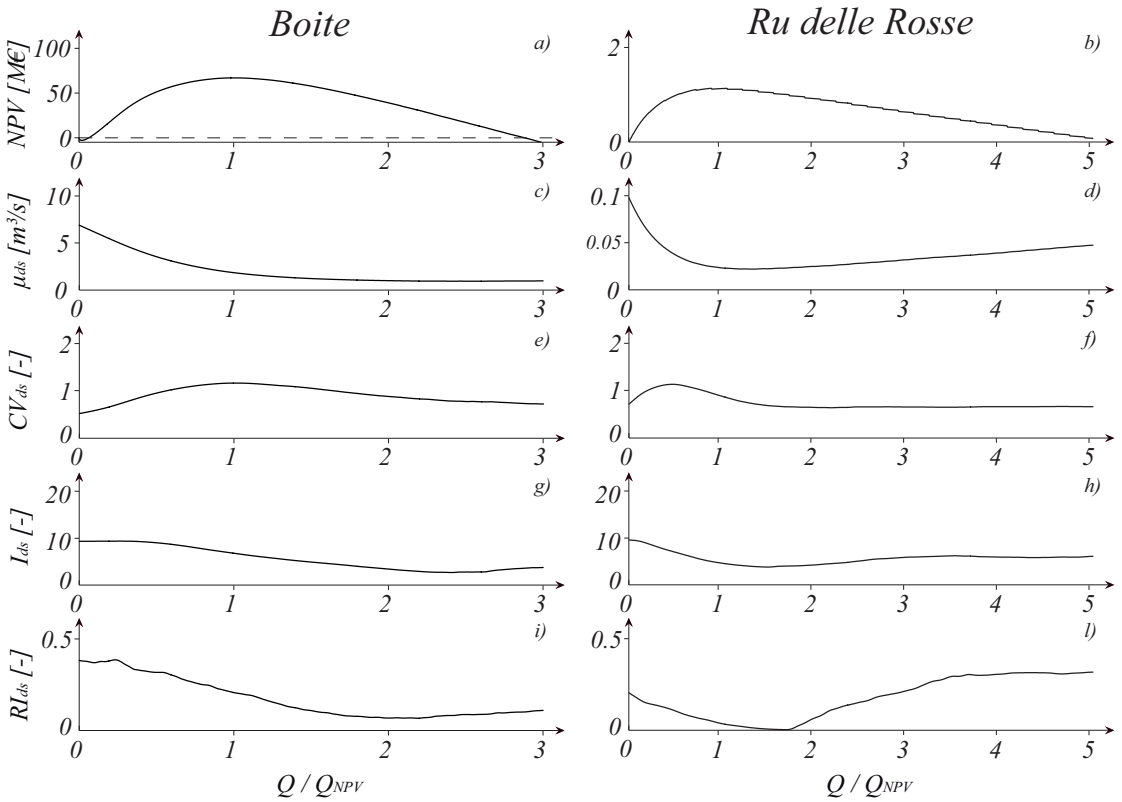

Figure 4.2: Behavior of the NPV and of the flow statistics downstream of the intake (μ, CV, I, RI) as a function of the plant capacity for the Boite river (left charts) and the Ru delle Rosse (right charts).

drologic disturbances is carried out in this application considering the following seasons: summer (June to August), fall (September to November), winter (December to February) and spring (March to May). Flow statistics during winter, when river ecosystems are almost inactive owing to the influence of snow dynamics [Schaefli et al., 2013], might be neglected [Brown et al., 2011]. The lowest hydrologic alteration is observed when the capacity is null and the natural flow regime remains unaltered. The plots show quite heterogeneous patterns for the different flow metrics (μ, CV, I and RI) in the two case studies.

A run-of-river plant always reduces the mean flow in the reach between the intake and the outflow. The rate of change of μ_{ds}, though, decreases with Q because of the reduced percentage of time during which the plant is activated implied by large plants. Note that μ_{ds} in the Ru delle Rosse creek (Figure 4.2d) exhibits a non-monotonic dependence on the capacity Q. Therein, the minimum value of μ_{ds} is observed for $Q \cong 1.2\,Q_{NPV}$, whereas the alteration of the mean flow decreases for larger capacities because of the increased percentage of time during which the plant is switched off. Conversely, the coefficient of variation of daily flows in the river reach downstream of the intake is generally increased by the water flows diverted to the plant (Figure 4.2e-f). In fact, the flow pdf observed in the impacted reach is characterized by a finite probability concentrated in $q_{ds} = MFD$ and by the translated tail of the original streamflow distribution, representing incoming flows large enough to saturate the plant capacity. The coefficient of variation of daily flows downstream of the intake, $CV_{ds}(Q)$, is a non monotonic function of Q. For small plants CV_{ds} increases with Q, while the opposite behavior is observed for large plants. In regimes featured by a significant flow variability, the capacity that maximizes the impact on the CV is smaller than Q_{NPV} (Figure 4.2f). Large plants may induce a reduced impact on flow variability than small plants because of the reduced contribution of flood events to the flow variability downstream of the intake. Run-of-river plants typically reduce the integral scale of correlation, I, and the regime instability index, RI (Figure 4.2g-l). This implies that the plant induces less correlated streamflows during each season/year, but more stable regimes across different years. In the Ru Delle Rosse creek, for $Q \cong 3\,Q_{NPV}$, RI_{ds} approaches the values observed in the absence of the plant, thereby leaving unaltered the natural inter-annual variability of streamflows. The fact that $CV_{up} > CV_{ds}$ and $RI_{up} < RI_{ds}$ implies that run-of-river plants induce an increase of the intra-annual variability of daily flows, but a decrease of the inter-annual

variability, with potential implications for adaptation strategies of aquatic biomes.
In order to quantitatively test the independence among the different flow metrics, the cross-correlations (across different years) among μ, CV, I and RI and those among the corresponding disturbance indexes in eq. (2.30) have been calculated for different capacities. The analyses provided empirical evidence of independence among the different flow attributes (and/or their response to flow abstractions) in the examined case studies (maximum correlation < 0.5).

4.2.1 Deterministic weighting factors

Objective functions dependent on the plant capacity Q, as defined by eqs. 2.33 and 2.34, assume values ranging between $f_i = 0$, when the i-th objective is completely fulfilled, and $f_i = 1$, in correspondence of the plant capacity implying worst performances of the i-th objective.
Figure 4.3 illustrates the economic (x-axis) and hydrologic (y-axis) components of the objective function for different values of the plant capacity Q when D_H is computed using deterministic weights (eq. 2.31). This curve is generated clockwise from the right-down corner (minimum profitability and lowest hydrologic impact) for increasing values of Q. Solid lines illustrate the Pareto front, while dominated capacities are indicated as dashed lines. The latter represent undesirable design conditions, for which both economic value of the plant and hydrologic impact could be simultaneously improved.
Plots on the top of Figure 4.3 shows the sensitivity of D_H to the single factors that contribute to the definition of the hydrologic disturbance, and they have been obtained by considering the disturbance induced by the plant on each flow metric of eq. (2.30) separately. In most cases, the range of efficient plant capacities is upwardly bounded by Q_{NPV}. The lowest value of the set of efficient capacities, instead, is highly variable from case to case. As a consequence, the set of Pareto-efficient capacities may be as wide as the interval $[0, Q_{NPV}]$ - implying that all plant sizes smaller than the economic optimum are efficient - or much narrower, implying that only specific ranges of Q should be preferred in the design of the plant.
In some instances the function representing the profitability and the hydrologic alteration of the plant in the plane (f_1, f_2) shows interesting features. For example, when the RI is considered, the Pareto front may be composed by two or more disconnected segments. Interestingly, in some cases the Pareto front includes also capacities which are

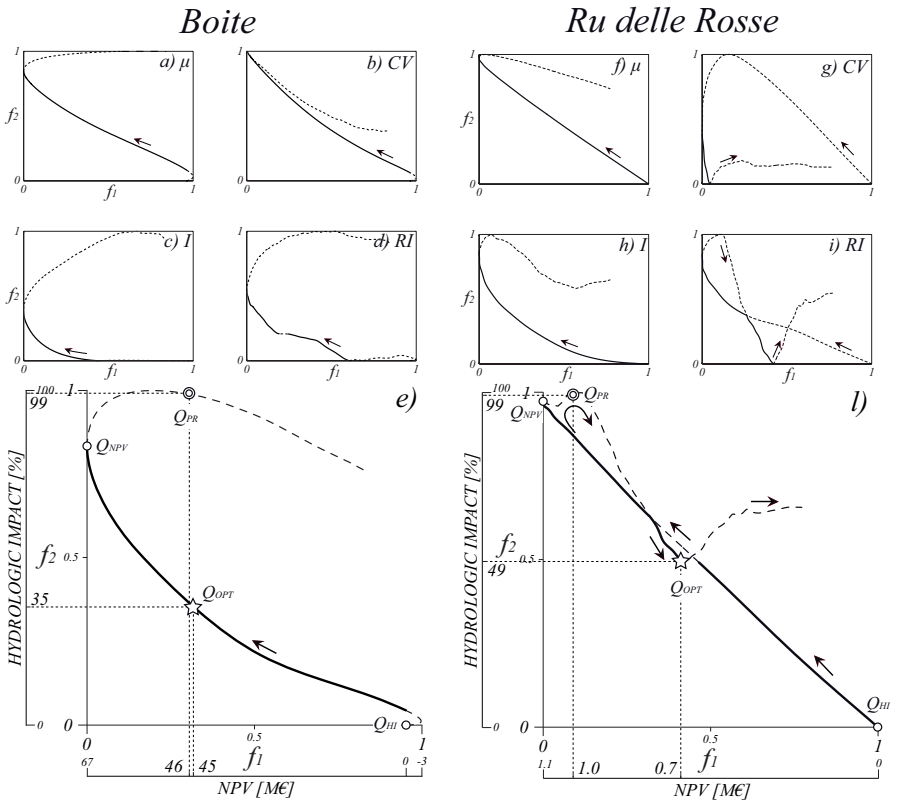

Figure 4.3: The economic component of the objective function, $f_1(Q)$ (x-axis), and the hydrologic component of the objective function, $f_2(Q)$ (y-axis), as a function of the plant capacity. The arrows indicate the direction along which the capacity Q increases.

significantly higher than Q_{NPV} (Figure 4.3g, 4.3i).

Figure 4.3e, 4.3l illustrate, for the two case studies investigated in the paper, the multi-objective optimization of the plant capacity which is achieved trading between the economic profitability and the overall hydrologic alteration when the latter is calculated via eq. (2.31), i.e. by weighting homogeneously all the flow statistics introduced in eq. (2.30). Solid lines represent the overall Pareto fronts, which include the plant capacities that maximize the economic profitability (Q_{NPV}) and those minimizing the hydrologic impact (Q_{HI}). Interestingly, for the Ru delle Rosse creek the set of dominant solutions is made up by three disconnected ranges of Q (0 m^3/s < Q < 0.05 m^3/s; 0.07 m^3/s < Q < 0.23 m^3/s; 0.56 m^3/s < Q < 0.66 m^3/s). The Pareto-optimal plant capacity, Q_{OPT}, minimizes the distance from the origin when the objective functions are dimensionless linear transformations of the economic profitability and the hydrologic impact. It represents the best choice to simultaneously fulfill the two contrasting objectives considered in the optimization. Q_{OPT} is equal to 2.9 m^3/s for the Boite river and to 0.66 m^3/s for the Ru delle Rosse creek. The size of the plant suggested by this methodology is almost equal to the maximum streamflow observed in the Ru delle Rosse (duration $D(Q_{OPT}) = 0.03$) and hence an erratic flow regime requires Pareto-optimal capacities which are proportionally larger than in persistent regimes ($D(Q_{OPT}) = 0.83$). It is worth to note that in the Ru delle Rosse creek the Pareto-optimal capacity is much larger than the economic optimum ($\frac{Q_{OPT}}{Q_{NPV}} = 2.87$), while in the Boite river the opposite trend is observed ($\frac{Q_{OPT}}{Q_{NPV}} = 0.39$). In both cases, the capacity chosen by the designers, $Q_{PROJECT}$, does not maximize the NPV, and implies larger costs than smaller plants with similar profitability. These results suggest that the two plants have been quite oversized, and that an equivalent profitability could have been achieved with smaller plants, with a sensible reduction of the overall alteration of the flow regime.

Table 4.2 summarizes the results of the analysis, when the hydrologic indexes are considered individually or when they are combined in a single index of hydrologic alteration by means of eq. (2.31).

4.2.2 Random weighting factors

When eq. (2.32) is used to compute D_H, a different value of Q_{OPT} is obtained for each combination of weights $\gamma_1, \gamma_2, \gamma_3, \gamma_4$. Figure 4.4 shows the probability density functions

	Q_{HI} [m^3/s]	Q_{NPV} [m^3/s]	Q_{OPT} [m^3/s]	$Q_{PROJECT}$ [m^3/s]
Boite				
μ	0	7.5	2.9	13.5
CV	0	7.5	3.2	13.5
I	1.1	7.5	3.7	13.5
RI	2.1	7.5	3.2	13.5
μ, CV, I, RI	0	7.5	2.9	13.5
Ru delle Rosse				
μ	0	0.23	0.05	0.35
CV	0.31	0.23	0.31	0.35
I	0	0.23	0.08	0.35
RI	0.66	0.23	0.61	0.35
μ, CV, I, RI	0	0.23	0.66	0.35

Table 4.2: Relevant plant capacities resulting from the application of the multi-objective optimization to a run-of-river hydropower plant in the Boite river and the Ru Delle Rosse creek: Q_{HI} (lowest hydrologic impact), Q_{NPV} (highest profitability) and Q_{OPT} (Pareto-optimal).

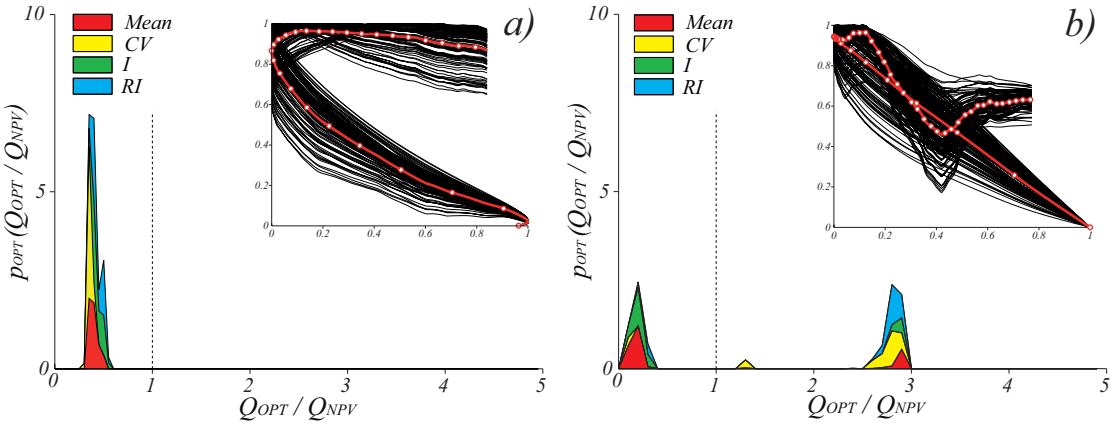

Figure 4.4: Probability density functions (pdfs) of the Pareto-optimal plant capacities for (a) the Boite river and (b) the Ru delle Rosse creek. Insets show the bundles of fronts (black curves) that originates by a 10^4 Monte Carlo sampling of the random weights γ_i in eq. (2.32).

(pdfs) of the Pareto-optimal plant capacity, $p_{OPT}(Q_{OPT})$, numerically obtained by 10000 Monte Carlo realizations of the vector $(\gamma_1, \gamma_2, \gamma_3, \gamma_4)$. In analogy to Figure 4.2, in the x-axis the plant capacity Q has been normalized by the capacity that maximizes the profits, Q_{NPV}.

In the Boite river (persistent flow regime, Figure 4.4a) p_{OPT} is narrow and peaks around $Q = 0.4\,Q_{NPV}$, suggesting that a trade-off between profitability and hydrologic alteration would be obtained by significantly reducing the plant capacity below Q_{NPV}, independently on the weight that is assigned to each flow statistics. In particular, the mean Pareto-optimal plant capacity is 3.1 m^3/s ($\frac{Q_{OPT}}{Q_{NPV}} = 0.41$), a value which is quite close to the optimal capacity derived using uniform values of γ_i in eq. (2.32). Conversely, in the Ru delle Rosse creek (erratic flow regime, Figure 4.4b) things are quite different. For high plant capacities, the coefficient of variation and the regime instability downstream of the intake closely resemble those observed in the natural regime. Hence, when the weights assigned to these flow statistics are large enough, the optimal plant capacity is much larger than the economic optimum. Otherwise, if the mean and the correlation of streamflows have a larger weight in eq. (2.32), the optimal capacity is smaller than Q_{NPV}. This explains the bimodal shape of p_{OPT} observed in Figure 4.4b. In the Ru delle Rosse, a satisfactory trade-off between the economic value of the plant and the hydrologic alteration downstream of the intake would be achieved either reducing the plant capacity below Q_{NPV} or increasing the capacity up to $3\,Q_{NPV}$, depending on the

weights assigned to each flow statistic.

In Figure 4.4, the area enclosed under p_{OPT} has been shaded with different colors to identify the distribution of Q_{OPT} obtained when each of the four flow statistics has the largest weight in the computation of D_H. The plot suggests that in the application to the Boite river (Figure 4.4a) the impact of the plant on the mean and the CV addresses the choice of the capacity toward slightly smaller values, while higher values are preferred when the disturbances on I and RI are more important. However, different combinations of weights for the flow statistics lead to similar results in terms of optimal trade-off between profitability and hydrologic disturbance. This is not the case for the Ru delle Rosse creek (Figure 4.4b), where red and green dominate the left peak of p_{OPT}, while yellow and blue prevail in the right peak. This suggests that the mean and the correlation downstream of the intake would be less impacted with a plant capacity smaller than Q_{NPV}. Conversely, a reduced impact on the flow variability and the regime instability would require large plant capacities.

This result can be better understood if the flow regime downstream of the intake is analysed for different plant capacities. Figure 4.5 shows (in a log-log plot) the natural flow duration curve at the intake of the Ru delle Rosse creek (solid curve), jointly with the flow duration curve between the intake and the outflow for two different values of the plant capacity. Dotted curve corresponds to a capacity $Q = Q_{NPV}$, while dashed curve refers to a capacity $Q = 3\,Q_{NPV}$. Flows have been normalized using the mean flow downstream of the plant, so as to better represent the relative flow variability in the chart. The plot shows that the increase of CV when the plant is designed to maximize the profits (dotted curve in Figure 4.5) is produced by the interplay between the right tail of the streamflow distribution and the mean. In this case, due to the erraticity of the natural flow regime, flows exceeding the plant capacity can be even 30 times larger than the mean flow in the impacted reach. When the capacity increases, instead, the tail is lighter (dashed curve in Figure 4.5), with maximum flows downstream of the intake that are closer to the mean flow. The role of extreme flows is thus crucial in determining the variability of daily streamflows downstream of the intake, and the corresponding value of D_H.

Figure 4.6 shows the annual flow pdf's observed downstream of the Ru delle Rosse plant intake for two plant capacities, approximately $Q = 1.5 \cdot Q_{NPV}$ (left) and $Q = 2 \cdot Q_{NPV}$ (right). Annual flow pdf's are shown from the first year (blue curve) to the last year

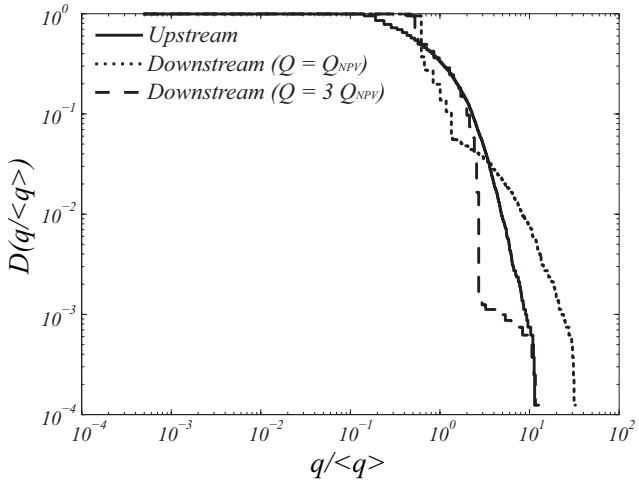

Figure 4.5: Upstream flow duration curve (solid curve) and flow duration curves observed downstream of the intake of the Ru delle Rosse power plant for a capacity $Q = Q_{NPV}$ (dotted curve) and $Q = 3\,Q_{NPV}$ (dashed curve). The flows have been scaled to the mean flow downstream of the plant (which is obviously different in each of the three cases), so as to better represent the relative flow variability.

(green curve) considered in the analysis of the economic value and the hydrologic impact of the plant. Fluctuations between annual pdf's are proportional to the Regime Instability, according to eq. (2.29). Fluctuations are much more accentuated in the right plot, even though the plant capacity increases from left to right plot. Crucial is the role of the cut-off flow, i.e. the minimum flow that the plant can process, which increases with the size of the plant, thus leaving natural fluctuations unaltered for a larger fraction of flow.

4.2.3 Identifiability of Pareto-optimal solutions

While random weights can be used to identify a set of optimal 'alternative' solutions through Pareto techniques, it is equally interesting to investigate whether these alternatives should be interpreted as local optima or if they are best interpreted as optimal ranges of capacity. Figure 4.7 shows, for different values of the plant capacity, the euclidean norm of the objective function ($|\boldsymbol{f}|$) calculated for the points belonging to the mean fronts (red curves in the insets of Figure 4.4). The identifiability of the Pareto-optimal plant capacities is assessed by identifying the range of capacities which are nearly

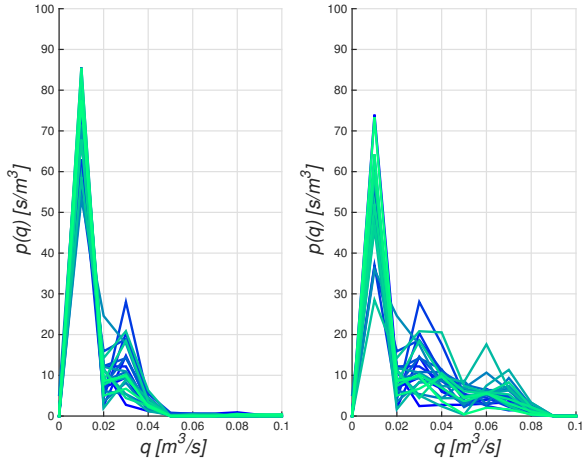

Figure 4.6: Annual flow pdf's observed downstream of the plant intake for different capacities.

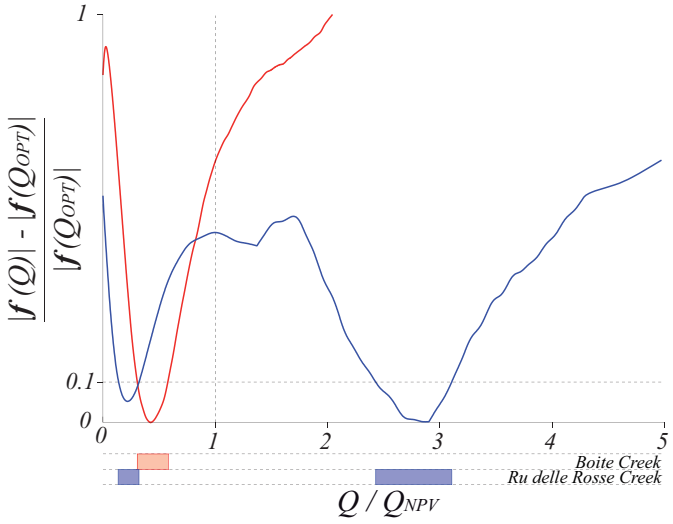

Figure 4.7: The distance from the origin of each point of the mean front (representing different values of the plant capacity, $|\boldsymbol{f}(Q)|$) is shown for the Boite river (red curve) and the Ru delle Rosse creek (blue curve). Colored bands located below the x-axis individuate the ranges of capacities which are nearly equivalent to the optimal capacity for each case study.

equivalent to the Pareto optimal capacity (being the norm of the corresponding objective function at most 10% larger than the minimum possible value). When a narrow range of capacities exists that fulfill the condition $|\boldsymbol{f}(Q) - \boldsymbol{f}(Q_{OPT})| / \boldsymbol{f}(Q_{OPT}) < 0.1$, the corresponding optimal solution is well identified, and the choice of Q should be restricted to a narrow range of Q around Q_{OPT} because weak departures from Q_{OPT} lead to significant changes in the degree of compliance of the objectives. For the Boite river (V-shaped red curve in Figure 4.7), the Pareto-optimal plant capacity is found to be well identified around 3.1 m^3/s. For the Ru delle Rosse (W-shaped blue curve in Figure 4.7), instead, two separated regions can be identified around the two modes of p_{OPT} which are almost equivalent to the global optimum. In this case, while the first optimal capacity is well identified around 0.05 m^3/s, the second optimal capacity is not, with a broad range of capacities (0.55 m^3/s < Q < 0.71 m^3/s) that produce similar values of the overall objective function.

Pareto techniques can be used to single out trade-offs and alternative solutions that incorporate both uncertainty in the knowledge of the most influential hydrologic attributes and degree of sensitivity of the objective functions to design attributes. In some cases the optimal trade-off between economic profitability and hydrologic disturbance is well identified, whereas in other cases wider ranges of optimal capacities may be devised. Even though well identified optima may facilitate the choice of designers providing to water managers an objective basis to identify efficient allocations of resources, less identifiability would give more flexibility in case of design errors and/or unexpected conditions.

4.2.4 Implications for policy actions

The multi-objective analysis carried out in previous sections provides some insight on how to identify policy actions that incorporate the actual evaluation of the hydrologic disturbance induced by run-of-river plants. Currently, feed-in tariffs that promote energy production from run-of-river hydropower plants are mainly based on the mean annual power produced by the plant. In Italy, for instance, plants that produce more energy get less incentives for selling it (but for longer periods). This type of prescriptions is grounded in the idea that the environmental footprint of a plant grows with the amount of energy produced. Even though the length of the impacted reach is roughly proportional to the power through the average slope between the intake and the outflow, and large plants may induce a more significant impact at the intake due to increased size

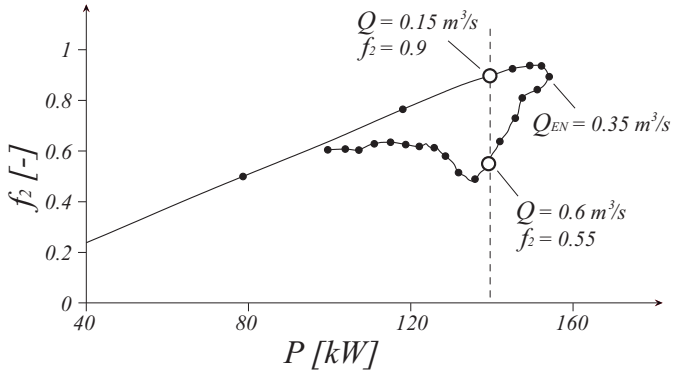

Figure 4.8: Hydrologic alteration ($f_2(Q)$ of the mean front) plotted against the mean annual power produced by the plant in the Ru delle Rosse creek. Dots indicate growing plant capacities with a step of 0.05 m^3/s.

of hydraulic works and infrastructures, other factors like the extent of the hydrologic alteration between the intake and the outflow could be equally important to define the overall impact of a run-of-river power plant.

Figure 4.8 shows the relationship between the mean annual power (computed through eq. (2.13)) and the hydrologic alteration (assessed through the objective function f_2 of the mean Pareto front) for the plant proposed in the Ru delle Rosse creek. The plot suggests that, especially in rivers featured by a pronounced variability of streamflows, the relationship between mean power ($E/\Delta T$) and hydrologic disturbance (f_2) is non monotonic and hysteretic. In particular, the plot emphasizes that a given mean power (say, 140 kW) can be produced with different plant capacities, that in turn imply different degrees of hydrologic alteration ($f_2 = 0.9$ for $Q = 0.15$ m^3/s and $f_2 = 0.55$ for $Q = 0.6$ m^3/s). Moreover, a plant that produces a relatively large amount of energy may be less impacting than a smaller plant in terms of flow regime disturbance between the intake and the outflow. Results suggest that feed-in tariffs for run-of-river plants should not be set as proportional to the produced energy (or to the plant size), but should rather account for the actual modifications of flow conditions downstream of the intake.

Chapter 5

Multi-objective optimization of the plant capacity: profitability and hydrological connectivity

In the application described in chapter 4, the problem of simultaneously combining economic and environmental objectives was carried out considering an overall hydrologic disturbance evaluated as the sum of the upstream/downstream changes of a set of flow statistics which are known to affect a variety of ecological processes in riverine environments. Under the proposed formulation, not only the impact on the natural streamflow pdf is considered, but information on ecologically-relevant features like discharge correlation and inter-annual variability of flows is accounted for. Hence, proposed tools for the definition of the optimal plant capacity aim at satisfying human needs (i.e. energy production in this case) while preserving the overall spectrum of ecosystem services supplied by the river, which are implicitly considered under the proposed approach.
In this chapter the same problem is addressed from a more specific point of view. Economic objectives (i.e. maximization of the Net Present Value) are not traded with the minimization of the overall hydrologic disturbance in the river reach between the intake and the outflow, but with the maintenance of the hydrological connectivity in the impacted reach. Discharges are known to represent a key variable in shaping ecologi-

cal processes within catchments, especially for fish communities. Their health indeed is strongly based on the availability of required habitats (e.g. feeding, spawning, refugia, etc.), but also on their reachability, provided that the physical connection between habitats is essentially given by available river discharges. Therefore, temporal variability of flows reflects in a variability of the hydrological connectivity, and thus might imply periods of strongly reduced connectivity, which represent a physical barrier for the movement of ecological species within the catchment, with associated environmental concerns. This is particularly important for migratory movements of anadromous fish, who grow in freshwater, spend large portions of their life cycle in salt water until they achieve sexual maturity and then return to native environments for spawning. Migrations are biologically constrained in time, and physical connectivity between habitats during those time windows is fundamental for the survival of fish communities. For example, when access to spawning sites is prevented, the number of new fish might be insufficient to overcome mature fish mortality thus implying a reduced health of the ecological community.

Since many regions of the world are experiencing a significant exploitation of riverine water resources for hydropower production (see the Introduction of this thesis), preserving the hydrological connectivity within a river network and, consequently, preventing environmental concerns on fish communities are becoming increasingly important tasks for water managers, who are asked to balance anthropogenic and environmental needs and thus require tools for a proper allocation of water resources among those contrasting goals. This chapter describes a quantitative analysis of how the presence of a run-of-river plant in a pristine Scottish catchment might induce losses of hydrological connectivity within the river network and thus affect the life cycle of an important salmon community homing in the same catchment.

To this aim, a novel probabilistic approach to quantitatively evaluate the strength of flow influence on hydrological connectivity under natural flow conditions on riverine ecosystem processes needs to be introduced. Proposed formulation is based on a simple outflux-influx model linking the number of Atlantic salmon emigrating and returning to the same stream, which explicitly accounts for the inter-annual variability of the hydrologic regime. Model parameters, in particular those defining fish passage dependence on available discharge, are calibrated against a detailed long-term hydroecological dataset for an Atlantic salmon spawning stream in Scotland which gives robustness and reliability to the proposed methodology.

Then, the presence of a run-of-river plant is simulated to quantify losses of connectivity induced by different scenarios of water abstraction for hydropower production. This chapter ends with a multi-criteria optimization analysis aimed at defining the plant capacity trading between the maximization of the economic profitability and the minimization of the losses of hydrological connectivity. This application, though specific, represents a noteworthy example of the need of balancing anthropogenic and environmental uses of water resources.

5.1 Study area and data

This section focuses on the specific application carried out in this chapter and introduces information and data required to meet the objective. In particular, this chapter aims at:

- developing a new, probabilistic tool for the quantitative evaluation of a synthetic index expressing the average probability for fish to move across river networks depending on seasonal availability and variability of flows;
- validating the proposed tool through an eco-hydrological model describing salmon returns for spawning based on the number of juveniles emigrated during previous years from the same catchment, explicitly including the influence of natural flow regime on the hydrological connectivity during pre-spawning season;
- simulating the presence of a run-of-river plant in the same river reach to investigate how water abstraction between the intake and the outflow limits local hydrological connectivity for salmon migrations, and how eco-hydrological concerns might be traded with economic goals to achieve sustainable design of hydropower plants maintaining satisfactory levels of connectivity in the altered river reach.

Atlantic salmon

Atlantic salmon (*Salmo salar*) is an economically and ecologically important fish species in North West Europe and the North East of the North American continent [MacCrimmon and Gots, 1979; Mills, 1991; Maitland and Campbell, 1992]. As an anadromous fish, salmon return from the sea as adults for spawning to the rivers and streams where they were juveniles. Adult fish typically return for spawning after 1-3 years at sea; this follows a juvenile phase of 1-4 years spent in freshwater [Youngson and Hay, 1996; Klemetsen et al., 2003; Bacon et al., 2005]. Spawning usually occurs during autumn in

headwater streams and it is a critical lifestage to the recruitment and the maintenance of salmon populations. Access into spawning streams is often mediated by streamflow, and discharge thresholds may need to be exceeded to facilitate entry [Tetzlaff et al., 2008; Cunjak et al., 2013].

Streamflow dynamics generally have a strong control on spawning entry because salmon usually remain in the main stem of the river network waiting for an increase in discharge that triggers the final upstream movement to the actual spawning site [Jonsson et al., 1990, 2007; Mitchell and Cunjak, 2007; Gibbins et al., 2008; Jonsson and Jonsson, 2009]. General relationships between fish entry into spawning tributaries and flow variability have been shown by direct trapping of returning fish and tracking of radio-tagged adult salmon [Webb and Hawkins, 1989; Tetzlaff et al., 2008]. In years when flows are insufficiently high, the size of returning spawning population may be limited as access to suitable habitat may be restricted or even prevented [Moir et al., 1998; Gibbins et al., 2008]. Headwater areas can often be reached only under relatively high flows [Baxter, 1961; Vadas, 2000; Cunjak et al., 2013], and progressively higher discharges are needed for increasing fish sizes and more upstream sites which are steep with high roughness [Moir et al., 2004]. Large fish homing to small streams during periods of low flows may find it physically impossible to reach their target when minimum depth requirement is not fulfilled [Youngson and Hay, 1996; Tetzlaff et al., 2005b] or may be particularly vulnerable to predation in shallow water [Jonsson et al., 2007]. The ascent of large salmonids at low flows in small streams is therefore often delayed compared to that of smaller ones [Jonsson et al., 1990; Jensen and Aass, 1995; Jonsson et al., 2007; Mitchell and Cunjak, 2007].

Although flow-related connectivity may act as an important control on salmon entry to spawning streams, its effects will be modulated by other factors. Density dependent controls have been identified whereby the larger number of returning spawning fish will increase competition for spawning sites and add dispersive pressures on habitat utilization. Thus, simple flow effects can be confounded by the number of returning adults, which in turn depends on the number of out-migrating juveniles in the preceding years and their survival rates in the ocean. Marine mortality is often high (> 95 %) as a result of predation, commercial fishing and variability of ocean food supplies. Moreover, the timing of the flow variability in the spawning migration can also have an important effect on discharge thresholds, with increasing the probability of fish trying to enter spawning

tributaries on lower flows when ovulation becomes closer. Fish are more likely to cease waiting for higher flows as spawning time approaches since they need to spawn promptly after ovulation, which in itself is temperature dependent. However, it is also important to note that some studies have shown that in larger rivers with more stable flow regimes, discharge may have limited effects on the upstream migration of adult salmon [Thorstad and Heggberget, 1998; Lilja and Romakkaniemi, 2003; Thorstad et al., 2003; Karppinen et al., 2004].

Girnock Burn catchment

The Scottish Highlands (UK) contain some of the least disturbed rivers in Europe and many form important spawning sites for Atlantic salmon [Gilvear et al., 2002]. Among those is the River Dee, flowing in north-east Scotland from the Cairngorms to the North Sea at Aberdeen (2300 km^2).

The Dee is the largest river in the UK that is not subject to the influence of river regulation by reservoirs and sustains an economically important salmon fishery. The Dee is particularly well known for its spring salmon - these are adult fish which return to freshwater habitat early in the year, allowing the fishing season to start early (in February). Genetic studies have shown that these fish mostly spawn in the high altitude headwater tributaries of the Dee [Youngson and Hay, 1996].

The Girnock Burn is one such relatively natural 9.5 km long tributary of the River Dee, draining a catchment of 30.3 km^2 with altitudes ranging between 230 m and 862 m (panel *A* in Figure 5.1) [Tetzlaff et al., 2005a]. Various glacial and fluvio-glacial deposits cover the bedrock, which is composed of granite in the upper part of the catchment and dominated by schists and other metamorphic rocks in the lower parts [Moir et al., 1998; Gibbins et al., 2002; Soulsby et al., 2005]. Land use is dominated by heather (*Calluna vulgaris*) moorland used for deer stalking.

Streamflow data

The hydrology of the Girnock has been extensively studied. Daily discharge data were measured from 1972 to 2011 at the gauging station of Littlemill (grey circle in Figure 5.1A), which is located about 1 km upstream of the confluence between the Girnock and the Dee. Figure 5.1B shows the frequency distribution of streamflows recorded at Littlemill. Mean annual discharge is 0.55 m^3/s, but flows can be smaller than 0.1

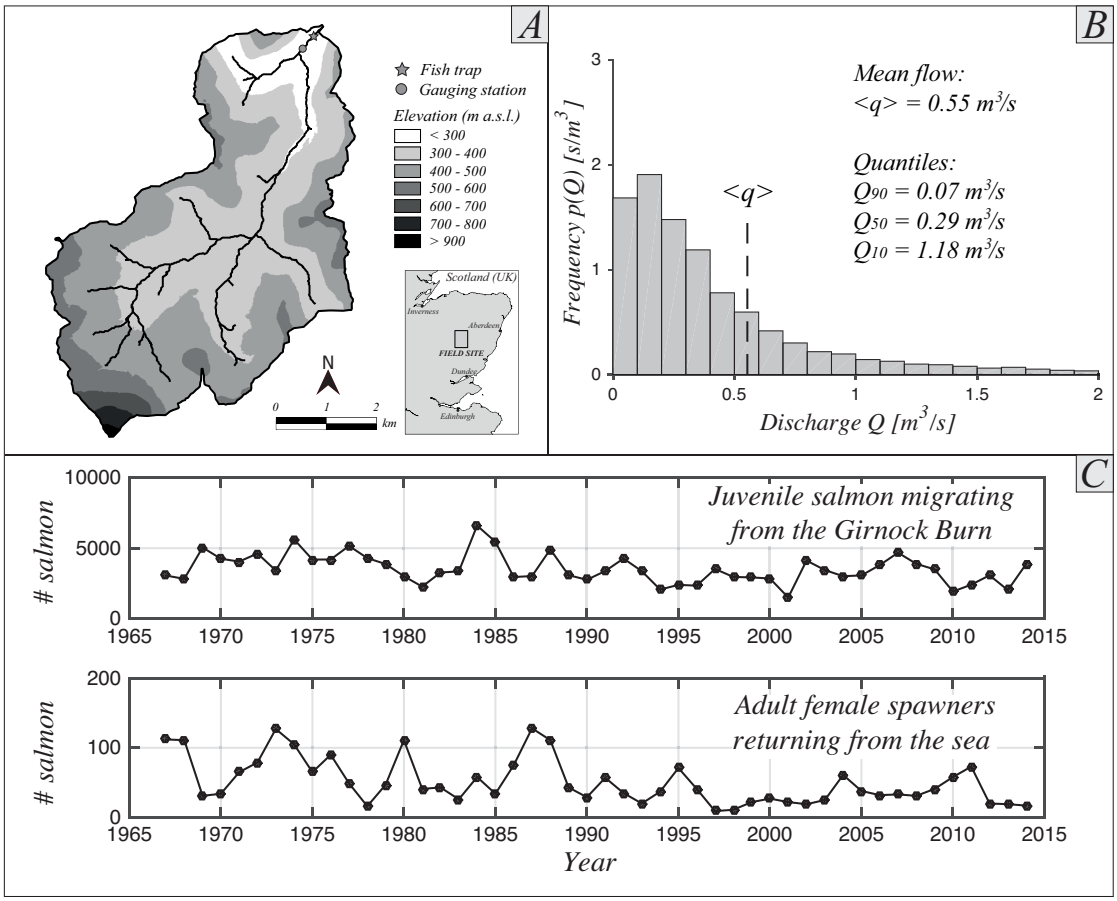

Figure 5.1: View of the Girnock Burn catchment with the location of the discharge gauging station and the fish trap (top left, A); probability density function of streamflows observed at the gauging station with mean flows and quantiles given (top right, B); annual number of smolt and parr emigrating downstream of the juvenile fish trap in the Girnock Burn (upper panel, C) and adult females returning for spawning (lower panel, C).

m^3/s in June and August or larger than 50 m^3/s during floods (usually in late autumn or early spring), implying a strong intra-annual variability of streamflows [Moir et al., 1998; Malcolm et al., 2003]. Moreover, the pronounced inter-annual flow variability is a distinctive feature of streamflow dynamics in the Girnock Burn [Moir et al., 1998; Soulsby et al., 2005].
The discharge characterized by a duration of 0.95 is considered the default residual flow, that must be preserved downstream of every kind of water abstraction for human needs, even though the Scottish Environmental Protection Agency (SEPA) may require specific prescriptions for every case study. In this case, at the cross section where the gauging station is located, a duration of 0.95 corresponds to a streamflow of about 0.04 m^3/s. This value, properly scaled if necessary, is considered as the Minimum Flow Discharge (MFD) in the present case study.

Salmon data

Salmon population dynamics in the Girnock Burn have been monitored for a long period. Most relevant studies and data acquisition include geomorphic and hydrologic characterization of spawning habitats [Moir et al., 2002], spawning observations within the river network [Moir et al., 2004] and hydraulic modelling of spawning sites Moir et al. [2005]. In the mid-1960s, two fish traps were built by Fisheries Research Services Freshwater Laboratory (FRS-FL) staff a few hundred meters downstream of the discharge gauging station at Littlemill. One trap is set to catch juvenile salmon emigrating out of the Girnock during their journey to the sea (smolts in spring and parr in autumn). Trapped juveniles are counted, measured and their scales are taken for age determination. Juveniles are released in the stream downstream of the trap. Another trap is located just downstream of the juvenile trap to monitor the number of adult salmon coming back in autumn for spawning from the ocean to the Girnock. The trap is temporary and is installed in the river only during the spawning season when adult salmon migrate from the River Dee into the Girnock. Adult female spawners undergo the same analysis as smolts and are released upstream of the traps.
The fish traps have continuously monitored emigration (smolt and parr) and immigration (adult female spawners) fluxes between the Girnock Burn and the River Dee since 1967 [Glover and Malcolm, 2015b,a]. The emigrants database is subdivided into smolts and parr depending on the season when emigration takes place. However, for the aim of

this work, smolt and parr are considered together, and the annual number of emigrants is the sum of all juveniles exiting the Girnock during spring and autumn of the same year. Comparative analyses were also carried out looking at adding the autumn migrants to the previous and following cohort of smolts, with no significant influences on the outcome. Unfortunately, the parr record exhibits some missing data during 80s (1982-1985 and 1988) and this is reflected in gaps in the total number of emigrants. This problem was circumvented by increasing the number of emigrating fish proportionally in these years (5 out of 40) to account for the missing parr data. Indeed, annually emigrating smolt runs during recent decades were on average as twice as large as those for parr. Figure 5.1C shows the number of juveniles exiting the Girnock (upper panel) and the number of females coming back for spawning (lower panel) every year (1 Jan - 31 Dec) through the fish trap since 1967. The mean number of emigrating salmon and immigrating females is 3500 and 50 (1967-2014), respectively. In common with a number of other salmon rivers in the United Kingdom and elsewhere, the number of female spawners returning to the Girnock has shown a substantial decline over the past 50 years, with mean annual returning spawners falling from 70 (1967-1984) to 30 (1997-2014). Fish population studies in the Girnock indicate that an average of 30 spawning females are needed to maintain optimum habitat use and maximum levels of productivity [Youngson and Hay, 1996].

Economic data

Estimating the economic profitability of a run-of-river hydropower plant requires the introduction of an additional set of economic parameters.
In Scotland, feed-in tariffs exist that promote selling of the energy produced by small hydropower plants. Though being continuously reviewed, this work refers to incentives on small hydropower proposed in 2013, as reported by Liu et al. [2013]. For nominal power between 100 kW and 500 kW, as in the case of a plant located in the Girnock, the energy selling price (e_p) is prescribed as 0.155 £/kWh and guaranteed for 20 years. Finally, construction cost parameters need to be provided to the model to quantify the NPV of the hydropower investment in the Girnock. This task was addressed by referring to an existing database on hydropower plants available for the entire UK containing information on plant characteristics and costs [Salford Civil Engineering Ltd, 1989]. This database was collected by Salford Civil Engineering Ltd. in 1989, therefore it is usually

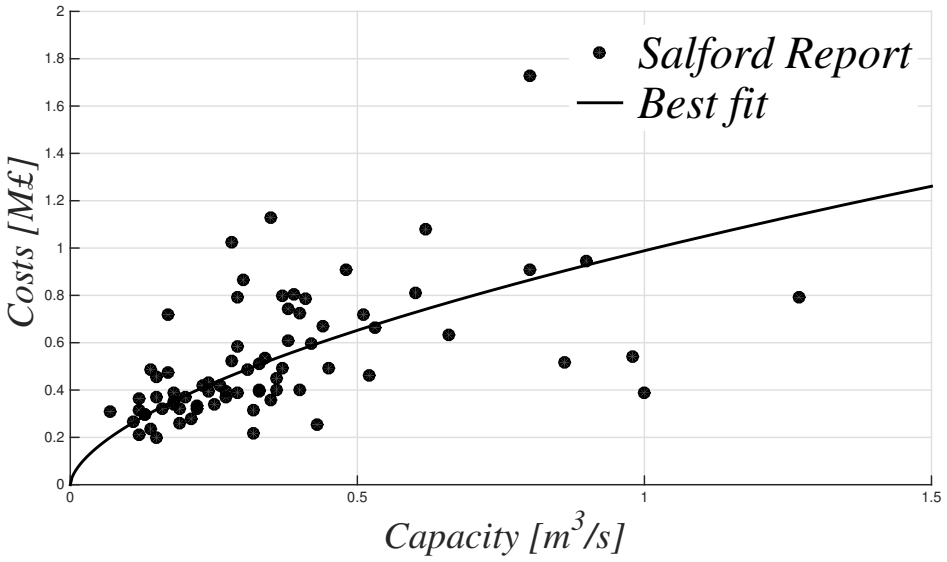

Figure 5.2: Comparison between construction costs data available as a function of correspondent plant capacity (black dots) and power-law fitting function of the ensemble of data (solid line).

referred as the Salford Study. Construction costs are reported in the Salford Study only for those plants built in England and Wales, but they were assumed to be valid also for Scotland. Construction costs (artificially corrected by inflation from 1989 to 2015) were then compared against the correspondent plant capacities for those plants with characteristics similar to small run-of-river plants in mountain regions, namely a capacity smaller than 1.5 m^3/s and an hydraulic head higher than 30 m. More than 70 plants satisfied the imposed characteristics, and they were used to calibrate the parameter $a = 0.97$ [M£/$(\frac{m^3}{s})^b$] of the power-law cost function (see eq. 2.18), in which b was again considered to be 0.6 [-] as in all previous applications. Figure 5.2 shows construction costs data reported in the available database as a function of correspondent plant capacity (black dots), as well as the function expressed by eq. (2.18) in which parameter b is 0.6 and parameter a is calibrated fitting the ensemble of data (solid line). The fitted power-law function accurately describes construction costs for smaller capacities, whereas increasing size of the plant implies that variability of observed costs increases accordingly.

5.2 Methods

In Section 5.2.1, a new formulation for the quantitative evaluation of the inter-annually varying hydrologic connectivity is introduced and validated through a model that describes annual return fluxes of adult salmon for spawning. Model parameters are calibrated against the eco-hydrological dataset described in Section 5.1.
Section 5.2.2 describes how losses of hydrological connectivity induced by a run-of-river power plant can be quantified for increasing plant capacities, and mathematically defines the objectives functions for a multi-criteria optimization of the plant capacity trading between the maximization of the economic profitability and preservation of the hydrologic connectivity between the intake and the outflow of the hydropower plant.

5.2.1 Modelling salmon returns for spawning

The first goal is to formulate a probabilistic tool to quantify the hydrologic connectivity for adult salmon explicitly accounting for the hydrologic regime at the confluence between the Girnock and the River Dee. Validation is then performed including the proposed tool in a simple and parsimonious model for the estimate of female salmon returns for spawning to the Girnock Burn. Female salmon returns are modelled based on the number of juveniles emigrated in previous years. Females are more important than males in determining subsequent juvenile recruitment because smolt and parr critically depend on the number of eggs deposited by female salmon. This is because each spawning female will produce ca 5000 eggs which can be fertilised by relatively few adult males or sexually mature resident parr [Youngson and Hay, 1996].
The model incorporates a number of factors relevant to the salmon life cycle derived from previous empirical and/or theoretical studies. The number of emigrants is approximately two orders of magnitude higher than the number of immigrating females. Hence, the high mortality rate characterizing the marine life stage needs to be accounted for. Spawner age determination at the fish trap has demonstrated that most salmon return to the Girnock two or three years after they left it. Observations have also shown that peaks of emigrants are often reflected by peaks of immigrants with a delay of two or three years (e.g. immigrants from 1986 to 1997 reflect emigrants from 1983 to 1994 implying a delay of three years). In addition, the access to spawning sites in the Girnock Burn strongly depends on the hydrological connectivity between the Girnock and the Dee

during the pre-spawning season, when females select spawning habitats [Moir et al., 1998]. Relatively dry spawning seasons reduce the probability of upstream migration and force females to spawn in the lower reaches of the Girnock. In such situations, uneven spawning distributions may result in sub-optimal use of potential habitats and compromise juvenile production [Tetzlaff et al., 2005b].
Hence, the following factors are identified as the main drivers of the flux of females returning to the Dee: marine survival rates (μ), the delay (number of years) between emigration from and return to the native stream (τ) and the fish passage probability between the Girnock and the Dee ($\bar{f}$), which is driven by the underlying hydrologic regime. Other types of environmental factors possibly involved in the selection of the spawning site and migratory movements (chemical stresses, water temperature, etc.) have been neglected in order to produce a parsimonious model that could be transferable to other sites and is able to test whether hydrologic dynamics are a first order control on fish migration, and quantify this relationship under natural flow conditions.

Marine survival rates, μ

The marine survival rate $\mu(t)$ during year t defines the fraction of adult salmon emigrated during the t-th year that will survive to the year $t+1$, and thus, will get a chance to return to the Girnock Burn for spawning. The survival rate $\mu(t)$ is therefore a dimensionless number that ranges between 0 (death of all emigrated salmon) and 1 (all emigrated salmon survive). The annual survival rate is known to have decreased with time. For this reason, salmon survival is defined as a linear function of time.

$$\mu(t) = \mu_0 + \frac{\mu_F - \mu_0}{t_F - t_0} \cdot (t - t_0) \tag{5.1}$$

According to eq. (5.1), two parameters are needed to evaluate $\mu(t)$ during the entire model simulation: μ_0, the survival rate for the first year of the simulation (t_0); μ_F, the survival rate for the last year of the simulation (t_F).

Delay between emigration and return, τ

The number of years between emigration and returns (hereafter termed delay, τ) is considered as a discrete random variable with a probability density function (pdf), $p_{d,t}(\tau)$, where the subscript t refers to a specific emigration year. The distribution $p_{d,t}$ is assumed to hold positive values only for $\tau = 2$ and $\tau = 3$ (Figure 5.3), since almost all salmon

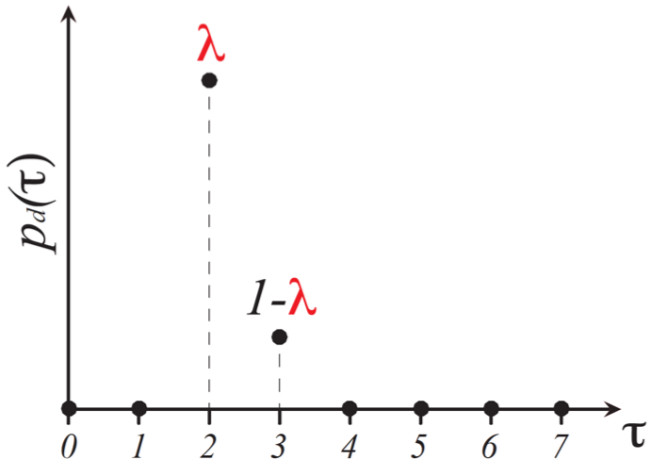

Figure 5.3: Probability density function $p_d(\tau)$ of the number of years between emigration and returns (delay, τ). A single parameter λ is required to define $p_d(\tau)$, which represents the probability of having salmon returns two years after juvenile emigration.

return two or three years after emigration. Hence, the model neglects the possibility that salmon can return after one year only, or after more than three years. Under these assumptions, for any emigration year t, the definition of $p_{d,t}$ relies on one parameter, $\lambda \in [0, 1]$, representing the probability that $\tau = 2$. Accordingly, the probability of having $\tau = 3$ must be $(1 - \lambda)$.

Finally, in order to reduce the number of parameters, the probability distribution of delays between emigrations and returns has been considered to be the same for all years of the simulation (i.e. $p_{d,t}(\tau) = p_d(\tau) \, \forall \, t$). In this framework, a single parameter (λ) is needed to model delays between emigrations and immigrations throughout the simulation.

Fish passage probability

A time-variable average passage probability $\bar{f}(t)$ is introduced to quantify the probability for spawners to successfully migrate from the confluence of the Dee and the Girnock Burn to upstream spawning sites of year t. This component of the model explicitly accounts only for the observed hydrologic conditions immediately prior to spawning (i.e. September to November - as indicated by long-term observations).

In the Girnock Burn, salmon spawning migrations have been found to be positively

correlated with streamflow conditions [Moir et al., 1998; Tetzlaff et al., 2007]. In fact, adult females utilise discharges greater than the long-term spawning season median flow (0.26 m^3/s) [Moir et al., 2004]. On the contrary, low discharges and associated reduced stages limit fish mobility and increases fish predation during immigration. Hence, low discharges can be seen as a physical barrier impeding upstream migratory movements. These factors have been incorporated into the model through a fish passage function f quantifying the probability of salmon to entering the Girnock Burn and accessing upstream spawning sites, and which is made dependent on the river discharge ($f(Q)$). An exponential fish passage function has been selected that relies upon two parameters (Figure 5.4).

$$f(Q) = \begin{cases} 0 & \text{if } Q \leq Q^* \\ 1 - \exp\left(-\frac{Q-Q^*}{\sigma}\right) & \text{if } Q > Q^*. \end{cases} \tag{5.2}$$

In eq. (5.2), Q^* represents a flow threshold that allows adult salmon movements while σ embeds the vulnerability of fish to flow conditions when $Q > Q^*$. Units of Q^* and σ are the same as the unit of the discharge.

According to eq. (5.2), the minimum threshold discharge, Q^*, separates two different situations (Figure 5.4): when $Q \leq Q^*$, salmon upstream movement is totally impeded by the physical limitation represented by low water stages; whereas if $Q > Q^*$, salmon are allowed to pass through and access the spawning stream.

However, for discharges higher than Q^* the connectivity increases with Q, and such increase depends on fish vulnerability σ. In particular, for $\sigma = 0$ (low vulnerability), $f(Q)$ becomes a step function always equal to 1 for $Q > Q^*$. In such circumstances, the probability of reaching upstream spawning sites is one whenever discharge is greater than the minimum threshold. Larger values of σ (higher vulnerability) imply an increased range of discharges where sub-optimal connectivity ($f < 1$) is experienced by salmon. An exponential increase of $f(Q)$ above Q^* was chosen because it implies that a given discharge increment produces higher increases of $f(Q)$ for low streamflows. In fact, the relationship between river discharge and the relevant eco-hydraulic variables controlling fish movement and predation (e.g. channel area, water level) is typically non-linear [Leopold and Maddock, 1953; Ceola et al., 2013].

Note that in eq. (5.2) any detrimental effect of high flows on fish movement is neglected because the exceedance probability of such high flows during an entire pre-spawning season is very small (e.g. $P[Q \geq 5\, m^3/s] \simeq 10^{-2}$).

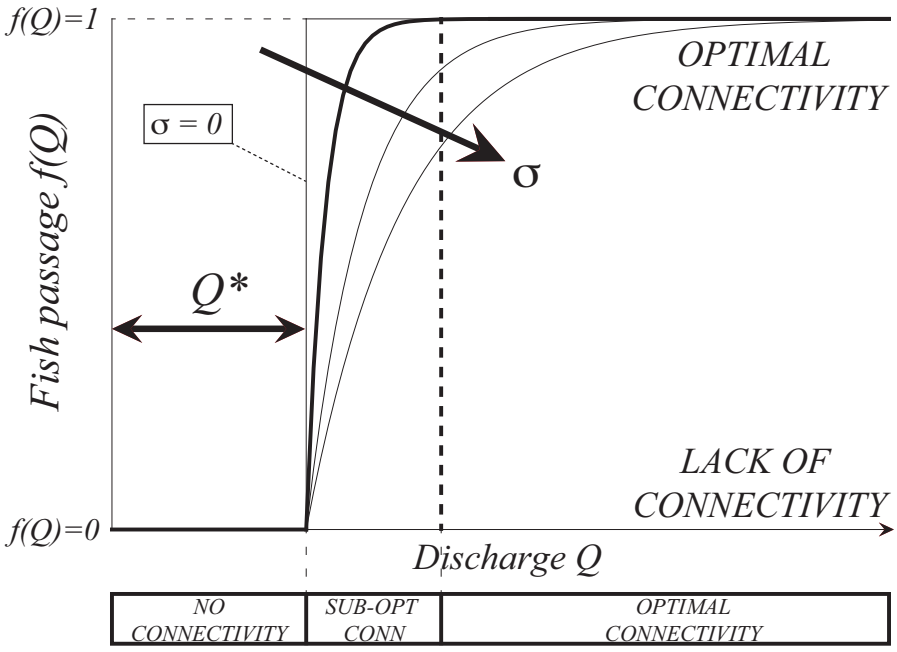

Figure 5.4: Exponential fish passage function f dependent on the river discharge (Q). The influence of the two parameters, namely the minimum threshold discharge (Q^*) and the fish vulnerability (σ), is also shown.

In this study, the annual number of females returning for spawning is assumed to depend on the seasonal average of the fish passage probability ($\bar{f}$) between the River Dee and the spawning sites located within the Girnock Burn. This can be defined as the integral over the entire range of experienced flows of the product between the fish passage function ($f(Q)$) introduced above and the streamflow distribution ($p_Q(Q)$) in the pre-spawning season (September to November).

$$\bar{f}(t) = \int_0^\infty f(Q)\; p_{Q,t}(Q)\; dQ \tag{5.3}$$

where t identifies the t-th year of the simulation. Note that in eq. (5.3), the fish passage function $f(Q)$ is kept constant (i.e. parameters Q^* and σ are not dependent on t). Considering that $\int p_Q(Q)dQ = 1$ and $f(Q) \leq 1$, $\bar{f}(t) \in [0, 1]$.
A complete lack of hydrological connectivity ($\bar{f}(t) = 0$) occurs if the observed autumn streamflows are always lower than Q^* during year t. During such low flow, the considered river section represents an hydrological discontinuity for upstream migratory fluxes and thus salmon returning in year t have a null probability of entering the Girnock

and reaching upstream spawning sites. Conversely, if the autumnal flow frequency distribution in year t only comprises discharges ensuring optimal fish passage conditions ($f(Q) = 1 \; \forall \; Q$), hydrological connectivity in that year is optimal ($\bar{f}(t) = 1$) and fish migration will not be limited by flow conditions. In general, most years, salmon experience hydrologic conditions that lie in between these two end members.
Inter-annual fluctuations of seasonal flows driven by climatic drivers such as rainfall and evapotranspiration [Zanardo et al., 2012; Botter et al., 2013; Botter, 2014] usually span a wide range of fish passage conditions $f(Q)$ and this leads to significant inter-annual variability in the average fish passage probability, $\bar{f}$.

Formulation of the mathematical model

Given the strong homing instinct of Atlantic salmon, with around 60-70 % of returning fish being from the Girnock [Youngson and Hay, 1996], adult females returning to the Girnock Burn in year t (Φ^{us}) can be expressed as a function of the number of juvenile females exiting the catchment during previous years (Φ^{ds}). The latter is estimated from the emigrants leaving the spawning site every year, assuming an even subdivision between males and females exiting the catchment.

$$\Phi^{us}(t) = \sum_{\tau=t_0}^{t-1} \Phi^{ds}(t-\tau) \left(\prod_{k=t-\tau}^{t-1} \mu(k) \right) p_d(\tau) \, \bar{f}(t) \, , \tag{5.4}$$

where t_0 is the initial year of the simulation.
Eq. (5.4) explicitly accounts for (i) marine survival rates (μ), (ii) the distribution of the delay between emigrations and immigrations ($p_d(\tau)$) and (iii) the annual fish passage probability ($\bar{f}$). In particular, the overall survival rate in eq. (5.4) is the product between survival rates of each year k, $\mu(k)$, spent by salmon in the sea. Therefore, the longer the duration of the period that a salmon spends at sea, the higher the mortality rate.
Fish passage probability reductions caused by loss of connectivity between the River Dee and spawning tributary of the Girnock, $\bar{f}(t)$, produce a similar effect, but only when female spawners come back from the sea. Although salmon have been continuously monitored since 1966, the hydrological connectivity between the River Dee and spawning sites can be evaluated only from 1972, when discharge measurements began. Similarly, simulations must end in 2011 because streamflow data are no longer available afterwards. Note that in eq. (5.4), μ depends on the year when salmon leave the Girnock ($t - \tau$),

whereas $\bar{f}$ is related to the year when salmon return for spawning (t). According to the model formulation, the parameter vector (θ) is composed of five elements, namely marine survival rates for the first (μ_0) and last (μ_F) year of the simulation, the probability of having females returning after two years in the sea (λ), the minimum flow allowing upstream movement (Q^*) and fish vulnerability to changes in flow (σ).

Model calibration

Parameters are estimated through a Markov Chain Monte Carlo (MCMC) calibration procedure using $DREAM_{ZS}$ [ter Braak and Vrugt, 2008; Vrugt et al., 2009] against observed annual salmon returns. Minimum and maximum values for model parameters during the MCMC calibration are reported in Table 5.1. Marine survival rates (μ_0 and μ_F) and the probability of having returns after two years in the sea (λ) can vary in their entire state space $[0, 1]$. Parameters of the average passage probability (Q^* and σ) are limited between 0 and 1 m^3/s (almost twice the long-term mean flow recorded at the gauging station of Littlemill). Model results are compared with the immigration dataset (annual number of adult females returning to the Girnock across the fish trap).
Standard optimization techniques are based on the maximization of the Mean Squared Error (MSE) or the Nash-Sutcliffe Error (NSE). However, Gupta et al. [2009]showed that models calibrated maximising the MSE or the NSE usually underestimate the observed variability of corresponding target outputs. They, thus, proposed an alternative criterion, namely the Kling-Gupta Efficiency ($KGE(\theta)$), which is adopted in this study as the objective function in the MCMC. The modelled mean m and standard deviation s (scaled with the same quantities observed in the dataset), as well as the cross-correlation r between model results and observations are considered as three independent objectives that need to be maximized. In particular, the following three components of the objective function can be defined: $\beta = m/m_{obs}$, $\alpha = s/s_{obs}$ and $r = Cov(mod, obs)/(s_{mod}\, s_{obs})$, where $Cov(mod, obs)$ represents the covariance between model results and observations. The optimal simulation is characterized by $\beta = 1$, $\alpha = 1$ and $r = 1$. The best simulation can thus be defined as the one for which the Euclidean distance (ED) from the optimal point (1,1,1) is the shortest. Accordingly, the Kling-Gupta Efficiency $KGE(\theta)$ is defined as:

$$KGE(\theta) = 1 - ED(\theta) = 1 - \sqrt{(r(\theta) - 1)^2 + (\alpha(\theta) - 1)^2 + (\beta(\theta) - 1)^2}\,. \tag{5.5}$$

The KGE has been widely used in the hydrological literature to identify optimal parameter ranges [Formetta et al., 2014; Dick et al., 2015; Piccolroaz et al., 2015].

5.2.2 Multi-objective optimization

The presence of a run-of-river power plant is now simulated in the Girnock Burn so as to alter the river reach between the confluence with the River Dee and upstream spawning sites in the Girnock, i.e. the same reach in which parameters of the fish passage function can be calibrated against data on salmon returns, according to the model described in the previous section. The objective in this case is to quantify the reduction of the hydrological connectivity induced by the presence of the hydropower plant. A fraction of natural streamflow is indeed diverted from the Girnock and processed for energy production implying the loss of hydrological connectivity for salmon, whose probability to successfully achieve upstream spawning sites might be endangered depending on the amount of water subtracted. The reduction of hydrological connectivity can be quantitatively evaluated adopting the same framework introduced in Section 5.2.1, but the natural flow regime during each fish migration season is replaced by the altered flow regime observed downstream of the intake of the run-of-river plant.
Incommensurable goals such as the maximization of the economic profitability and the maximization (better said, the minimization of the losses) of hydrological connectivity are then jointly considered in the definition of the optimal plant capacity trading between those objectives. The latter is directly proportional to the number of adult female salmon returning for spawning: e.g., $\bar{f}(t) = 0.35$ in eq. (5.4) means that in year t only the 35 % of salmon which are ready to complete the final run could achieve their target.

Plant characteristics

The definition of the plant location is made aiming at altering the same river reach where hydrological connectivity for salmon return can be quantitatively evaluated (see Section 5.2.1).
The plant outflow, i.e. where processed water is returned to the original stream, is thus considered to correspond with the fish trap. Whereas, the intake is chosen trying to maximize the gross hydropower potential. Particular attention is made in the protection of upstream spawning sites that represent the target of adult female's final run and

must not be altered by water abstraction otherwise any action aimed at preserving hydrological connectivity would be meaningless. Therefore, positioning the plant intake is constrained relatively downstream in the catchment, provided that available spawning sites for salmon are mainly distributed in upstream tributaries of the Girnock.
The gross hydropower potential to be maximized is proportional to the product between the contributing area at a certain cross section and the elevation difference with the outflow (i.e. the fish trap whose elevation is 248.3 m a.s.l.). This is valid only assuming that the catchment equally contributes to river streamflow and thus the contributing area is proportional to the mean flow. Furthermore, in this analysis hydraulic energy losses are considered null for simplicity.
Intake position maximizing the gross hydropower potential is 4 km upstream of the outflow (i.e. the fish trap). Under this configuration, contributing catchment at the plant intake is 20.15 km^2, and the available hydraulic head is 48.8 m, the intake elevation being 297.1 m a.s.l.. A single Francis turbine is chosen for energy production, provided that relatively low hydraulic heads and high contributing catchments usually lead designers to the same choice (e.g. see the Piova hydropower plant described in Section 3.1 which has similar characteristics).

Multi-criteria optimization

The economic profitability of the run-of-river plant in the Girnock Burn is estimated considering government incentives guaranteed for 20 years. Provided that streamflow measurements at the plant intake are available (properly scaled with the catchment area), the Net Present Value of the investment is estimated according to eqs. (2.11) and (2.20). Streamflow data are available from 1972 to 2011 (40 years), but only last 20 years are considered in this analysis. All possible time windows were analysed, and results were quite similar.
Losses of connectivity with increasing plant capacity are evaluated with eq. (5.3), where the natural flow regime during pre-spawning period (Sep to Nov) is now replaced by the flow regime downstream of the plant intake in the same season. The latter is obtained through by eq. (2.28), where the Minimum Flow Discharge is 0.03 m^3/s (that at the fish trap scaled with the different contributing area). Downstream flow regimes considered for the quantification of the hydrological connectivity in the altered river reach are those from 1992 to 2011 (same years as for NPV evaluation). A long-term (20 years) average

connectivity ($CONN$) function of the plant capacity (Q) is defined as the mean average fish passage probability.

$$\begin{aligned} CONN(Q) &= \frac{1}{20}\sum_{t=1992}^{2011}\bar{f}(t,Q) \\ &= \frac{1}{20}\sum_{t=1992}^{2011}\int_0^{\infty} f(q_{ds})\, p_{ds,Q,t}(q_{ds})\, dq_{ds} \end{aligned} \tag{5.6}$$

where:

- q_{ds} is discharge in the altered river reach downstream of the intake;
- Q is the proposed plant capacity;
- $f(q_{ds})$ is the fish passage function (see eq. 5.2 in Section 5.2.1) which is a function of observed downstream streamflows. Parameters Q^* and σ that define $f(t,q)$ are based on fish characteristics and derive from calibration of the model described in Section 5.2.1 against the salmon returns dataset;
- $p_{ds,Q,t}(q_{ds})$ is the pre-spawning flow regime observed in year t in the altered river reach between the intake and the outflow, and is thus function of the plant capacity Q (subscripts Q and t);
- $\bar{f}(t,Q)$ is the average fish passage probability in the altered river reach during year t. For simplicity the long-term (20 years) mean of $\bar{f}(t,Q)$ is considered in this analysis as a function of the plant capacity Q.

Under the proposed formulation, one may expect that the altered flow regime observed downstream of the plant intake provides values of the inter-annual hydrological connectivity which are lower than those observed under natural flow conditions. The loss of connectivity, directly proportional to reduced salmon returns for spawning, is thus function of the amount of water withdrawn from the river, which in turn depends on the plant capacity Q (the decision variable in this problem). Reduction of connectivity needs to be evaluated against improvements of the economic value of the plant induced by increasing plant capacities.

The optimal allocation of water resources between economic (maximization of $NPV(Q)$) and environmental needs (maximization of $CONN(Q)$) is based on the definition of different objective functions corresponding to different goals as a function of the only decision variable, i.e. the plant capacity.

In analogy with previous applications (chapter 4), the economic objective function is

defined as:

$$f_1(Q) = \frac{NPV_{max} - NPV(Q)}{NPV_{max} - NPV_{min}} \tag{5.7}$$

where NPV_{max} and NPV_{min} are the maximum and minimum economic values of the run-of-river plant. The economic optimization of the plant capacity (Q_{NPV}) determines $f_1 = 0$.

The objective function for the maximization of the long-term mean hydrological connectivity in the altered river reach is:

$$f_2(Q) = \frac{CONN_{max} - CONN(Q)}{CONN_{max} - CONN_{min}} \tag{5.8}$$

where $CONN_{max}$ and $CONN_{min}$ are the maximum and minimum mean connectivities values observed with increasing plant capacity. When the reduction of connectivity is minimum ($CONN(Q) = CONN_{max}$), $f_2 = 0$ since this goal is completely fulfilled and $Q = Q_{CONN}$ (environmental optimal plant capacity). Conversely, the maximum reduction of connectivity experienced in the altered river reach implies $f_2 = 1$.

In agreement with the analyses performed in chapter 4, the plant capacity is varied up to a discharge value which corresponds to a duration of 0.01. The multi-criteria optimal plant capacity (Q_{OPT}) is defined as that minimizing the distance from the origin of the Pareto chart.

5.3 Results and Discussion

This section presents main results of the application of the methodology outlined in Section 5.2. The remainder of this chapter is organized as follows: Section 5.3.1 shows performances of the modelling exercise to describing salmon returns to the Girnock Burn, which are based on a quantitative evaluation of the hydrological connectivity between the Girnock and upstream spawning sites; Section 5.3.2 describes how losses of hydrological connectivity can be compared against the increase of economic profitability of a run-of-river power plant to define the multi-criteria optimal plant capacity; finally, Section 5.3.3 discusses main implications of the obtained results.

5.3.1 Eco-hydrological model

The upper panel in Figure 5.5 shows the comparison between observed and modelled annual salmon returns for spawning. The red dots of the simulation indicate the model

results corresponding to the best simulation ($KGE_{max} = 0.65$), while the shadowed area represents the ensemble of simulations featured by acceptable performances (i.e. $KGE/KGE_{max} > 0.9$). Model results are generally in good agreement with the observations. The observed dynamic is not well described at the beginning of the simulation (1972-1977) and only occasionally in the following years (1981-1982, 1985). Panel B

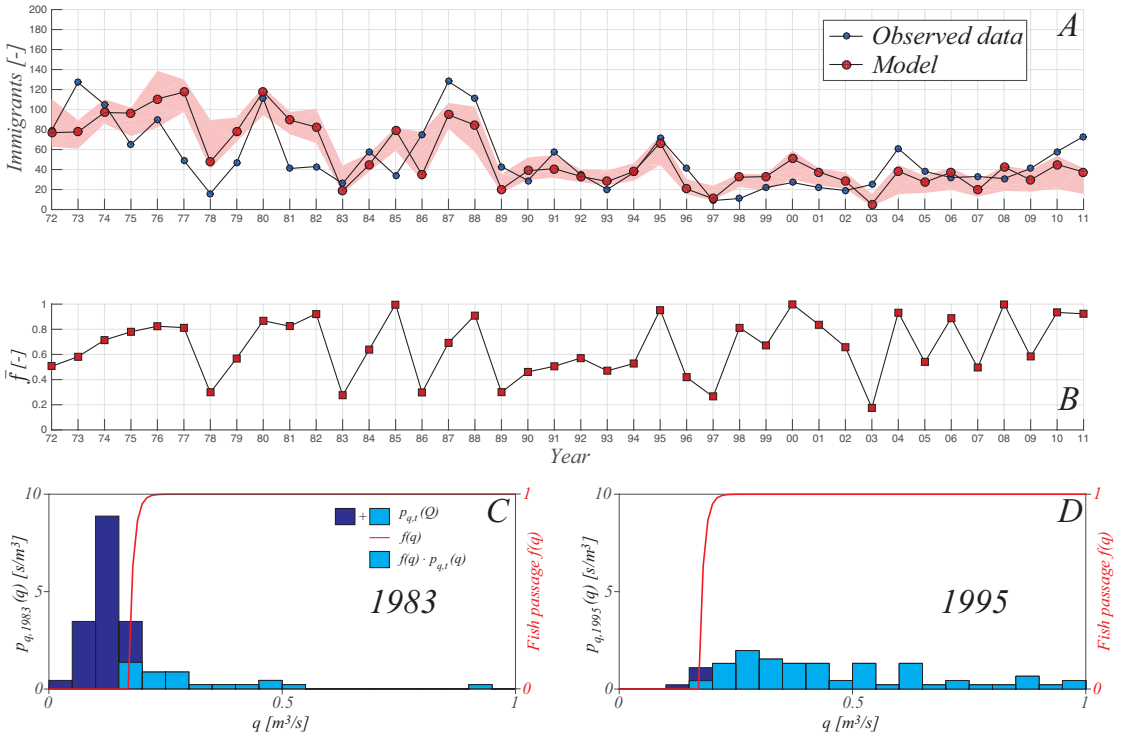

Figure 5.5: The upper panel shows observed annual salmon returns (blue dots), model results corresponding to the best simulation (red dots) and the ensemble of simulation featured by acceptable performances (shadowed red area); the annual average passage probability characterizing the best model run is shown in panel B. Panels C and D show that the annual average passage probability has been calculated by the model as the area of the product (light blue) between a fish passage function (red curve) and the flow regime annually observed in fall (dark blue). These plots refer to years characterized by relatively dry (1983, panel C) or wet (1995, panel D) hydrologic regimes, which gave $\bar{f}(1983) = 0.24$ and $\bar{f}(1995) = 0.96$.

of Figure 5.5 shows the annual average passage probability ($\bar{f}$) for the best model run in terms of the KGE. Important findings emerge from the comparison between the observed data and the corresponding seasonal average of the passage probability. In particular, positive peaks in the observed salmon returns (e.g. 1988, 1995 and 2004)

Table 5.1: Minimum and maximum values for the Markov Chain Monte Carlo (MCMC) calibration of each parameter of the model. The parameter set giving the highest performance of the model is also reported in the table (last column).

Parameter	Symbol	Units	Min	Max	Best
Minimum threshold discharge	Q^*	[m^3/s]	0	1	0.17
Fish vulnerability	σ	[m^3/s]	0	1	0.01
Marine survival rate (first year)	μ_0	[-]	0	1	0.37
Marine survival rate (last year)	μ_F	[-]	0	1	0.23
Probability of 2-years delay	λ	[-]	0	1	0.24

are well captured by the model mainly because the average passage probability in those years approaches one (i.e. an optimal hydrological connectivity). Likewise, low values of the average passage probability induced by seasonal droughts allow the model to capture negative peaks of the observed dataset (e.g. 1978, 1983 and 1997).

Panels C and D of Figure 5.5 highlight the temporal variability of the annual average passage probability $\bar{f}(t)$. These examples refer to the flows observed between September and November of 1983 (panel C) and 1995 (panel D), that were the driest and wettest falls of the last 50 years, respectively. Red curves represent the shape of the fish passage function $f(q)$ determined by parameters Q^* and σ giving best performances of the model (Table 5.1). The product between $p_{q,t}(q)$ (dark and light blue bars) and $f(q)$ determines the light blue histogram which carries information about the occurrence probability of those flows that allow salmon to reach upstream spawning sites. The area underlying this histogram is the average passage probability $\bar{f}(t)$ during year t. The inter-annual variability of the flow regime produces different values for $\bar{f}(t)$, as shown by Figure 5.5B. In particular, arid years imply average passage probabilities approaching zero ($\bar{f}(1983) = 0.24$) whereas higher flows ensure much higher fish passage probabilities ($\bar{f}(1995) = 0.96$). In the best simulation, salmon vulnerability σ is very low (0.01 m^3/s). Therefore the optimal fish passage function shown by Figure 5.5C-D is basically a step function rapidly increasing from 0 to 1 for $Q^* = 0.17\, m^3/s$. Therefore, a simplified version of the model in which fish vulnerability is assumed to be zero ($\sigma = 0$) and $f(q)$ is a step function was also tested. Performances are quite satisfactory also in this

case ($KGE_{max} = 0.64$), especially in view of the low number of parameters (see Section 5.3.3).

Figure 5.6 shows the stationary posterior pdf of each parameter provided by the MCMC calibration. The vertical dashed line in each plot marks the parameter value giving the best model output (i.e. shown in the upper panel of Figure 5.5). The posterior pdf of the minimum threshold discharge (Q^*) ranges between 0 and 0.3 m^3/s, with a mean of 0.07 m^3/s. The posterior pdf of the fish vulnerability (σ) varies across the full range of values explored. However, higher probabilities characterize low vulnerabilities ($\sigma < 0.5$ m^3/s). Marine survival rates in the first (μ_0) and last (μ_F) year of the simulation are both described by hump-shaped posterior distributions with μ_0 ranging between 0.2 and 0.6, and μ_F ranging between 0.1 and 0.4. It is worth noting that the optimal survival rates decrease from 0.37 (first year) to 0.23 (last year). This confirms that mortality during the marine period has increased during the last fifty years [Chaput, 2012; Lacroix, 2014; Moore et al., 2014]. The posterior distribution of parameter λ is characterized by an enhanced variability. However, observed salmon returns seem to be better represented by low values of λ, which correspond to a preferential delay of three years. The value of λ giving best model results is 0.24. The corresponding average delay between emigration and immigration is larger than 2 years.

To better assess the relationship between the inter-annual variability of the hydrologic regime observed in the Girnock Burn and salmon migratory dynamics, results obtained through eq. (5.4) (hereafter termed Variable Hydrological Connectivity model, VHC) were compared against those from a modified version of the model where the annual fish passage probability is constant and independent on the observed streamflow regime (i.e. $\bar{f}(t) = 1\,,\ \forall\ t$) (hereafter termed Constant Hydrological Connectivity model, CHC). Under the latter assumption, the CHC model parameter vector (θ) is composed of three elements $\theta = (\mu_0, \mu_F, \lambda)$.

Figures 5.7A-B compare the observed number of female spawners returning to the Girnock with the optimal simulations performed using both the VHC and CHC models. Green dots in Figure 5.7A indicate the best simulation obtained assuming a constant hydrological connectivity. Conversely, red dots in Figure 5.7B represent the optimal simulation when the annual average fish passage probability is seen as a function of the observed pre-spawning flow regime (VHC model).

Overall, model performances decline if the influence of the observed streamflow regime is

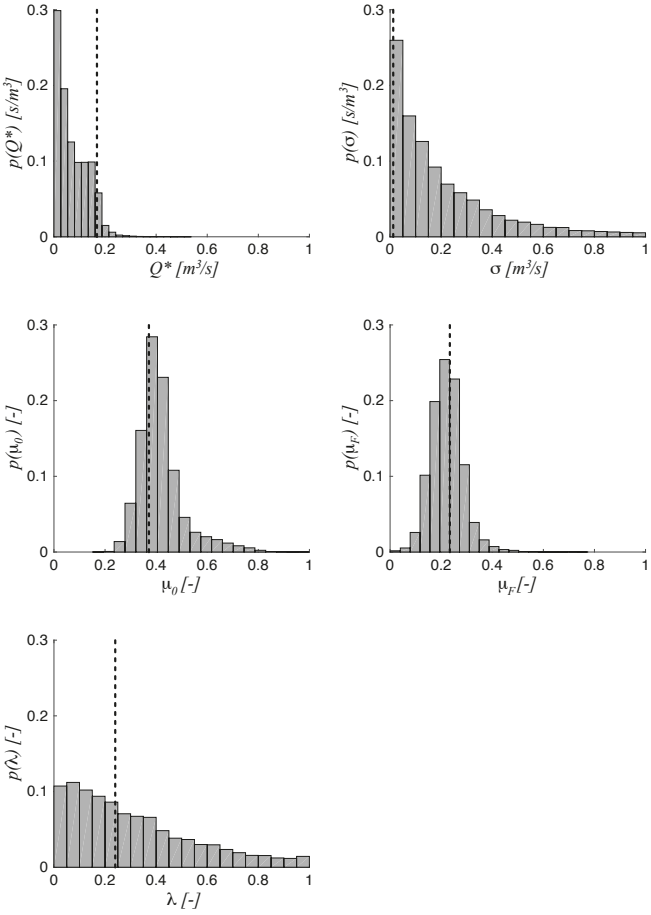

Figure 5.6: Stationary posterior frequency distribution of each parameter provided by the Markov Chain Monte Carlo calibration. Vertical dashed lines mark the value giving the best model output: Q^* =0.17 m^3/s, σ =0.01 m^3/s, μ_0 =0.37, μ_F =0.23 and λ =0.24.

no longer taken into account ($KGE_{VHC} = 0.65$ vs. $KGE_{CHC} = 0.61$). In particular, the VHC model outperforms the CHC model in reproducing the mean and the standard

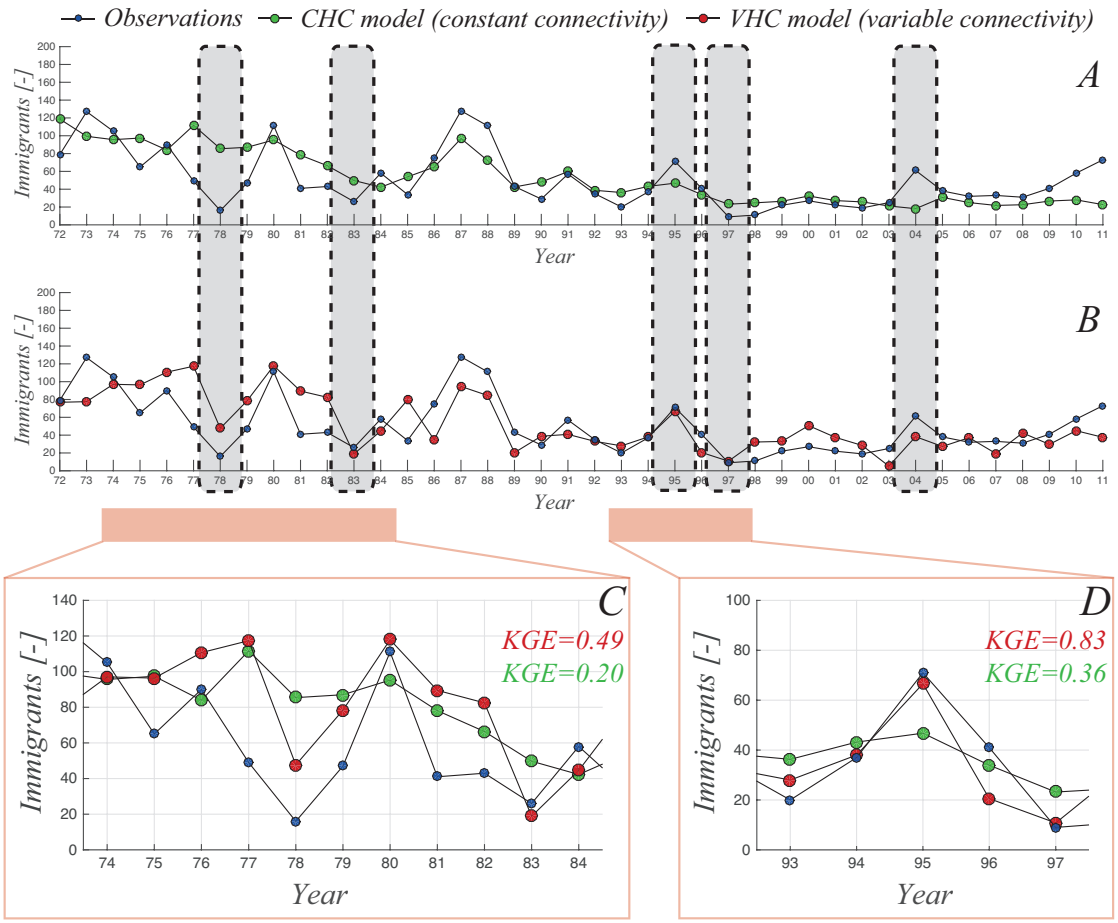

Figure 5.7: Comparison between the observed number of female spawners returning to the Girnock Burn and the optimal simulation performed using the Variable Hydrologic Connectivity model (VHC, panel A) and the Constant Hydrologic Connectivity model (CHC, panel B). Shadowed grey areas highlight years where the VHC model better reproduces positive and negative peaks in the observed dataset. Panels C and D emphasize the reduced performances of the CHC model in 1974-1984 and 1993-1997 by showing VHC (red dots) and CHC (green dots) together against the observed dataset (blue dots).

deviation of the observed number of returning salmon ($m_{obs} = 51.0$ and $s_{obs} = 31.7$; $m_{VHC} = 52.8$ and $s_{VHC} = 30.9$ vs. $m_{CHC} = 53.1$ and $s_{VHC} = 30.0$). In addition, the cross-correlation between observed and modelled salmon returns is higher when adopting a variable hydrological connectivity ($r_{VHV} = 0.65$ vs. $r_{CHV} = 0.62$).

In those years highlighted by the shadowed grey areas, a time-variant connectivity allows the VHC model to better reproduce positive and negative peaks in the observed

dataset. This is not the case for the CHC model. For instance, the relative absolute error between observed and modelled salmon returns in 1978 is almost 2.5 times larger when the CHC is used. Similarly, in 1997 the error decreases from 160 % to 20 % if the influence of the observed flow regime on salmon migration is taken into account.
The importance of the inter-annual variability of the hydrological connectivity on salmon migratory dynamics is further emphasized in Figure 5.7C-D. The CHC best simulation (green dots) shows a poor agreement with the observed data in 1974-1984 and 1993-1997. When the hydrologic control is removed, the KGE of the model falls from 0.49 to 0.20 in 1974-1984 and from 0.83 to 0.36 in 1993-1997. The CHC model is strongly penalised by the different variability of the observed and modelled number of salmon returns ($s_{obs} < s_{mod}$) but also because the observed and CHC-modelled time series are poorly correlated (e.g., $r = 0.37$ in 1974-1984).

5.3.2 Trade-offs between NPV and connectivity

The hydrological connectivity in the river reach between the intake and the outflow of the run-of-river plant proposed in the Girnock is quantified according to eq. (5.6) considering the altered flow regime function of the plant capacity Q ($p_{ds,Q}(q_{ds})$) and parameters of the fish passage function ($f(q_{ds})$) which resulted from the calibration shown in the previous section. Parameters $Q^* = 0.17$ m^3/s and $\sigma = 0.01$ m^3/s define the fish passage function that give highest performances in modelling female salmon returns for spawning. These values of Q^* and σ are considered here to model losses of hydrological connectivity induced by different plant capacities.
Solid lines in the left charts of Figure 5.8 show how the Net Present Value of the plant (NPV, upper chart) and the hydrological connectivity in the altered river reach (CONN, lower chart) vary with increasing plant capacity. The NPV shows the typical hump shape that was found in previous applications analysed in this work (see e.g. Figure 4.2). In particular, it reaches a maximum for $Q_{NPV} = 0.67$ m^3/s, which provides an economic profitability of about 860 k£ in 20 years. However, if the plant is designed to maximize the economic value, the mean hydrological connectivity in the altered river reach during the functioning period of the plant is 0.11. In this case, the river reach between the intake and the outflow would represent a barrier for salmon upstream migration with only the 11 % of adult females arrived at the confluence between the Dee and the Girnock that successfully reaches their final target (i.e. upstream spawning sites). Under natural flow

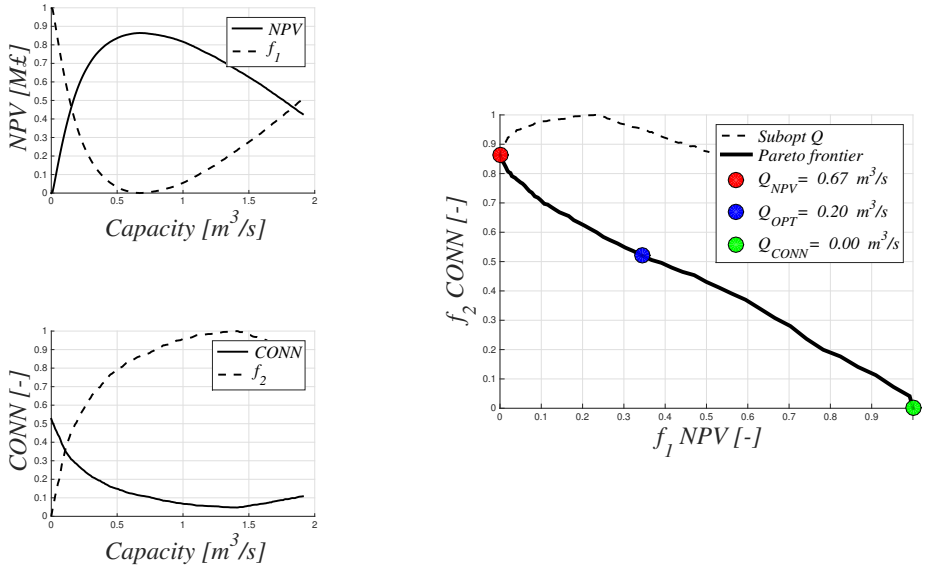

Figure 5.8: Left charts describe economic (NPV, upper) and environmental ($CONN$, lower) performances of the run-of-river plant in the Girnock Burn with increasing plant capacity (Q) and correspondent objectives function $f_1(Q)$ and $f_2(Q)$. The right chart shows efficient (solid line, i.e. the Pareto frontier) and non-efficient (dashed line) plant capacities obtained in this application, with remarkable capacities highlighted by markers.

conditions, this fraction would grow up to more than 50 % ($CONN(Q = 0) = 0.53$), implying that about 80 % of the natural hydrological connectivity is lost by the presence of the run-of-river plant when economy is maximized.

In the left plots of Figure 5.8, dashed lines are the objective functions corresponding to each goal, as defined by eqs. (5.7) and (5.8). Objective functions $f_1(Q)$ and $f_2(Q)$ assume values equal to zero (one) when the correspondent goal is completely fulfilled (unfulfilled) in the range of plant capacities investigated. In this case, $f_1(Q_{NPV}) = 0$ and $f_1(Q = 0) = 1$, the latter implying that the economic worst situation is when the plant is absent and no incomes are generated. Avoiding the construction of the plant simultaneously corresponds to the best condition for salmon upstream migration (i.e., $f_2(Q_{CONN} = 0) = 1$), which progressively becomes more difficult when capacity increases (i.e., $f_2(Q)$ increases with Q).

Objective functions $f_1(Q)$ and $f_2(Q)$ clearly represent contrasting goals dependent only on the plant capacity. They can thus be simultaneously optimized identifying the Pareto

frontier in a f_1-f_2 chart, as shown in the right plot of Figure 5.8. Accordingly, each point in the plot represents a tentative plant capacity for which economic and connectivity performances are evaluated. Solid line represents the Pareto frontier, i.e. the set of capacities for which improvements in one objective need to be made at the detriment of the other objective. Every plant capacity in the Pareto frontier represents an efficient design choice among these two contrasting goals. The Pareto frontier contains $Q_{NPV} = 0.67$ m^3/s and $Q_{CONN} = 0$ m^3/s, respectively red and green dots in the right plot of Figure 5.8, which are the capacities maximizing the economic value of the plant or minimizing the loss of connectivity in the altered river reach. Non-efficient capacities are those located along the dashed line in the same plot. They are capacities larger than Q_{NPV} for which both profitability and alteration of hydrological connectivity could be improved with a different design choice (i.e. selecting a plant capacity on the Pareto frontier).
The plant capacity which is the nearest to the origin of axis is the multi-objective optimal plant capacity, and in this case is $Q_{OPT} = 0.20$ m^3/s. Correspondent performances are $NPV(Q_{OPT}) = 566$ k£ and $CONN(Q_{OPT}) = 0.28$. Therefore, multi-criteria optimal allocation of water resources among the two contrasting goals considered in this analysis suggests that limiting the profitability at the 65 % of the maximum economic value of the plant could benefit the hydrological connectivity in the altered river reach, which almost triples from 0.11 (if $Q = Q_{NPV}$) to 0.28 (if $Q = Q_{OPT}$).

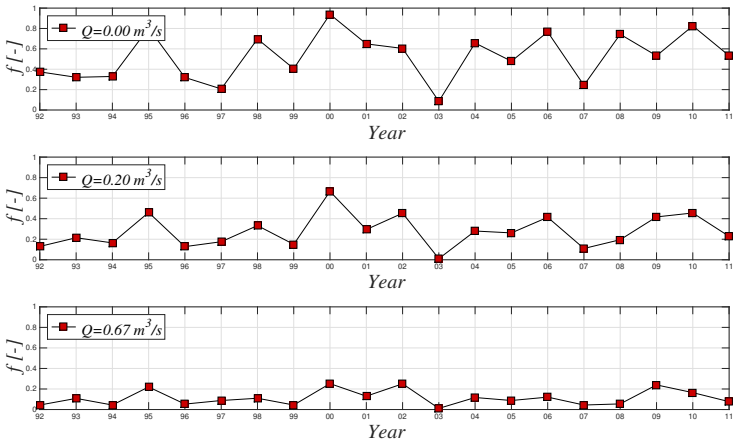

Figure 5.9: Inter-annual variability of the average passage probability ($\bar{f}(t)$) under different design scenarios: natural flow conditions $Q = 0$ m^3/s in the top, $Q = Q_{OPT} = 0.20$ m^3/s in the middle, and $Q = Q_{NPV} = 0.67$ m^3/s in the bottom.

Figure 5.9 shows the inter-annual variability of the average passage probability ($\bar{f}(t)$) under different design scenarios. The long-term mean of the average passage probability is the mean hydrological connectivity ($CONN(Q)$) whose maximization is here considered as the environmental goal. Top panel in Figure 5.9 represents the inter-annual passage probability under natural flow conditions ($Q = Q_{CONN} = 0$ m^3/s, the green dot in in the right plot of Figure 5.8), for which $CONN(Q_{CONN}) = 0.53$.

Interesting findings emerge analysing how the system responds to different withdrawal scenarios. In Figure 5.9, middle and bottom panels show $\bar{f}(t)$ when, respectively, multi-criteria optimal or economic optimal plant capacities are accounted for. In the latter, reduction of connectivity is maximum, with $CONN(Q_{NPV}) = 0.11$. When a larger fraction of water is left to the Girnock, and the trade-off between economic and environmental goals is achieved, $CONN(Q_{OPT}) = 0.28$.

These findings are the result of non-linear processes affecting the reduction of the connectivity with increasing removal of discharge available for fish movements. Main drivers of this non-linearity are the tails of the annual distribution of streamflows during pre-spawning season. In particular, in pre-spawning seasons frequently characterized by moderately high flows, it is highly probable to observe discharges bypassing the plant (i.e. exceeding the maximum flow that the plant can process, which is the plant capacity). In such cases, increasing the capacity induces limited reductions of $\bar{f}$ because bypass flows still maintain a satisfactory connectivity in the altered river reach. The same does not occur if the exceedance probability of moderately high flows is low. In such circumstances, the hydrological connectivity in the altered river reach is mainly given by flows which can be processed by a run-of-river plant. Hence, increments of the plant capacity progressively remove fractions of water which are fundamental for maintaining good connectivity between the intake and the outflow. Reductions of $\bar{f}$ with Q are thus more (less) pronounced in years where exceedance probability of such relatively high flows is low (high). In Figure 5.9, e.g. 2009 and 2010 clearly show that, even if $\bar{f}(2009) < \bar{f}(2010)$ in absence of the plant, increases of Q progressively make the relationship changing: for $Q = Q_{OPT}$, 2009 and 2010 are characterized by similar values of $\bar{f}$; whereas for $Q = Q_{NPV}$, connectivity is higher in 2009 (which was less connective than 2010 under natural flow conditions).

Particularly important is also the role of the Minimum Flow Discharge in supporting the hydrological conditions downstream of the plant intake, which deserves specific ad-

ditional analyses. The definition of the fish passage function in eq. (5.2) that provides (once calibrated) satisfactory reproductions of adult salmon returns, eliminates any contribution to connectivity of discharges lower than Q^*. For this reason, an alternative management policy at the plant intake is tested here, which prescribes that during pre-spawning seasons the default value of residual flow (i.e. Q_{95}) is increased above Q^*. In particular, in this case MFD is set to 0.18 m^3/s, a value ensuring optimal connectivity (i.e. $f(0.18\,m^3/s) \approx 1$ if $\sigma = 0.01$ m^3/s). This management scenario is based on the concept that in seasons when hydrological connectivity is fundamental for salmon upstream migration, Water Managers might reduce incomes from energy selling to guarantee in the Girnock flow conditions completely allowing fish movements. Certainly, this management rule could not be performed when flows are insufficient independently on the presence of the run-of-river plant (i.e. climatic-driven drought in pre-spawning seasons). Figure 5.10 compares economic (NPV, left) and environmental ($CONN$, right) perfor-

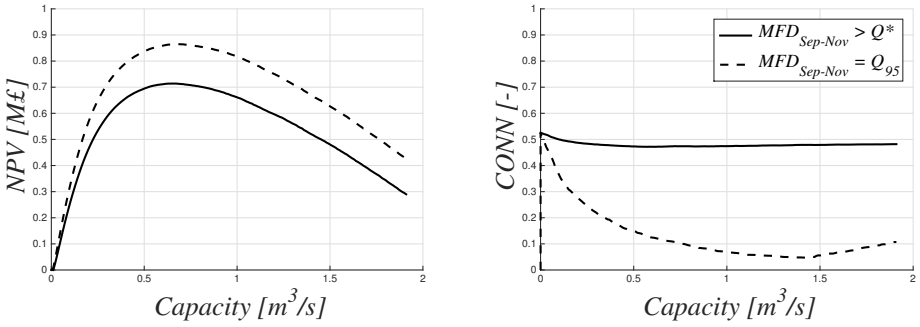

Figure 5.10: Comparison between economic (NPV, left) and environmental ($CONN$, right) performances of the run-of-river plant in the Girnock Burn with increasing plant capacity (Q) under different pre-spawning Minimum Flow Discharge scenarios. Dashed lines represent NPV and $CONN$ when the MFD prescribed by law (Q_{95}) is maintained downstream, whereas solid lines represent same quantities when MFD is increased and equalled to Q^* only in the pre-spawning season (Sep to Nov).

mances of the run-of-river plant in the Girnock Burn with increasing plant capacity (Q) under different Minimum Flow Discharge scenarios. When the MFD prescribed by law (Q_{95}) is maintained downstream, performances are the same showed by left charts in Figure 5.8. Interestingly, if MFD is increased above Q^*, reductions of the hydrological connectivity in the altered river reach are strongly limited, regardless of the choice of the plant capacity. Therefore, one may speculate that the best choice for the plant

capacity is that maximizing the economic profitability ($Q_{NPV} = 0.65$ m^3/s) which guarantees about 700 k£ in 20 years, with almost any alteration of the natural hydrologic connectivity.

5.3.3 Discussion

Although the general influence of the hydrological connectivity on fish migratory dynamics has been already documented in the literature [Freeman et al., 2007; Jonsson et al., 2007; Mitchell and Cunjak, 2007; Gibbins et al., 2008; Tetzlaff et al., 2008; Cunjak et al., 2013], the quantitative assessment of ecologically-relevant flow thresholds remains problematic. From this perspective, this work represents a proof of concept about how availability and variability of flows during the migration season could affect salmon returns for spawning. The modelling exercise also illustrates how the effect of seasonal flow regimes can be summarised by a synthetic index ($\bar{f}$) that expresses the average probability for fish to move across river networks during a given year/season.
The novelty of this work stems from the development of a simple and parsimonious model based on a probabilistic assessment of the hydrological connectivity to reproduce seasonal fish migratory dynamics. The framework is quite general in the mathematical formulation and could be extended to include the effect of other environmental factors (e.g. temperature, density-dependent competition) and identify the hydrologic controls on spawning migrations in rivers where sufficient data are available. Many other countries with rivers hosting Atlantic salmon populations have similar long term monitoring sites like the Girnock (e.g. Kennedy and Crozier [2010]; Cunjak et al. [2013]).
Results confirm that the inter-annual variability of hydrological connectivity contributes to explain the observed temporal pattern of salmon returns. Lack of hydrological connectivity can reduce the number of immigrating salmon by up to 80 % of the potential value under optimal hydrologic condition (Figure 5.5B).
Interestingly, the value of minimum discharge required to guarantee the hydrological connectivity between the Girnock and the Dee ($Q < 0.30$ m^3/s) suggested by this modelling exercise corresponds well with those found, in a more qualitative analysis, by Tetzlaff et al. [2008], who stated that only 30 % of fish enter the Girnock on flows lower than the long term median discharge during the spawning season (0.25 - 0.30 m^3/s). Based on the stage-discharge relationship at the Girnock gauging station, this implies that the persistence of water stages lower than 0.28 m may threaten adult salmon migrations to

the Girnock Burn.

When fish vulnerability (σ) is set to zero, model performances are still satisfactory in the case study examined in this paper. In this case, the minimum flow threshold (Q^*) becomes the only parameter required to define fish passage function ($f(q)$). Whereas the physical underpinning of stepwise fish passage functions may be questioned, this simplified version of the model can be useful for management applications, where the impact of different minimum flow requirements on hydrological connectivity could be easily assessed.

These findings, however, are case-specific as they depend on local characteristics of the considered river (e.g. bed morphology and flow regime) and calibration of parameters is unavoidable. Hence, the model has limited predictive potential in the absence of hydro-ecological datasets. Stage and discharge thresholds identified in this work can be different from those of other rivers. However, this work sets a general and transferable quantitative framework that establishes causal relationship between salmon influx and outflux, and helps in disentangling hydrological and ecological controls on fish migratory dynamics.

The eco-hydrological framework adopted for modelling salmon migratory dynamics may provide useful information in the analysis of the impact induced by anthropogenic uses of water resources on fish communities. Many regions of the world are experiencing a significant exploitation of riverine water resources for anthropogenic uses [Jackson et al., 2001; Postel and Richter, 2003; Nilsson et al., 2005; Carlisle et al., 2011; Destouni et al., 2013; Birkel et al., 2014]. While the human exploitation of freshwater is introducing strong alterations of hydrologic conditions at multiple spatial and temporal scales, the ecological and morphological consequences of water abstractions are still poorly understood [Nilsson and Berggren, 2000; Rosenberg et al., 2000]. Hence, the proposed tool may help including the hydrological connectivity in the planning of restoration and conservation initiatives aimed at preserving and revitalising ecological services provided by streams and rivers. For instance, simple influx/outflux models explicitly quantifying the influence of streamflow on riverine ecosystems as the one proposed in this chapter (if properly supported by extensive hydro-ecological datasets from other long-term monitoring sites) could be used to identify hotspots of connectivity [Fullerton et al., 2010; Nunn et al., 2010] and to define flow requirements and policy rules that are deemed necessary to achieve target levels of connectivity in relation to critical ecological processes. Nu-

merical investigations carried out in this chapter evidenced the key role of environmental flow prescriptions, which is fundamental in supporting hydrological connectivity in river reaches altered by water abstractions. As the Scottish Environmental Protection Agency (SEPA) prescribed, Q_{95} is the minimum residual flow to be maintained downstream of water withdrawals, but particular attention should be made when regulating water abstractions in catchments hosting well structured and developed fish communities whose survival is based on the availability and physical connection between different habitats (feeding, spawning, refugia, etc.).

River network fragmentation at catchment-scale possibly induced by local drops of connectivity is still poorly understood. Local drops of connectivity induced by run-of-river plants not only have direct negative impact on the reaches between intake and outflow, but may contribute to the fragmentation of the overall river network [Widder et al., 2014], disconnecting different type of habitats supplied by the river system. For instance, plants built in remote upstream tributaries could have very limited impact on riverine ecosystems if they are not limiting access to fundamental habitats hosted therein. However, considerable portions of the catchment may become unavailable to fishes and biomes due to local loss of connectivity in critical nodes of the river network. The application carried out in this chapter evidenced the simplicity and potential utility for designers and water managers of the proposed tools. However, the multi-objective optimization should be performed based on the optimization of catchment-scale measures of network connectivity, therefore accounting for the actual position of the plants within the catchment. Further investigations should thus investigate the resilience of river networks to local reductions of connectivity induced by human exploitation of water resources.

Chapter 6

Conclusions and future developments

Given the recent expansion of run-of-river plants in mountain regions and the implied disturbance on riverine ecosystems addressed in this thesis, alterations between the intake and the outflow should be carefully considered in the design of new plants. Moreover, policy actions aimed at supporting small hydropower should explicitly account for the environmental impact induced by water abstractions, and not only be based on the nominal/maximum power of plants. The relationship between energy production and impacts was found to be typically non-linear and strongly dependent on the flow regime at the plant intake. This thesis aims at providing objective tools to address the preliminary choice of the capacity of a run-of-river hydropower plant when the economic value of the plant is maximized against environmental goals, such as the minimization of the hydrologic disturbance in the altered river reach, or the maximization of the hydrological connectivity allowing fish migrations. This is done using the concept of Pareto-optimality, which is a powerful tool suited to face multi-objective optimization in presence of conflicting goals.
Main findings of this work can be summarized as follows:

- The analytical model developed and applied in chapter 3 consists of a set of analytical expressions for the design capacity which maximizes the produced energy and the profitability of the plant. Such expressions can be easily applied to different hydrologic/economic contexts, or further simplified to provide immediate estimates of the duration of the optimal capacity of a plant. The ease of appli-

cation of the method makes it a valuable tool for scenario analysis and decision making. The robustness of the method, as well as its flexibility and generality, makes it a useful tool for selecting the optimal design flow in practical application, as demonstrated by the applications presented in chapter 3. In particular, the duration of economic optimal capacity was found to strongly depend on the incoming streamflow regime. Flow regimes in mountain regions are usually characterized as persistent, when the variability of daily flows is limited ($CV(q) < 1$), or erratic, when $CV(q) > 1$, depending on climatic and landscape attributes. Run-of-river plants built in persistent rivers are economically optimized by capacities corresponding to relatively large durations if compared with those in erratic case studies. The choice of higher capacities in erratic flow regimes suggests that it is more convenient to activate the plant less frequently and thus process less probable but larger streamflows in regimes where the variability of flows is pronounced.

- The thesis provides a set of objective tools to address the choice of the capacity when the economic value of the plant and the hydrologic alteration of the flow regime are simultaneously accounted for. Results show that optimal design features are strongly affected by the flow regime at the plant intake. In the persistent case study, the emerging Pareto front is upwardly bounded by the capacity that maximizes the profits, and a trade-off between profitability and hydrologic alteration is achieved reducing the plant capacity below the economic optimum. This choice is well identified regardless of the specific hydroloigc index considered in the optimization. Conversely, in the erratic case study, the Pareto front is made up by disconnected ranges of capacities, and distinct optimal trade-offs are available depending on which statistic is predominant. The latter optimal capacities may be less identified because a broad range of capacities exists that would produce analogous earnings and a similar hydrologic disturbance.
- A detailed, long-term dataset on Atlantic salmon migration in the River Dee catchment (Scottish Highlands, UK) is adopted to test an eco-hydrological model addressing the influence of the inter-annual variability of natural flow regime on migratory dynamics of salmon. The model is grounded on a probabilistic approach for the quantitative evaluation of the hydrological connectivity for adult salmon under natural or disturbed flow conditions. This modelling exercise confirms that water abstractions for human needs induce ecologically-meaningful and quantifi-

able impacts on the connectivity of altered river reaches, in turn limiting salmon migratory dynamics.

- Reductions of connectivity can be analytically included in a multi-objective optimization of the capacity of run-of-river hydropower plants, to get a trade off between connectivity and economic profitability.

  Non-linear processes affecting the reduction of connectivity with increasing removal of discharge for fish movements are observed, when the impact of run-of-river plants on the flow regime is considered. Main drivers of this non-linearity are the tails of the annual distribution of streamflows during pre-spawning season. Reductions of the annual hydrological connectivity are indeed more pronounced in years where exceedance probability of relatively high flows is low.

  A relevant feature of management scenarios when hydrological connectivity is concerned is the Minimum Flow Discharge (i.e. the constant residual flow maintained downstream of water abstractions). Analyses show that if MFD is suitably increased, reductions of the hydrological connectivity in the altered river reach are limited, regardless of the choice of the plant capacity. In this case, the most important decision variable for Water Managers facing the need of maintaining good levels of connectivity in the catchment is an accurate definition of the Minimum Flow Discharge, which must be carefully determined and quantified. If minimum flows are mis-quantified, the chance of maintaining the natural connectivity between the intake and the outflow through the plant capacity is strongly reduced.

The multi-objective approach developed in this thesis offers an objective basis to identify optimal design solutions and policy actions that explicitly account for the actual disturbance of small power plants on river flow regimes and hydrological connectivity.
Nevertheless, further validations of the proposed methodology shall be recommended, especially in those regions hosting ecologically and economically important biological communities where long-term eco-hydrological data are available. Design tools as those identified in this work may be helpful in practical applications either for engineering companies or public authorities.
Similar analyses could be extended from reach- to network-scale through the assessment of the overall catchment-scale impact of multiple plants installed along the same river expressed in terms of reduction of the global connectivity within the river network.
Small hydro technology is likely to gain a higher social value in the next decades if

the environmental and hydrologic footprint associated to the energetic exploitation of surface water will take a higher priority in civil infrastructures planning.

Bibliography

Aggidis, G., Luchinskaya, E., Rothschild, R., and Howard, D. (2010). The costs of small-scale hydro power production: Impact on the development of existing potential. *Renewable Energy*, 35(12):2632 – 2638.

Anagnostopoulos, J. S. and Papantonis, D. E. (2007). Optimal sizing of a run-of-river small hydropower plant. *Energy Conversion and Management*, 48(10):2663 – 2670.

Anderegg, W. R. L., Prall, J. W., Harold, J., and Schneider, S. H. (2010). Expert credibility in climate change. *Proceedings of the National Academy of Sciences*, 107(27):12107–12109.

Bacon, P. J., Gurney, W. S. C., Jones, W., McLaren, I. S., and Youngson, A. F. (2005). Seasonal growth patterns of wild juvenile fish: Partitioning variation among explanatory variables, based on individual growth trajectories of Atlantic salmon (Salmo salar) parr. *J. Anim. Ecol.*, 74:1–11.

Bartle, A. (2002). Hydropower potential and development activities. *Energy Policy*, 30(14):1231–1239.

Basso, S. and Botter, G. (2012). Streamflow variability and optimal capacity of run-of-river hydropower plants. *Water Resources Research*, 48(10).

Basso, S., Schirmer, M., and Botter, G. (2015). On the emergence of heavy-tailed streamflow distributions. *Advances in Water Resources*, 82:98 – 105.

Baxter, G. (1961). River utilization and the preservation of migratory fish life. *Proceedings of the Institution of Civil Engineers*, 18(3):225–244.

Birkel, C., Soulsby, C., Ali, G., and Tetzlaff, D. (2014). Assessing the cumulative impacts of hydropower regulation on the flow characteristics of a large atlantic salmon river system. *River Research and Applications*, 30(4):456–475.

Biswal, B. and Marani, M. (2010). Geomorphological origin of recession curves. *Geophysical Research Letters*, 37(24). L24403.

Bombino, G., Boix-Fayos, C., Gurnell, A. M., Tamburino, V., Zema, D. A., and Zimbone, S. M. (2014). Check dam influence on vegetation species diversity in mountain torrents of the mediterranean environment. *Ecohydrology*, 7(2):678–691.

Bombino, G., Gurnell, A. M., Tamburino, V., Zema, D. A., and Zimbone, S. M. (2009). Adjustments in channel form, sediment calibre and vegetation around check-dams in the headwater reaches of mountain torrents, Calabria, Italy. *Earth Surface Processes and Landforms*, 34(7):1011–1021.

Botter, G. (2014). Flow regime shifts in the Little Piney creek (US). *Advances in Water Resources*, 7:44–54.

Botter, G., Basso, S., Porporato, A., Rodriguez-Iturbe, I., and Rinaldo, A. (2010). Natural streamflow regime alterations: Damming of the Piave river basin (Italy). *Water Resources Research*, 46(6).

Botter, G., Basso, S., Rodriguez-Iturbe, I., and Rinaldo, A. (2013). Resilience of river flow regimes. *Proceedings of the National Academy of Sciences*, 110(32):12925–12930.

Botter, G., Porporato, A., Rodriguez-Iturbe, I., and Rinaldo, A. (2007). Basin-scale soil moisture dynamics and the probabilistic characterization of carrier hydrologic flows: Slow, leaching-prone components of the hydrologic response. *Water resources research*, 43(2).

Brown, R. S., Hubert, W. A., and Daly, S. F. (2011). A primer on winter, ice, and fish: what fisheries biologists should know about winter ice processes and stream-dwelling fish. *Fisheries*, 36(1):8–26.

Brutsaert, W. and Nieber, J. L. (1977). Regionalized drought flow hydrographs from a mature glaciated plateau. *Water Resources Research*, 13(3):637–643.

Budyko, M. I. (1974). *Climate and life*. Academic, New York.

Carlisle, D., Wolock, D., and Meador, M. (2011). Alteration of streamflow magnitudes and potential ecological consequences: A multiregional assessment. *Frontiers in Ecology and the Environment*, 9(5):264–270.

Castelletti, A., Pianosi, F., Soncini-Sessa, R., and Antenucci, J. P. (2010). A multiobjective response surface approach for improved water quality planning in lakes and reservoirs. *Water Resources Research*, 46(6).

Ceola, S., Botter, G., Bertuzzo, E., Porporato, A., Rodriguez-Iturbe, I., and Rinaldo, A. (2010). Comparative study of ecohydrological streamflow probability distributions. *Water Resources Research*, 46(9).

Ceola, S., Hodl, I., Adlboller, M., Singer, G., Bertuzzo, E., Mari, L., Botter, G., Waringer, J., Battin, T. J., and Rinaldo, A. (2013). Hydrologic variability affects invertebrate grazing on phototrophic biofilms in stream microcosms. *PLoS ONE*, 8(4):1–11.

Chaput, G. (2012). Overview of the status of atlantic salmon (salmo salar) in the north atlantic and trends in marine mortality. *ICES Journal of Marine Science: Journal du Conseil*.

Comiti, F., Canal, M. D., Surian, N., Mao, L., Picco, L., and Lenzi, M. (2011). Channel adjustments and vegetation cover dynamics in a large gravel bed river over the last 200 years. *Geomorphology*, 125(1):147 – 159.

Cunjak, R. A., Linnansaari, T., and Caissie, D. (2013). The complex interaction of ecology and hydrology in a small catchment: a salmon's perspective. *Hydrological Processes*, 27(5):741–749.

Destouni, G., Jaramillo, F., and Prieto, C. (2013). Hydroclimatic shifts driven by human water use for food and energy production. *Nat Clim Change*, 3:213–217.

Dick, J. J., Tetzlaff, D., Birkel, C., and Soulsby, C. (2015). Modelling landscape controls on dissolved organic carbon sources and fluxes to streams. *Biogeochemistry*, 122(2):361–374.

Doulatyari, B., Basso, S., Schirmer, M., and Botter, G. (2014). River flow regimes and vegetation dynamics along a river transect. *Advances in Water Resources*, 73:30 – 43.

Doulatyari, B., Betterle, A., Basso, S., Biswal, B., Schirmer, M., and Botter, G. (2015). Predicting streamflow distributions and flow duration curves from landscape and climate. *Advances in Water Resources*, 83:285 – 298.

ESHA (1998). Guida all'idroelettrico minore. per un corretto approccio alla realizzazione di un piccolo impianto. Technical report, European Small Hydropower Association (ESHA), Directorate General for Energy (DG XII-97/010), European Commission.

Fahlbuch, F. (1983). Optimum capacity of a run-of-river plant. *J. Int. Water Power Dam Constr.*, 35(3):25–37.

Formetta, G., Antonello, A., Franceschi, S., David, O., and Rigon, R. (2014). Hydrological modelling with components: A GIS-based open-source framework. *Environmental Modelling and Software*, 55:190 – 200.

Freeman, M. C., Pringle, C. M., and Jackson, C. R. (2007). Hydrologic connectivity and the contribution of stream headwaters to ecological integrity at regional scales1. *JAWRA Journal of the American Water Resources Association*, 43(1):5–14.

Fullerton, A. H., Burnett, K. M., Steel, E. A., Flitcroft, R. L., Pess, G. R., Feist, B. E., Torgesen, C. E., Miller, D. J., and Sanderson, B. L. (2010). Hydrological connectivity for riverine fish: measurement challenges and research opportunities. *Freshwater Biology*, 55(11):2215–2237.

Gibbins, C. N., Moir, H. J., Webb, J. H., and Soulsby, C. (2002). Assessing discharge use by spawning atlantic salmon: A comparison of discharge electivity indices and phabsim simulations. *River Research and Applications*, 18(4):383–395.

Gibbins, C. N., Shellberg, J., Moir, H. J., and Soulsby, C. (2008). Hydrological Influences on Adult Salmonid Migration, Spawning, and Embryo Survival. *American Fisheries Society Symposium*, 65:195–223.

Gilvear, D. J., Heal, K. V., and Stephen, A. (2002). Hydrology and the ecological quality of Scottish river ecosystems. *The Science of the Total Environment*, (294):1–29.

Glover, R. and Malcolm, I. (2015a). Girnock and baddoch: Adult returns to the traps.

Glover, R. and Malcolm, I. (2015b). Girnock and baddoch: Emigrant numbers by year of emigration.

Gordon, J. L. (1981). Estimating hydro stations costs. *J. Int. Water Power Dam Constr.*, 33:31–33.

Gordon, J. L. (1983). Hydropower costs estimates. *J. Int. Water Power Dam Constr.*, 35:30–37.

Gordon, J. L. and Noel, C. R. (1986). The economic limits of small and low-head hydro. *J. Int. Water Power Dam Constr.*, 38:23–26.

Gordon, J. L. and Penman, A. C. (1979). Quick estimating techniques for small hydro potential. *J. Int. Water Power Dam Constr.*, 31:46–55.

Gupta, H. V., Kling, H., Yilmaz, K. K., and Martinez, G. F. (2009). Decomposition of the mean squared error and NSE performance criteria: Implications for improving hydrological modelling. *Journal of Hydrology*, 377(1-2):80 – 91.

Harman, C. J., Sivapalan, M., and Kumar, P. (2009). Power law catchment-scale recessions arising from heterogeneous linear small-scale dynamics. *Water Resources Research*, 45(9).

IEA (2015). Technology roadmap: hydropower. Technical report, International Energy Agency, Paris, France.

IPCC (2014). Climate Change 2014: Synthesis Report. Contribution of Working Groups I, II and III to the Fifth Assessment Report of the Intergovernmental Panel on Climate Change. Technical report, IPCC, Geneva, Switzerland.

Jackson, R. B., Carpenter, S. R., Dahm, C. N., McKnight, D. M., Naiman, R. J., Postel, S. L., and Running, S. W. (2001). Water in a changing world. *Ecological Applications*, 11(4):1027–1045.

Jensen, A. J. and Aass, P. (1995). Migration of a fast-growing population of brown trout (Salmo trutta l.) through a fish ladder in relation to water flow and water temperature. *Regulated Rivers: Research and Management*, 10(2-4):217–228.

Jonsson, B. and Jonsson, N. (2009). A review of the likely effects of climate change on anadromous Atlantic salmon (Salmo salar) and brown trout (Salmo trutta), with particular reference to water temperature and flow. *Journal of Fish Biology*, 75(10):2381–2447.

Jonsson, B., Jonsson, N., and Hansen, L. P. (2007). Factors affecting river entry of adult Atlantic salmon in a small river. *Journal of Fish Biology*, 71(4):943–956.

Jonsson, N., Jonsson, B., and Hansen, L. P. (1990). Partial segregation in the timing of migration of atlantic salmon of different ages. *Animal Behaviour*, 40(2):313 – 321.

Karki, P. (2008). Briefing: IHA sustainability guidelines and assessment protocol. *Eng Sustain*, 161(1):3–5.

Karppinen, P., Erkinaro, J., Niemela, E., Moen, K., and Ø kland, F. (2004). Return migration of one-sea-winter atlantic salmon in the river tana. *Journal of Fish Biology*, 64(5):1179–1192.

Kennedy, R. J. and Crozier, W. W. (2010). Evidence of changing migratory patterns of wild atlantic salmon salmo salar smolts in the river bush, northern ireland, and possible associations with climate change. *Journal of Fish Biology*, 76(7):1786–1805.

Kern, J. D., Characklis, G. W., Doyle, M. W., Blumsack, S., and Whisnant, R. B. (2012). Influence of deregulated electricity markets on hydropower generation and downstream flow regime. *Journal of Water Resources Planning and Management*, 138(4):342–355.

Klemetsen, A., Amundsen, P.-A., Dempson, J. B., Jonsson, B., Jonsson, N., O'Connell, M. F., and Mortensen, E. (2003). Atlantic salmon Salmo salar L., brown trout Salmo trutta L. and Arctic charr Salvelinus alpinus (L.): a review of aspects of their life histories. *Ecology of Freshwater Fish*, 12(1):1–59.

Lacroix, G. L. (2014). Large pelagic predators could jeopardize the recovery of endangered atlantic salmon. *Canadian Journal of Fisheries and Aquatic Sciences*, 71(3):343–350.

Lazzaro, G., Basso, S., Schirmer, M., and Botter, G. (2013). Water management strategies for run-of-river power plants: Profitability and hydrologic impact between the intake and the outflow. *Water Resources Research*, 49(12):8285–8298.

Lazzaro, G. and Botter, G. (2015). Run-of-river power plants in Alpine regions: Whither optimal capacity? *Water Resources Research*, 51(7):5658–5676.

Ledger, M. E., Brown, L. E., Edwards, F. K., Milner, A. M., and Woodward, G. (2013). Drought alters the structure and functioning of complex food webs. *Nat Clim Change*, 3(3):223–227.

Leopold, L. B. and Maddock, T. (1953). The hydraulic geometry of stream channels and some physiographic implications. Technical report, U.S. Geol. Survey Prof. Paper No. 252, U.S. Government Printing Office, Washington, DC.

Lilja, J. and Romakkaniemi, A. (2003). Early-season river entry of adult Atlantic salmon: its dependency on environmental factors. *Journal of Fish Biology*, 62(1):41–50.

Liu, H., Masera, D., and Esser, L. (2013). World small hydropower development report 2013. Technical report, United Nations Industrial Development Organization.

Loucks, D. P., Van Beek, E., Stedinger, J. R., Dijkman, J. P., and Villars, M. T. (2005). *Water resources systems planning and management: an introduction to methods, models and applications*. UNESCO, Paris.

Lu, L., Anderson-Cook, C. M., and Robinson, T. J. (2011). Optimization of Designed Experiments Based on Multiple Criteria Utilizing a Pareto Frontier. *Technometrics*, 53(4):353–365.

Lucchetti, E., Barbier, J., and Araneo, R. (2013). Assessment of the technical usable potential of the TUM Shaft Hydro Power plant on the Aurino River, Italy. *Renewable Energy*, 60:648–654.

Lytle, D. A. and Poff, N. (2004). Adaptation to natural flow regimes. *Trends in Ecology and Evolution*, 19(2):94 – 100.

MacCrimmon, H. R. and Gots, B. L. (1979). World Distribution of Atlantic Salmon, Salmo solar. *Journal of the Fisheries Research Board of Canada*, 36(4):422–457.

Maitland, P. S. and Campbell, R. N. (1992). *Freshwater fishes of the British Isles*. Harper Collins, London.

Malcolm, I. A., Youngson, A. F., and Soulsby, C. (2003). Survival of salmonid eggs in a degraded gravel-bed stream: effects of groundwaterâĂŞsurface water interactions. *River Research and Applications*, 19(4):303–316.

Marler, R. and Arora, J. (2004). Survey of multi-objective optimization methods for engineering. *Structural and Multidisciplinary Optimization*, 26(6):369–395.

Mills, D. (1991). *Strategies for the rehabilitation of Atlantic salmon*. The Atlantic Salmon Trust, Pitlochry.

Mitchell, S. C. and Cunjak, R. A. (2007). Relationship of upstream migrating adult Atlantic salmon (Salmo salar) and stream discharge within Catamaran Brook, New Brunswick. *Canadian Journal of Fisheries and Aquatic Sciences*, 64(3):563–573.

Moir, H., Gibbins, C., Soulsby, C., and Youngson, A. F. (2005). Validation of PHABSIM predictions for simulating salmon spawning habitat. *Riv. Res. Appl.*, 21:1–14.

Moir, H., Soulsby, C., and Youngson, A. (2002). Hydraulic and sedimentary controls on the availability and use of Atlantic salmon (Salmo salar) spawning habitat in the River Dee system, north-east Scotland. *Geomorphology*, 45(3-4):291 – 308.

Moir, H. J., Gibbins, C. N., Soulsby, C., and Webb, J. (2004). Linking channel geomorphic characteristics to spatial patterns of spawning activity and discharge use by Atlantic salmon (Salmo salar L.). *Geomorphology*, 60(1-2):21–35.

Moir, H. J., Soulsby, C., and Youngson, A. F. (1998). Hydraulic and sedimentary characteristics of habitat utilized by Atlantic salmon for spawning in the Girnock Burn, Scotland. *Fisheries Management and Ecology*, 5:241–254.

Montanari, R. (2003). Criteria for the economic planning of a low power hydroelectric plant. *Renewable Energy*, 28(13):2129 – 2145.

Moore, J.-S., Bourret, V., Dionne, M., Bradbury, I., O'Reilly, P., Kent, M., Chaput, G., and Bernatchez, L. (2014). Conservation genomics of anadromous Atlantic salmon across its North American range: outlier loci identify the same patterns of population structure as neutral loci. *Molecular Ecology*, 23(23):5680–5697.

Muneepeerakul, R., Azaele, S., Botter, G., Rinaldo, A., and Rodriguez-Iturbe, I. (2010). Daily streamflow analysis based on a two-scaled gamma pulse model. *Water Resources Research*, 46(11). W11546.

Muneepeerakul, R., Bertuzzo, E., Lynch, H. J., Fagan, W. F., Rinaldo, A., and Rodriguez-Iturbe, I. (2008). Neutral metacommunity models predict fish diversity patterns in mississippi–missouri basin. *Nature*, 453(7192):220–222.

Najmaii, M. and Movaghar, A. (1992). Optimal design of run-of-river power plants. *Water Resources Research*, 28(4):991–997.

Nilsson, C. and Berggren, K. (2000). Alterations of riparian ecosystems caused by river regulation: Dam operations have caused global-scale ecological changes in riparian ecosystems. how to protect river environments and human needs of rivers remains one of the most important questions of our time. *BioScience*, 50(9):783–792.

Nilsson, C., Reidy, C. A., Dynesius, M., and Revenga, C. (2005). Fragmentation and flow regulation of the world's large river systems. *Science*, 308(5720):405–408.

Nunn, A. D., Copp, G. H., Vilizzi, L., and Carter, M. G. (2010). Seasonal and diel patterns in the migrations of fishes between a river and a floodplain tributary. *Ecology of Freshwater Fish*, 19(1):153–162.

Ogayar, B. and Vidal, P. (2009). Cost determination of the electro-mechanical equipment of a small hydro-power plant. *Renewable Energy*, 34(1):6 – 13.

Pargett, M., Rundell, A. E., Buzzard, G. T., and Umulis, D. M. (2014). Model-based analysis for qualitative data: An application in drosophila germline stem cell regulation. *PLoS Comput Biol*, 10(3):1–18.

Park, J., Botter, G., Jawitz, J. W., and Rao, P. S. C. (2014). Stochastic modeling of hydrologic variability of geographically isolated wetlands: Effects of hydro-climatic forcing and wetland bathymetry. *Advances in Water Resources*, 69:38 – 48.

Piccolroaz, S., Majone, B., Palmieri, F., Cassiani, G., and Bellin, A. (2015). On the use of spatially distributed, time-lapse microgravity surveys to inform hydrological modeling. *Water Resources Research*, 51(9):7270–7288.

Poff, N. L., Allan, J. D., Bain, M. B., Karr, J. R., Prestegaard, K. L., Richter, B. D., Sparks, R. E., and Stromberg, J. C. (1997). The natural flow regime. *BioScience*, 47(11):769–784.

Poff, N. L. and Ward, J. V. (1989). Implications of streamflow variability and predictability for lotic community structure: A regional analysis of streamflow patterns. *Canadian Journal of Fisheries and Aquatic Sciences*, 46(10):1805–1818.

Postel, S. L. and Richter, B. (2003). *Rivers for life*. Island Press, Washington, D.C.

Reed, P., Hadka, D., Herman, J., Kasprzyk, J., and Kollat, J. (2013). Evolutionary multiobjective optimization in water resources: The past, present, and future. *Advances in Water Resources*, 51:438 – 456.

Reynolds, L. V., Shafroth, P. B., and Poff, N. L. (2015). Modeled intermittency risk for small streams in the Upper Colorado River Basin under climate change. *Journal of Hydrology*, 523:768 – 780.

Richter, B. D., Baumgartner, J. V., Powell, J., and Braun, D. P. (1996). A method for assessing hydrologic alteration within ecosystems. *Conservation Biology*, 10(4):1163–1174.

Rodriguez-Iturbe, I., Muneepeerakul, R., Bertuzzo, E., Levin, S. A., and Rinaldo, A. (2009). River networks as ecological corridors: A complex systems perspective for integrating hydrologic, geomorphologic, and ecologic dynamics. *Water Resources Research*, 45(1). W01413.

Rosenberg, D. M., McCully, P., and Pringle, C. M. (2000). Global-scale environmental effects of hydrological alterations: Introduction. *BioScience*, 50(9):746–751.

Rye, C. J., Willis, I. C., Arnold, N. S., and Kohler, J. (2012). On the need for automated multiobjective optimization and uncertainty estimation of glacier mass balance models. *Journal of Geophysical Research: Earth Surface*, 117(F2).

Sabo, J. L., Finlay, J. C., Kennedy, T., and Post, D. M. (2010). The role of discharge variation in scaling of drainage area and food chain length in rivers. *Science*, 330(6006):965–967.

Sabo, J. L., Finlay, J. C., and Post, D. M. (2009). Food chains in freshwaters. *Annals of the New York Academy of Sciences*, 1162(1):187–220.

Salford Civil Engineering Ltd (1989). Small Scale Hydroelectric Generation Potential in the UK. Technical report, Department of Energy, London.

Santolin, A., Cavazzini, G., Pavesi, G., Ardizzon, G., and Rossetti, A. (2011). Techno-economical method for the capacity sizing of a small hydropower plant. *Energy Conversion and Management*, 52(7):2533 – 2541.

Scarlat, N., Dallemand, J., Motola, V., and Monforti-Ferrario, F. (2013). Bioenergy production and use in Italy: Recent developments, perspectives and potential. *Renewable Energy*, 57:448 – 461.

Schaefli, B., Rinaldo, A., and Botter, G. (2013). Analytic probability distributions for snow-dominated streamflow. *Water Resour Res*, 49:2701–2713.

Soulsby, C., Malcolm, I. A., Youngson, A. F., Tetzlaff, D., Gibbins, C. N., and Hannah, D. M. (2005). Groundwater-surface water interactions in upland scottish rivers: hydrological, hydrochemical and ecological implications. *Scottish Journal of Geology*, 41(1):39–49.

Stanimirovic, I. P., Zlatanovic, M. L., and Petkovic, M. D. (2011). On the linear weighted sum method for multi-objective optimization. *Facta Acta Universitatis*, 26:49–63.

Tealdi, S., Camporeale, C., and Ridolfi, L. (2011). Modeling the impact of river damming on riparian vegetation. *Journal of Hydrology*, 396(3-4):302 – 312.

ter Braak, C. J. F. and Vrugt, J. A. (2008). Differential Evolution Markov Chain with snooker updater and fewer chains. *Statistics and Computing*, 18(4):435–446.

Tetzlaff, D., Gibbins, C. N., Bacon, P. J., Youngson, A. F., and Soulsby, C. (2008). Influence of hydrological regimes on the pre-spawning entry of Atlantic salmon (Salmo salar L.) into an upland river. *River Research and Applications*, 24(5):528–542.

Tetzlaff, D., Soulsby, C., Bacon, P. J., Youngson, A. F., Gibbins, C. N., and Malcolm, I. A. (2007). Connectivity between landscapes and riverscapes - a unifying theme in integrating hydrology and ecology in catchment science? *Hydrological Processes*, 21(10):1385–1389.

Tetzlaff, D., Soulsby, C., Gibbins, C., Bacon, P., and Youngson, A. (2005a). An approach to assessing hydrological influences on feeding opportunities of juvenile atlantic salmon (salmo salar): A case study of two contrasting years in a small, nursery stream. *Hydrobiologia*, 549(1):65–77.

Tetzlaff, D., Soulsby, C., Youngson, A. F., Gibbins, C. N., Bacon, P. J., Malcolm, I. A., and Langan, S. (2005b). Variability in stream discharge and temperature: a preliminary assessment of the implications for juvenile and spawning Atlantic salmon. *Hydrology and Earth System Sciences*, pages 1–16.

Thorstad, E. B. and Heggberget, T. G. (1998). Migration of adult Atlantic salmon (Salmo salar); the effects of artificial freshets. *Hydrobiologia*, 371(0):339–346.

Thorstad, E. B., Ø kland, F., Johnsen, B. O., and Næ sje, T. F. (2003). Return migration of adult atlantic salmon, salmo salar, in relation to water diverted through a power station. *Fisheries Management and Ecology*, 10(1):13–22.

Tockner, K., Pusch, M., Borchardt, D., and Lorang, M. S. (2010). Multiple stressors in coupled river-floodplain ecosystems. *Freshwater Biology*, 55:135–151.

Vadas, R. L. (2000). *Instream-Flow Needs For Anadromous Salmonids And Lamprey On The Pacific Coast, With Special Reference To The Pacific Southwest*. Springer Netherlands.

Voros, N., Kiranoudis, C., and Maroulis, Z. (2000). Short-cut design of small hydroelectric plants. *Renew. Energy*, 19:545–563.

Vrugt, J. A., ter Braak, C. J. F., Diks, C. G. H., Robinson, B. A., Hyman, J. M., and Higdon, D. (2009). Accelerating Markov chain Monte Carlo simulation by differential evolution with self-adaptive randomized subspace sampling. *Int. J. Nonlin. Sci. Num.*, 10(3):273–290.

Wang, X., Sun, Y., Song, L., and Mei, C. (2009). An eco-environmental water demand based model for optimising water resources using hybrid genetic simulated annealing algorithms. Part I. Model development. *Journal of Environmental Management*, 90(8):2628 – 2635.

Webb, J. H. and Hawkins, A. D. (1989). The movement and spawning behaviour of adult salmon in the Girnock Burn, a tributary of the Aberdeenshire Dee. Technical report.

Widder, S., Besemer, K., Singer, G. A., Ceola, S., Bertuzzo, E., Quince, C., Sloan, W. T., Rinaldo, A., and Battin, T. J. (2014). Fluvial network organization imprints

on microbial co-occurrence networks. *Proceedings of the National Academy of Sciences*, 111:12799–12804.

Youngson, A. and Hay, D. (1996). *The lives of salmon*.

Zanardo, S., Harman, C., Troch, P., Rao, P., and Sivapalan, M. (2012). Intra-annual rainfall variability control on interannual variability of catchment water balance: A stochastic analysis. *Water Resources Research*, 48(1):W00J16.

Ziv, G., Baran, E., Nam, S., Rodriguez-Iturbe, I., and Levin, S. A. (2012). Trading-off fish biodiversity, food security, and hydropower in the mekong river basin. *Proceedings of the National Academy of Sciences*, 109(15):5609–5614.